12-15-2014

Ferric Reductases and Transporters that Contribute to Mitochondrial Iron Homeostasis

Anshika Jain
University of South Carolina - Columbia

FERRIC REDUCTASES AND TRANSPORTERS THAT CONTRIBUTE TO MITOCHONDRIAL IRON HOMEOSTASIS

by

ANSHIKA JAIN

Bachelor of Technology
Guru Gobind Singh Indraprastha University, 2008

Submitted in Partial Fulfillment of the Requirements

For the Degree of Doctor of Philosophy in

Biological Sciences

College of Arts and Sciences

University of South Carolina

2014

Accepted by:

Erin Connolly, Major Professor

Johannes Stratmann, Chaiman, Examining Committee

Rehka Patel, Committee Member

Zhengqing Fu, Committee Member

Thomas Makris, Committee Member

Lacy Ford, Vice Provost and Dean of Graduate Studies

Dedication

To my Baba, Jagjot Singh Jain

Acknowledgements

I would first like to acknowledge my advisor, Dr. Erin Connolly, for having faith in me and giving me the opportunity to work in her lab. I am grateful for all the knowledge, guidance and support she has provided over these past few years. I would also like to thank my current committee members, Dr. Johannes Stratmann, Dr. Rehka Patel, Dr. Zhengqing Fu and Dr. Thomas Makris as well as my former committee members Dr. Beth Krizek and Dr. Wayne Outten for all of the helpful advice and suggestions throughout the years. I am immensely grateful to all our funding sources, NSF, Aspire and SPARC for supporting our research.

I would like to thank our collaborators, Dr. Jeeyon Jeyong, Dr. Mary Lou Guerinot, Dr. David Salt, Dr. Brian Jackson, Dr. Nigel Robinson, Dr. Jerry Kaplan and Dr. Janneke Balk for providing us with the materials, expertise and their timely technical suggestions. I would like to thank Center for Elemental Mass Spectrometry and Mrs. Elizabeth Bair for their time and guidance required through the ICP experiments. I am particularly thankful to Krizek lab, Stratmann lab and Vance lab for letting me use their equipment at any time of the day.

I would also like to acknowledge and thank my current and former lab mates: Grandon Wilson for his input and helpful discussions. Margo Maynes and Amanda

Havighorst for their support, Dr. Indrani Mukherjee, who initiated the FRO3 project and Huijun Yang for teaching me various techniques, lab procedures and help me get independent in the lab.

I would also like to thank all my friends I made in graduate school, Gehana, Rahul, Avneesh, Madhurima, Nirnimesh, Sunil, Suvarthi, Suraj, Rupa, Swati without whom I could not have gotten through my time here at USC and my friends in the Biology department namely, Han, CJ, Janaki, and Claire, for always being there to discuss science and life.

I would also like to thank my undergraduate research advisor Dr. Meenu Kapoor for teaching me the basics of molecular biology and getting me interested in research.

Finally, I would like to thank my entire family, especially my parents for their immense patience, support and faith in me which got me through my years here. Lastly, I would like to thank my pillar, my Fiancé, whose role through this period cannot be described in words.

Abstract

Iron (Fe) is the fourth most abundant element in the Earth's crust, yet the availability of Fe to plants is often limited. This is because in most soil types, Fe precipitates as ferric-oxyhydroxy complexes, making it unavailable for uptake by plants. While the mechanisms involved in Fe uptake from the soil are relatively well understood, the mechanisms involved in its further distribution to the aerial portion of the plant and to subcellular compartments are not fully understood. During Fe deprivation, plants up-regulate root Fe acquisition machinery. How plants sense Fe deprivation and tie the Fe status of the plant to appropriate rates of root Fe uptake, is not well understood. Chloroplasts and mitochondria represent significant Fe sinks in plants and it is assumed that plants monitor the Fe status of these two compartments; if chloroplasts or mitochondria sense Fe limitation, a long distance signal is generated, which serves to upregulate the root Fe acquisition machinery. A number of enzymes involved in the process of energy production in mitochondria are dependent on Fe either as Fe-S clusters or heme cofactors. Thus adequate import of Fe to the mitochondria is vital for the function of this organelle, which becomes all the more essential during Fe starvation. Despite this, not much is known about the Fe trafficking to/from mitochondria. In this study, I describe the mechanisms involved in mitochondrial iron acquisition from the

cytoplasm in plants. Two types of proteins, a ferric chelate reductase (FRO3) and two functionally redundant transporters (MIT1 and MIT2 for **M**itochondrial **I**ron **T**ransporter) mediate Fe uptake by mitochondria. In the absence of either FRO3 or MIT1/MIT2, total Fe content of the mitochondria is reduced and the plants exhibit signature Fe deficiency phenotypes. Furthermore, while it is presumed that MITs are localized to the mitochondrial inner membrane, our membrane topology studies place FRO3 on the outer mitochondrial membrane with its catalytic site facing the inter membrane space of the organelle. Thus we believe that FRO3 and MITs work together during Fe deprivation to reduce and shuttle the ferric iron pools of the IMS to the matrix to meet mitochondrial Fe requirements. Additionally, we found that, while FRO3 is absolutely essential for seed production during Fe deprivation, loss of MIT1 and MIT2 leads to embryo lethality. In this study, we show that FRO3 and the MITs are essential for mitochondrial Fe homeostasis and thus for proper growth and development of the plant.

Table of Contents

List of Figures

Chapter 1

Mitochondrial Iron Transport and Homeostasis in Plants

General Introduction [1]

Iron (Fe) is a vital nutrient for virtually all living organisms. It functions as an essential cofactor for various metabolic processes including respiration and DNA synthesis. In addition, Fe is vital for the synthesis of the oxygen carriers, hemoglobin and myoglobin in mammals. Iron's utility in myriad biochemical processes stems from its ability to readily accept and donate electrons. It is most often associated with protein complexes either as a component of heme or Fe-S clusters. The ability of Fe to participate in electron transfer reactions is nevertheless problematic as well, since Fe^{3+} ions and Fe^{2+} ions are able to participate in the generation of the highly reactive hydroxyl radical (Halliwell et al., 1992). As a result, it is critical that cells carefully control cellular Fe metabolism. Along with Fe-deficiency anemia, which is a widespread human nutritional disorder, Fe-overload results in several pathologies too. Thus, to maintain appropriate amounts of the element while avoiding over-accumulation, all species tightly regulate Fe

---

1

Portions of this chapter have been adapted from
Jain, A., and Connolly, E.L. (2013). Mitochondrial Iron Transport and Homeostasis in Plants. *Frontiers in Plant Science* 4:348.
Jain, A., Wilson, G.T., and Connolly, E.L. (2014). The diverse roles of FRO family metalloreductases in iron and copper homeostasis. *Frontiers in Plant Science* 5:100.

uptake, metabolism, storage and distribution. While red meat serves as a major and an ample source of dietary Fe, Fe acquisition is difficult for people and animals that subsist on a largely plant-based diet. In fact, the World Health Organization estimates that ~2 billion people around the world are afflicted by Fe deficiency anemia (http://www.who.int/nutrition/topics/ida/en/). Thus, studies are being conducted for a comprehensive understanding of Fe homeostasis in plants which, in turn, can inform strategies for the development of Fe fortified food crops.

As in other species, Fe plays an important role in the growth and development of plants. It is required for the function of a large number of enzymes involved in processes like photosynthesis, respiration and DNA synthesis. After nitrogen and phosphorus, Fe is the third most common nutrient that limits plant growth. Fe deficiency is known to be the leading cause of chlorosis in plants (Koenig and Kuhns, 1996). Fe limits plant growth in many soil types despite the fact that it is usually quite abundant in nature. In the presence of oxygen, Fe precipitates into insoluble Fe(III)- oxyhydroxide complexes which limits the availability of Fe to the plants. Thus, the molecular mechanisms utilized by plants for Fe acquisition often include a first step that solubilizes ferric Fe followed by a second step in which Fe is transported from the soil and into root cells. Plants have evolved two types of strategies for Fe acquisition. Strategy I is a reduction-based method used by all dicots and non-grass monocots while strategy II is used by grass species and involves chelation of ferric iron followed by uptake (Guerinot and Yi, 1994). Following transport of Fe into root cells, it may be shuttled into various intracellular organelles for their specific purposes and/or trafficked to the aerial part of the plant.

For my dissertation, I have focused on the intracellular trafficking of Fe to the mitochondria. This work demonstrates a novel, reduction-based mechanism that is employed by plant mitochondria for Fe acquisition. In chapter 2, I describe the characterization of a novel mitochondrial ferric reductase that is important for reducing Fe at the surface of the organelle. Chapter 3 describes the characterization of two functionally redundant transporters that are involved in transporting Fe across the mitochondrial inner membrane.

Background

Fe is an essential micronutrient for virtually all organisms, including plants. Indeed, photosynthetic organisms are distinguished by the high Fe requirement for photosynthetic complexes. Fe deficiency represents an enormous problem in human populations as well, with approximately 2 billion people afflicted (Wu et al., 2002). Plant foods (especially staples like rice, maize and wheat) tend to be poor sources of dietary Fe and thus significant interest surrounds efforts to develop crop varieties with elevated levels of bioavailable Fe. Although Fe is generally quite abundant in the soil, it has a low bioavailability in aerobic environments at neutral to basic pH and as a result, approximately 30% of the world's soils are considered Fe-limiting for plant growth.

Iron Uptake by Strategy I Plants

In response to Fe deficiency, strategy I plants engage in a three stage process to acquire Fe (Figure 1.1). First, the surrounding rhizosphere is acidified via proton

extrusion by a root plasma membrane-localized proton ATPase, AHA2 [***A**rabidopsis* **H**$^+$**A**TPase 2; (Santi and Schmidt, 2009)]. In addition, the secretion of phenolic compounds, particularly coumarins, serves to increase solubility of ferric iron complexes (Rodriguez-Celma et al., 2013a;Schmid et al., 2014;Schmidt et al., 2014). Ferric iron is then reduced to ferrous iron by FRO2 (**F**erric **R**eductase **O**xidase 2) and Fe^{2+} ions are subsequently taken up into root cells by the divalent metal transporter, IRT1 [**I**ron **R**egulated **T**ransporter 1; (Eide et al., 1996;Yi and Guerinot, 1996;Robinson et al., 1999;Vert et al., 2002;Connolly et al., 2003)]. In addition to the induction of these molecular components, the response to low Fe availability is also accompanied by morphological changes including alterations of root architecture such as enhanced root elongation, formation of additional root hairs and formation of transfer cells (Santi and Schmidt, 2009b;Marschner and Marschner, 2012).

The plasma membrane H^+-ATPase family in *Arabidopsis* consists of 12 family members, some of which are regulated by Fe deficiency (Baxter et al., 2003;Colangelo and Guerinot, 2004). H^+-ATPase-mediated extrusion of protons across the plasma membrane of rhizodermal cells is one of the earliest responses to Fe deficiency and is believed to assist in the mobilization of sparingly soluble Fe chelate complexes (Dell'Orto et al., 2002;Schmidt et al., 2003) . While AHA2 is believed to be the key protein responsible for the acidification of the rhizosphere in response to Fe deficiency, AHA7 was recently shown to function in the development of root hairs in response to Fe starvation. This increases the surface area of the root, thus facilitating enhanced Fe uptake during nutrient stress (Santi and Schmidt, 2009a).

In addition, solubilization of ferric-complexes may be mediated by phenolic exudates secreted by roots into the rhizosphere. The response of plants to various organic exudates has been known for over a decade (Romheld and Marschner, 1983). However, the transporters responsible for secretion and the chemical nature of the phenolic compounds were only recently characterized (Schmidt et al., 2014). An ABC (**A**TP-**B**inding **C**assette) transporter, ABCG37 or **P**leiotropic **D**rug **R**esistant9 [(PDR9; (Fourcroy et al., 2014)] in concert with *F6'H* genes (**F**e(II)- and 2.oxoglutarate dependent dioxygenase Feruloyl-CoA 6′-**H**ydroxylase; (Schmidt et al., 2014)] was shown to mediate the extrusion of fluorescent phenolic compounds, particularly coumarins, which aid in solubilization as well as mobilization of Fe(III) complexes in the soil. Mutation in either one of the genes abolishes the secretion of phenolics and results in compromised Fe-uptake in *Arabidopsis* (Fourcroy et al., 2014;Schmid et al., 2014). These *in vitro* studies indicate the role of phenolic compounds in Fe uptake from the soil, however their significance to access metal in calcareous environment is still not clear.

The reduction of solubilized ferric iron to ferrous iron at the root surface is a process that has been well documented and characterized across several plant species including *Arabidopsis* (Yi and Guerinot, 1996) pea (Waters et al., 2002) and tomato (Li et al., 2004), as well as the green alga *Chlamydomonas reinhardtii* (Eckhardt and Buckhout, 1998). The first plant metalloreductase gene was cloned from *Arabidopsis* (Robinson et al., 1999). *FRO2* was identified based on its sequence similarity to the yeast ferric reductase, *FRE1* (**F**erric **RE**ductase1), as well as to a subunit of the human NADPH oxidase, gp91phox, which is involved in the production of reactive oxygen species to protect against invading pathogens (Robinson et al., 1999;Vignais, 2002).

FRO2 was shown to complement the phenotype of an *Arabidopsis* **f**erric **r**eductase **d**efective1 mutant (*frd1*), thus proving that *FRO2* encodes the root surface ferric chelate reductase (Robinson et al, 1999). As expected for an enzyme involved in iron acquisition from the soil, *FRO2* is expressed in the root epidermis and is strongly induced by Fe limitation (Connolly et al., 2003). FRO2 belongs to a superfamily of flavocytochromes and is involved in transfer of electrons from the cytosol across the plasma membrane to reduce extracellular ferric iron to ferrous iron. Studies of the topology of FRO2 show that the protein contains 8 transmembrane (TM) helices, 4 of which build up the highly conserved core of the protein (Schagerlof et al., 2006). This core is conserved throughout the flavocytochrome b family. The large water-soluble domain of FRO2, which contains the NADPH and FAD binding domains and the oxidoreductase sequence motifs, is located in the cytosol. FRO2 also contains four highly conserved histidine residues that likely coordinate two intramembranous heme groups that are instrumental in the electron transfer process (Robinson et al., 1999).

A mechanism similar to strategy I was demonstrated for Fe uptake in yeast; upon the reduction of Fe(III) by FRE1 and FRE2 (Hassett et al., 1998), the reduced Fe(II) is subsequently transported into the cells via high affinity (**F**e **TR**ansporter1; FTR1); and low affinity transporters (**Fe**rrous **T**ransporter4; FET4) (Dix et al., 1994;Hassett et al., 1998). In addition to these, a multicopper oxidase, FET3, is also required for high affinity Fe transport (Askwith et al., 1994;Dix et al., 1997). The double mutant *fet3fet4* is impaired in both low and high affinity Fe transport in yeast (Dix et al., 1994). This mutant was employed to screen for the gene responsible for Fe transport into root cells in *Arabidopsis* (Eide et al., 1996). Thus, the first Fe transporter in plants, IRT1 was

identified by functional complementation of the yeast *fet3fet4* double mutant (Eide et al., 1996). Although the Fe deficiency-limited growth phenotype of *fet3fet4* was successfully rescued by IRT1, IRT1 does not show any sequence homology with either FET3 or FET4.

IRT1 is the founding member of the ZIP (**Z**RT, **I**RT-like **P**rotein) family of metal ion transporters (Eide et al., 1996;Connolly et al., 2002;Vert et al., 2002). It is predicted to contain 8 TM domains with a long intracellular loop between domains 3 and 4 (Eng et al., 1998). This domain contains a conserved histidine rich motif (HCHGHGH) that is believed to play a role in iron sensing and perhaps protein stability (Eng et al., 1998;Grossoehme et al., 2006;Kerkeb et al., 2008;Shin et al., 2013;Kobayashi and Nishizawa, 2014). Although IRT1 is a non-specific transporter of divalent metal ions [with a broad substrate range that includes Fe^{2+}, Mn^{2+}, Zn^{2+}, Co^{2+}, Cd^{2+} (Eide et al., 1996;Korshunova et al., 1999;Rogers et al., 2000;Connolly et al., 2002)], it serves as the predominant route for Fe uptake in Fe limited plants (Eide et al., 1996;Korshunova et al., 1999;Vert et al., 2002;Grossoehme et al., 2006). Loss of function *irt1* mutants are extremely chlorotic and exhibit severe growth defects which can only be rescued by exogenous supply of Fe, indicating its crucial role in Fe homeostasis (Henriques et al., 2002;Varotto et al., 2002;Vert et al., 2002).

IRT1 is primarily expressed in root epidermal cells and flowers (Vert et al., 2002), While IRT1 is known to function as a primary Fe transporter at the plasma membrane, the protein was recently shown to localize to the trans-golgi network/early endosomes of root hair cells (Barberon et al., 2011). This dual localization was explained by the

necessity of a constant recycling of IRT1 for adequate Fe uptake at the plasma membrane. Following metal uptake at the plasma membrane, it is thought that IRT1 is monoubiquitinated on two lysine residues located in an intracellular loop (Kerkeb et al., 2008). It is then trafficked to vacuoles for turn over (Kerkeb et al., 2008;Barberon et al., 2011). However, upon sensing Fe-deficiency, IRT1 can be recycled back to the plasma membrane, a process, that is mediated in part by an endosomal protein, **S**orting **Nex**in1 (SNX1) (Ivanov et al., 2014). The *snx1* mutant exhibits enhanced Fe-deficiency responses presumably due to improper trafficking and premature degradation of IRT1 (Ivanov et al., 2014).

Ubiquitination of IRT1 was shown to be mediated by IDF1 [**I**RT1-**D**egrading **F**actor1; (Shin et al., 2013)]. *idf1* lines are defective in ubiquitination of IRT1, and therefore display increased IRT1 levels at the plasma membrane and seedling lethality. IRT1 ubiquitination however, appear to be independent of the Fe status of the plant (Barberon et al., 2011;Ivanov et al., 2014). In fact, the abundance of secondary non-iron metal substrates of IRT1 (Zn, Mn, and Co) was shown to modulate the shuttling of IRT1 between the plasma membrane and the endosomes in root epidermal cells (Barberon et al., 2014). Furthermore, recent studies showed that IRT1 displays polar localization and is found localized to plasma membrane domains that face the soil solution (Barberon et al., 2014). Together, these studies demonstrate the complex regulation of IRT1 and provide a connecting link between the dynamic localization of IRT1 and metal transport by IRT1.

Iron Uptake by Strategy II Plants

In contrast to strategy I, strategy II plants follow a chelation-based mechanism for Fe acquisition. They secrete **P**hyto**S**iderophores (PS), such as **M**ugineic **A**cid (MA), which bind to ferric iron with high affinity (Ma, 2005). The resulting Fe(III)-PS complexes are transported across the root plasma membrane by a specific iron transporter called **Y**ellow **S**tripe1 (YS1) [(Curie et al., 2001); Figure 1.2].

Phytosiderophores are synthesized through a conserved pathway in which three molecules of **S**-**A**denosyl-L-**M**ethionine (SAM) are condensed with the help of **N**icoti**A**namine **S**ynthase (NAS) to form a molecule of **N**icoti**A**namine (NA) (Higuchi et al., 1999;Bashir et al., 2006). Then, by the action of **N**icotian**A**mine **A**mino**T**ransferase (NAAT), NA is converted to **D**eoxy**M**ugineic **A**cid (DMA) (Takahashi et al., 1999). DMA, the precursor of all PSs then undergoes a series of hydroxylation reactions to form MA (Ma et al., 1999).

The genes responsible for MA secretion into the rhizosphere were unidentified for a long time. However, a recent study showed that **T**ransporter **O**f **M**ugenic acid1 (TOM1), a member of **M**ajor **F**acilitator **S**uperfamily (MFS) of transporters, is responsible for MA extrusion in rice and barley (Pao et al., 1998;Nozoye et al., 2011). The MAs secreted into the rhizosphere solubilize Fe(III), and the resulting Fe(III)-MA complexes are taken up into root cells by YS1 or **Y**ellow **S**tripe 1–**L**ike (YSL) transporters (Curie et al., 2001;Inoue et al., 2009;Lee et al., 2009).

The YS1 transporter was first identified in maize in a mutant screen for defective Fe(III)-PS complex transport. The *ys1* mutant exhibits severe growth defects and interveinal chlorosis. Yeast complementation studies demonstrated successful complementation of the yeast *fet3fet4* double mutant by ZmYS1 under low Fe conditions, suggesting that YS1 functions in transportation of Fe-complexes across the plasma membrane (Curie et al., 2001). The up-regulation of *YS1* under Fe-deficiency in roots and leaves supports their role in Fe uptake and perhaps Fe- distribution to the aerial parts of the plant.

Iron Translocation from Roots to Shoots

Because of its poorly soluble and highly reactive nature, Fe must be associated with chelating agents following uptake into cells. Chelation helps to carefully maintain its redox state between ferric and ferrous iron in the different plant tissues with the varying redox environments (Kobayashi and Nishizawa, 2012). Citrate (Tiffin, 1966;Brown and Chaney, 1971) and NA (Hell and Stephan, 2003;Takahashi et al., 2003) have emerged to be the principal Fe chelators which function in Fe trafficking/translocation in non-graminaceous plants (Figure 1.3).

Once Fe enters the root symplast, it is translocated laterally across the root and effluxed into the xylem for long distance transport through apoplastic spaces. Fe is transported from roots to shoot as a Fe(III)- citrate complex via the xylem (Tiffin, 1970;Lopez-Millan et al., 2000). Fe(III) loading from stele into the xylem sap is believed to be mediated by **F**erro**p**orti**n**1/ **I**ron **REG**ulated1 (FPN1/IREG1) (Morrissey et al.,

2009). Similarly, a transporter of the **M**ultidrug **a**nd **T**oxin **E**fflux (MATE) family, FRD3, has been shown to mediate citrate efflux into the xylem vessels (Rogers and Guerinot, 2002;Durrett et al., 2007). Following translocation to the shoot, Fe(III) from the xylem is then unloaded into the source tissues and phloem for further translocation. Although the process of Fe unloading from xylem to the source tissue is not fully understood, a mechanism similar to strategy I has been postulated for Fe uptake across the plasma membrane of leaf mesophyll cells. A plausible reduction of Fe(III)-citrate mediated by either FRO6, secreted ascorbic acid or light may facilitate the transport of Fe across the plasma membrane of mesophyll cells via an IRT-like transporter (Grillet et al., 2014). IRT3 has been suggested to be a potential candidate for Fe transport across the plasma membrane in shoot tissues (Lin et al., 2009). Although the cytosolic species of Fe are not yet known, upon its entry into the cytoplasm, it is thought that Fe forms Fe chelates and it is likely that the levels of free cellular Fe are exceedingly low. While the role of NA as an Fe(II) chelator has been well documented, additional chelators may function to chelate and stabilize the Fe(III) iron pool of the cell. Fe(II)-NA is believed to circulate symplastically through plasmodesmata to enter the sieve cells (Grillet et al., 2014). The apoplastic Fe(II)-NA is transported into the cells via YSL proteins. Studies have shown the involvement of YSL2 in the transport of Fe-NA across the plasma membrane of leaf cells (DiDonato et al., 2004). On the other hand, YSL1 and YSL3 were shown to function in Fe transport in leaves, pollen and seeds (Waters et al., 2006). Recently, the role of OPT3 (**O**ligo **P**eptide **T**ransporter3, a member of the oligo peptide transporter family) has emerged in Fe loading into phloem cells and in redistribution of Fe from source to sink tissues (Mendoza-Cozatl et al., 2014;Zhai et al., 2014). Although,

OPT3 primarily mediates the transport of Fe(II) ions, its physiological substrate is still unknown (Zhai et al., 2014).

Iron Translocation to Subcellular Compartments

Following the uptake of Fe into cells, it is shuttled into various organelles where it serves as a cofactor for numerous enzymes (Figure 1.4). Organelles like chloroplasts and mitochondria are thought to play a central role in the cellular Fe economy of a plant cell. This is because Fe serves as an essential cofactor for many enzymes involved in the electron transport chain in mitochondria and in the photosynthetic complexes found in chloroplasts. Indeed, recent work has shown that Fe deficiency results in significant changes in the structure and function of mitochondria (Vigani et al., 2009;Vigani and Zocchi, 2009). PS1-LHC1 supercomplexes also exhibit structural and functional alterations under Fe-limited conditions (Yadavalli et al., 2012). Thus, Fe-deficiency affects respiratory and photosynthetic output. However, excessive Fe exacerbates the generation of reactive oxygen species in these redox centers, which can have exceedingly deleterious effects on cells. Thus, mitochondrial and chloroplast Fe metabolism are of particular importance to cellular Fe homeostasis (Nouet et al., 2011).

Chloroplast Iron Transport

Although the precise mechanisms involved in chloroplast Fe acquisition are still somewhat murky (Landsberg, 1984; Terry and Abadia, 1986; Shikanai et al., 2003), it seems likely that chloroplasts take up both Fe(II) and Fe(III) via multiple pathways as

observed in modern day cyanobacteria. Free living cyanobacteria have been shown to acquire Fe through Fe(II) iron transporters from a pool of Fe(III)-dicitrate complexes (Katoh et al., 2001) and it is thus clear that some species of cyanobacteria are able to use a reduction-based mechanism for iron uptake (Kranzler et al., 2014). Plant chloroplasts, which are thought to have originated from ancient cyanobacteria, appear to utilize a similar strategy for Fe uptake as studies of *Arabidopsis* FRO7 demonstrate that chloroplasts employ a reduction-based strategy for Fe acquisition. FRO7 localizes to chloroplasts and loss of FRO7 function results in a significant reduction in chloroplast surface ferric reductase activity. In addition, *fro7* chloroplasts show a ~30% reduction in chloroplast Fe content. *fro7* grows poorly on medium lacking sucrose and shows reduced photosynthetic efficiency, consistent with the idea that FRO7 is critical for delivery of Fe for proper assembly of photosynthetic complexes. When sown on alkaline soil, *fro7* seeds germinate but the resulting seedlings are severely chlorotic and the plants fail to set seed unless supplemented with excess Fe (Jeong et al., 2008). Recent work in sugar beet further supports the existence of a reduction-based mechanism for Fe uptake by chloroplasts, as well (Solti et al., 2012). A presumptive Fe transporter, **P**ermease **I**n **C**hloroplasts1 (PIC1), has been identified that localizes to the chloroplast envelope (Duy et al., 2007). Whether FRO7 and PIC1 work together in chloroplast iron uptake currently remains unknown and it is not yet clear whether PIC1 transports ferric or ferrous iron. Other proteins that are presumed to function in chloroplast Fe transport are MAR1 (**M**odifier of **AR**G1; a homolog of ferroportin 1 and 2), which may transport a Fe chelator (Conte et al., 2009), MFL1/2 (**M**ito**F**errin **L**ike1/2) which resemble mitoferrins but function in chloroplasts; (Tarantino et al., 2011)] and NAP14 [**N**on intrinsic **A**BC binding

Protein; (Shimoni-Shor et al., 2010)]. In addition, a chloroplast-and mitochondria-localized NEET-type protein was recently identified which may be involved in Fe–S cluster transfer to apoproteins (Nechushtai et al., 2012).

Mitochondrial Iron Transport

The recent discovery and characterization of rice MIT1 (**M**itochondrial **I**ron **T**ransporter), which is involved in iron uptake by mitochondria, and the mitochondrial Fe chaperone, Frataxin (FH) have demonstrated the significance of mitochondrial iron uptake and trafficking/distribution to plant growth and development (Busi et al., 2006;Bashir et al., 2011;Maliandi et al., 2011;Vigani, 2012). Despite this, we are far from a comprehensive understanding of mitochondrial Fe homeostasis (Nouet et al., 2011;Vigani et al., 2013). Although two *Arabidopsis* metalloreductases (FRO3 and FRO8) have been predicted to localize to mitochondrial membranes, neither one has been functionally characterized. A mitochondrial proteomics study has placed FRO8 at the mitochondrial membrane (Heazlewood et al., 2004). The expression patterns of FRO3 and FRO8 are largely non-overlapping, suggesting that they do not function redundantly (Jain and Connolly, 2013). FRO3 is expressed in both roots and shoots (Mukherjee et al., 2006). Little information is available for FRO8 but its expression is concentrated in the vasculature of senescing leaves (Wu et al., 2005). Mitochondria also supply Fe and sulfur to the **C**ytoplasmic **I**ron-sulfur cluster **A**ssembly machinery (CIA) (Balk and Pilon, 2011). While sulfur scaffolded with glutathione is likely exported to the cytosol via an ABC transporter, ATM3 (Bernard et al., 2009;Schaedler et al., 2014), putative transporters required for Fe efflux are still unknown. The recent discovery of a

Mitochondrial **I**ron **E**xporter (MIE) in mice (**A**TP-**B**inding **C**assette **B**8, ABCB8) and its role in CIA-mediated Fe-S synthesis has provided new insight into understanding of intracellular Fe homeostasis (Ichikawa et al., 2012) and may facilitate the identification of MIE proteins in other species. Finally, the discovery of YSL4 and YSL6 transporters involved in Fe(II)-NA release from chloroplasts of *Arabidopsis*, suggest a possible role for other members of the YSL family in mitochondrial Fe efflux (Divol et al., 2013).

Vacuolar Iron Trafficking

Acidic compartments like vacuoles have a relatively oxidizing atmosphere as compared to the cytosol. In yeast, Fe in vacuoles is largely present as ferric polyphosphate complexes (Raguzzi et al., 1988). The remobilization of Fe from the yeast vacuolar compartment is mediated by the FRE6 (Singh et al., 2007). FRE6 also plays a role in copper remobilization from vacuoles; reduced copper is subsequently exported to the cytosol via CTR2 [**C**opper **TR**ansporter2; (Rees and Thiele, 2007)]. Vacuolar Fe transporters have been reported in plants; *Arabidopsis* **V**acuolar **I**ron **T**ransporter1 (VIT1), transports iron into the organelle while NRAMP3 (**N**atural **R**esistance **A**gainst **M**icrobial **P**athogens3) and NRAMP4 mediate the export of iron (Lanquar et al., 2005;Kim et al., 2006). However, no vacuolar metalloreductases have been reported in plants, to date.

Iron Storage

Metal homeostasis in plants is accomplished via a set of elegantly regulated mechanisms that control various aspects of Fe metabolism (including uptake, efflux, chelation and storage). Ferritins are clearly essential to overall Fe homeostasis as they function in Fe sequestration and thus serve to prevent oxidative damage (Zhao et al., 2002;Arosio et al., 2009). Ferritins are localized to both chloroplasts and mitochondria, two major sites for ROS production. Plant ferritins are conserved proteins that oligomerize to form a hollow sphere. They exhibit ferroxidase activity and oxidize Fe^{2+} and store it within the ferritin core in the form of hydrous ferric oxides along with phosphates (Arosio et al., 2009). Ferritin can accommodate 2000-4000 Fe^{3+} atoms per ferritin molecule (Carrondo, 2003). The molecular mechanism underlying the release of Fe from ferritins is not very well understood. *In vitro* studies in animals suggest that release of Fe requires iron chelators or reducing agents (Bienfait and van den Briel, 1980). In contrast, *in vivo* studies in animals have demonstrated the release of Fe by proteolytic degradation of ferritin protein (Voss et al., 2006;Briat et al., 2010;Zhang et al., 2010). To date, the process is not described in plant systems. Plant ferritins are primarily localized to plastids, as opposed to animal ferritins which are usually cytoplasmic. Mitochondrial localization of ferritins was first reported in mammals (Levi et al., 2001). Subsequently, mitochondrial ferritins were also identified in plants (Zancani et al., 2004;Tarantino et al., 2010a). *Arabidopsis* possesses four ferritin (FER1-4) proteins, all of which are known to be localized to chloroplasts. FER4 is unique in that it contains dual targeting signals and is therefore found in mitochondria as well as chloroplasts (Tarantino et al., 2010b), FER1 is the predominant ferritin and is primarily

expressed in the vasculature of the leaves, pollens and anthers (Tarantino et al., 2003;Ravet et al., 2009). This indicates the role of leaves, pollen and anthers as major sinks for Fe accumulation (Roschzttardtz et al., 2013).

However, in addition to chloroplast and mitochondria, histochemical staining studies have also shown the accumulation of Fe in the cell wall of the stele (Roschzttardtz et al., 2013). Furthermore, during embryo development, the Fe is transported via VIT1 and stored in the vacuolar compartment of the plant (Kim et al., 2006;Roschzttardtz et al., 2009). At the beginning of germination, induction of NRAMP3 and NRAMP4 help in the remobilization of these stores and provide enough Fe to developing seedlings for their metabolic requirements (Lanquar et al., 2005;Divol et al., 2013).

Iron Homeostasis and Iron Deficiency-Induced Signaling

Genes involved in Fe acquisition are transcriptionally up-regulated in response to Fe deprivation. Several transcription factors are known to control the Fe deficiency response. The key regulator in non-graminaceous plants was first identified in tomato. A gene encoding for a bHLH transcription factor, FER was shown to control the strategy I response in tomato (Ling et al., 2002). The ortholog of FER, **F**er-like **I**ron deficiency induced **T**ranscription factor (FIT) was soon identified in *Arabidopsis* (Colangelo and Guerinot, 2004). FIT, in association with two other transcription factors, bHLH38 and bHLH39 was shown to regulate the expression of FRO2 and IRT1 and thus modulate Fe uptake from the soil (Yuan et al., 2008). In addition, microarray analysis showed that FIT modulates the expression of 72 other genes involved in Fe homeostasis (Colangelo and

Guerinot, 2004). However, post-translational regulation of FIT by proteasomal degradation suggests the presence of regulatory proteins that control the expression of this master regulator of Fe deficiency responses (Sivitz et al., 2011). In an attempt to search for the regulators of FIT, two other transcription factors involved in ethylene signaling [**E**thylene **IN**sensitive3 (EIN3) and **E**thylene **I**nsensitive3-**L**ike1 (EIL1)] were shown to interact with FIT and prevent its degradation under Fe deficiency. This enhanced stabilization of FIT in turn facilitates an enhanced Fe-deficiency response. Thus, the plant stress hormone ethylene was discovered as a signaling molecule that promotes Fe acquisition (Lingam et al., 2011). Other plant hormones affecting the FIT-regulated Fe uptake regulon have also been discovered in the recent years. While auxin (Wu et al., 2012), **N**itric **O**xide (NO) (Meiser et al., 2011) and ethylene serve as positive regulators of FIT, cytokinin (Seguela et al., 2008) and jasmonic acid (Maurer et al., 2011) on the other hand have been demonstrated as negative regulators of Fe uptake in non-graminaceous plants (Hindt and Guerinot, 2012).

Using a cell type-specific transcriptional profiling approach, the root pericycle was identified as a regulatory center for sensing the Fe status of the plant (Dinneny et al., 2008). A few years later, the same group discovered two tightly co-regulated transcription factors [**P**OPE**YE** (PYE) and **B**RU**T**U**S** (BTS)], which are expressed in the pericycle and control the expression of several other Fe-response genes (Long et al., 2010). Both PYE and BTS are induced by Fe deficiency. PYE, a bHLH transcription factor, was identified as a regulator of Fe-deficiency induced genes whereas BTS was identified as a negative regulator of PYE. BTS possesses three putative domains: a putative DNA binding domain (CHY-type zinc finger), a putative E3 ubiquitin ligase

domain (RING/FYVE/PHD type-Zn finger domain), and a putative hemerythrin (HHE) domain for Fe binding (Long et al., 2010). Recent studies have shown the role of proteins with HHE binding domains in sensing of Fe and oxygen status in mammals [**F**-**B**o**X** and **L**eucine-rich repeat protein 5 (FBXL5); (Chollangi et al., 2012)] and rice [**H**aemerythrin motif-containing **R**eally interesting New Gene (RING)-and **Z**inc-finger protein 1 (HRZ1 and HRZ2); (Kobayashi et al., 2013)]. Both of these proteins have been reported to function as Fe sensors (Chollangi et al., 2012;Kobayashi et al., 2013). Under Fe-sufficient conditions, the E3 binding domain (F-box) of FBXL5 in mammals mediates the proteasomal degradation of a repressor protein, IRP2, which, in turn, results in the increased transcription of Fe-storage genes (Chollangi et al., 2012). Similarly, HRZs were also demonstrated as potential negative regulators of Fe-deficiency inducible gene regulators like OsIRO2 and OsIRO3, the PYE homologs in rice. HRZs are believed to sense the Fe/Zn ratio of the plant and repress or modulate the expression of Fe-utilization genes. This suggests the potential of HRZs to function at the core of Fe sensing (Kobayashi et al., 2013). The presence of the HHE and E3 ligase domains in BTS suggests that BTS may also function in Fe sensing. While the substrates of BTS are not characterized, potential substrates might include all the Fe responsive proteins which undergo ubiquitination, such as FIT or an unknown repressor of ferritin synthesis or the bHLH proteins, related to PYE (bHLH115 and ILR3) (Samira et al., 2013;Kobayashi and Nishizawa, 2014). The fact that BTS physically interacts with PYE homologs supports the hypothesis that BTS targets these two proteins for degradation (Long et al., 2010).

A new set of transcription factors were reported recently, which provide an indirect connection between the aforementioned FIT and PYE networks. MYB10 and

MYB72 are strongly up-regulated under Fe-starvation and have been shown to positively control the expression of NAS2 and NAS4 in roots. NAS2/4 encode nicotianamine synthase which function in the generation of NA, an important chelator of Fe. While PYE is a negative regulator of NAS4, MYB72 functions downstream of FIT and positively regulates NAS4 expression. On the other hand, MYB10, a direct target of PYE and FIT is responsible for the tight regulation of NAS4 and Fe-deficiency response (Li et al.;Palmer et al., 2013;Li et al., 2014).

Another FIT independent pathway for Fe regulation was recently demonstrated (Sivitz et al., 2012) Two transcriptional factors, bHLH100 and bHLH101, also induced by Fe deficiency are believed to regulate the genes involved in Fe distribution within the plant (Sivitz et al., 2012). These transcription factors regulate several genes including OPT3, which was the first identified shoot-expressed gene shown to function in systemic signaling of Fe status in the plant (Mendoza-Cózatl et al., 2014;Zhai et al., 2014).

Conclusion

Several studies have highlighted the role of various gene families and metabolites that are involved in Fe uptake, metabolism, distribution and storage to maintain Fe homeostasis in plants. New tools that provide insight into the redox status and types of Fe species found in each of the various cellular compartments will go a long way toward the development of a comprehensive understanding of Fe metabolism in plants. These studies will be critical to efforts to understand both organellar iron homeostasis and the mechanisms employed by plants to coordinate and prioritize Fe utilization by the various

iron containing compartments of the cell. This new knowledge should facilitate novel strategies aimed at improving crop yields on nutrient-poor soils and biofortification of plant foods to help ameliorate nutrient deficiencies in humans.

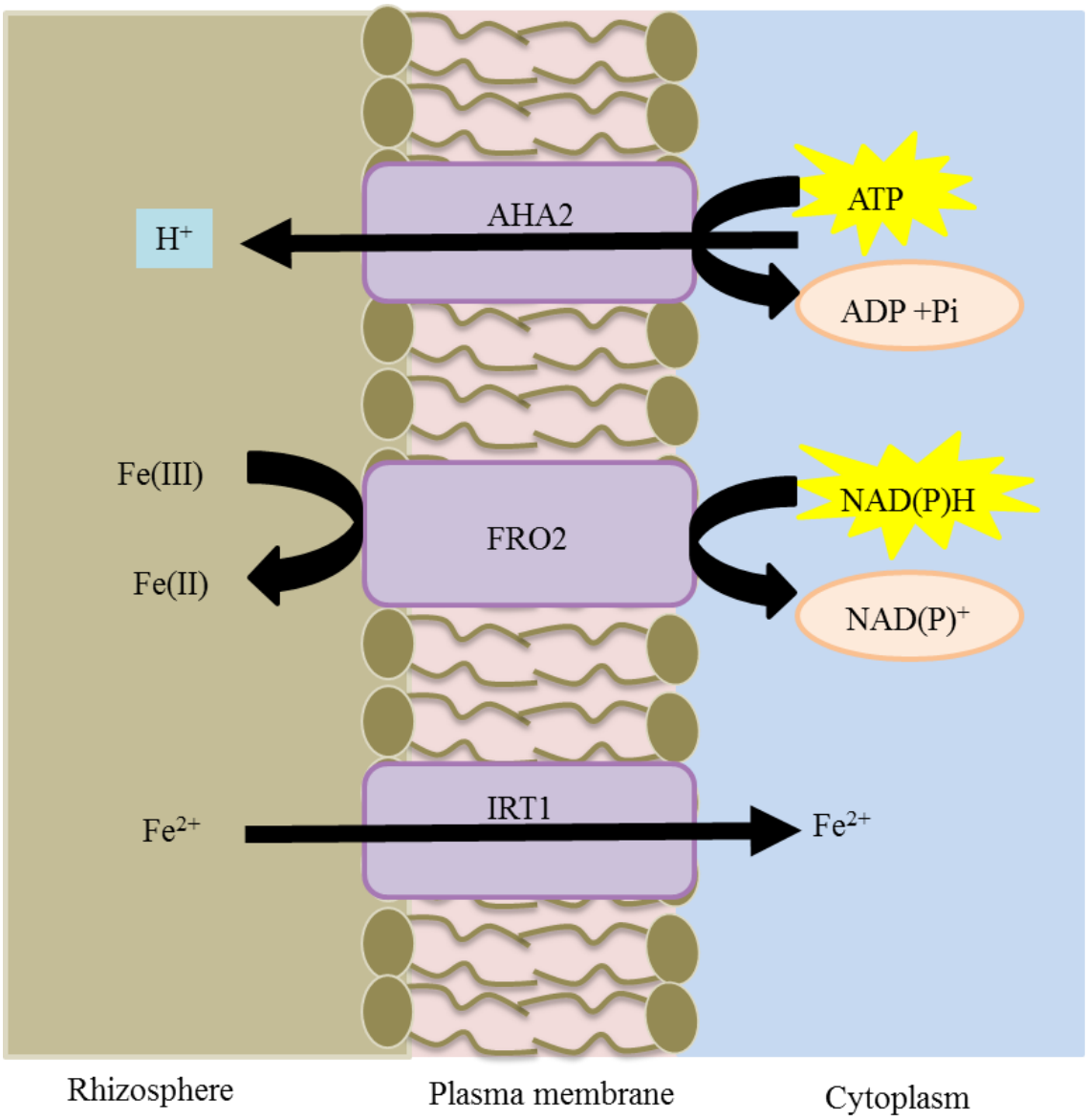

Figure 1.1: Iron uptake mechanism in strategy-I plants.
Adapted from Buchanan, Gruissem and Jones, 2002

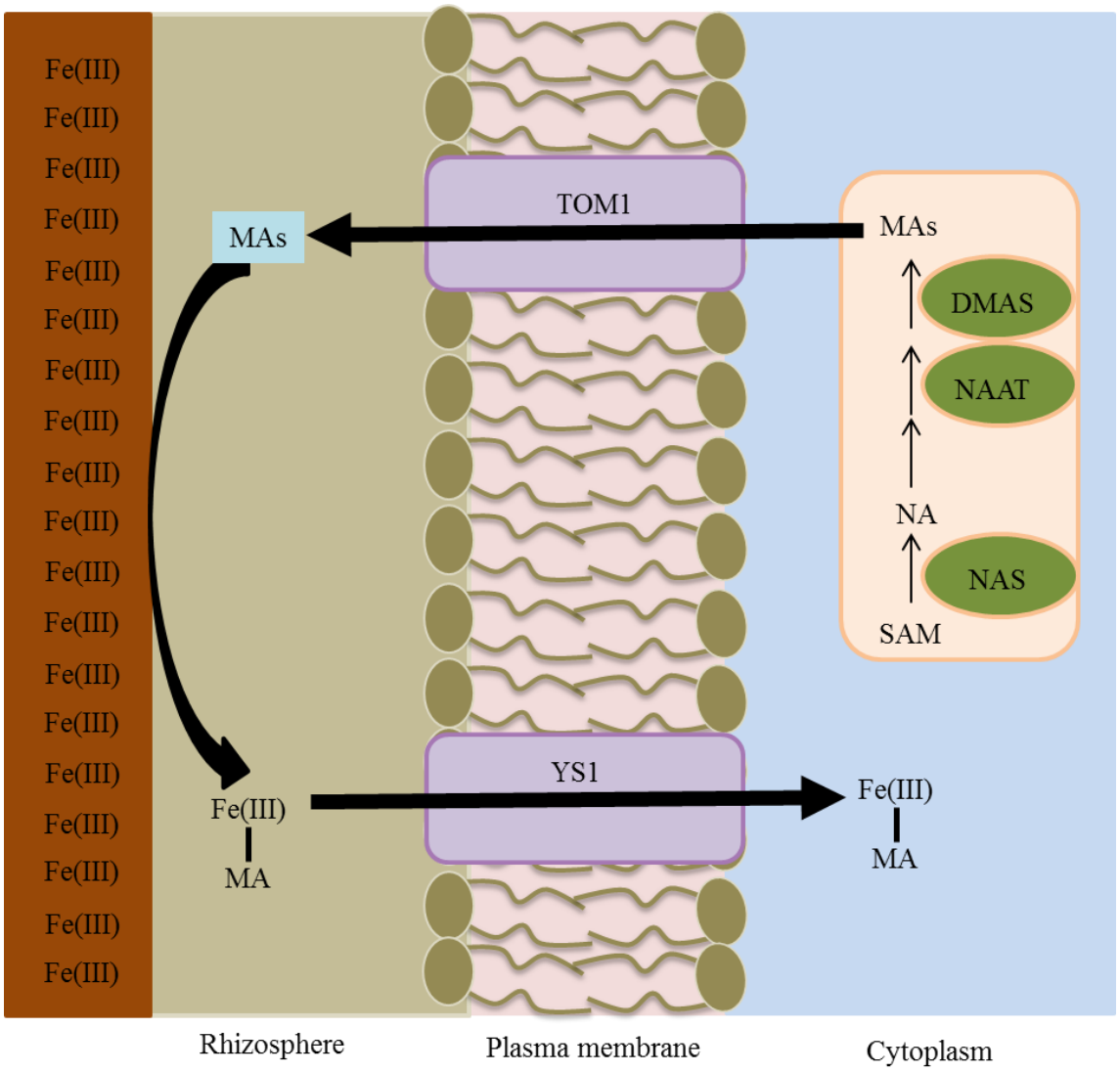

Figure 1.2: Iron uptake mechanism in Strategy II plants.
Adapted from Kobayashi and Nishizawa, 2012

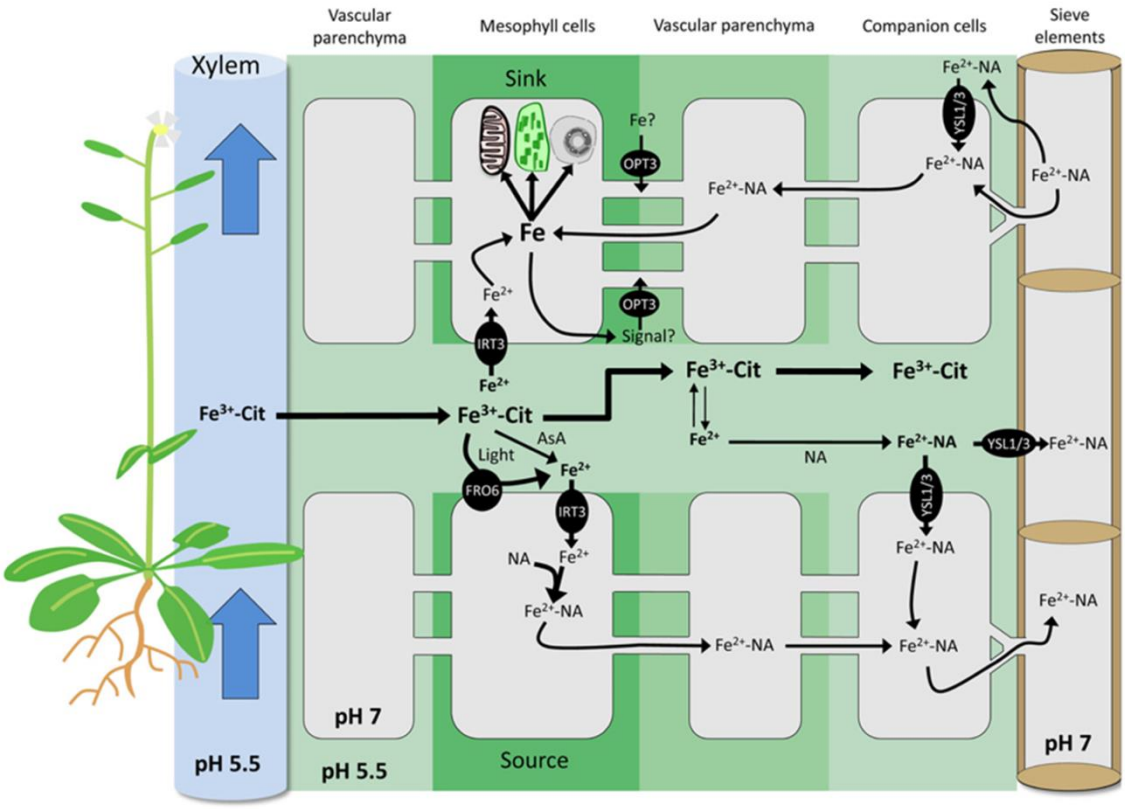

Figure 1.3: Schematic representation of iron translocation from roots to shoots in *Arabidopsis*

Adapted from Grillet et al, 2014

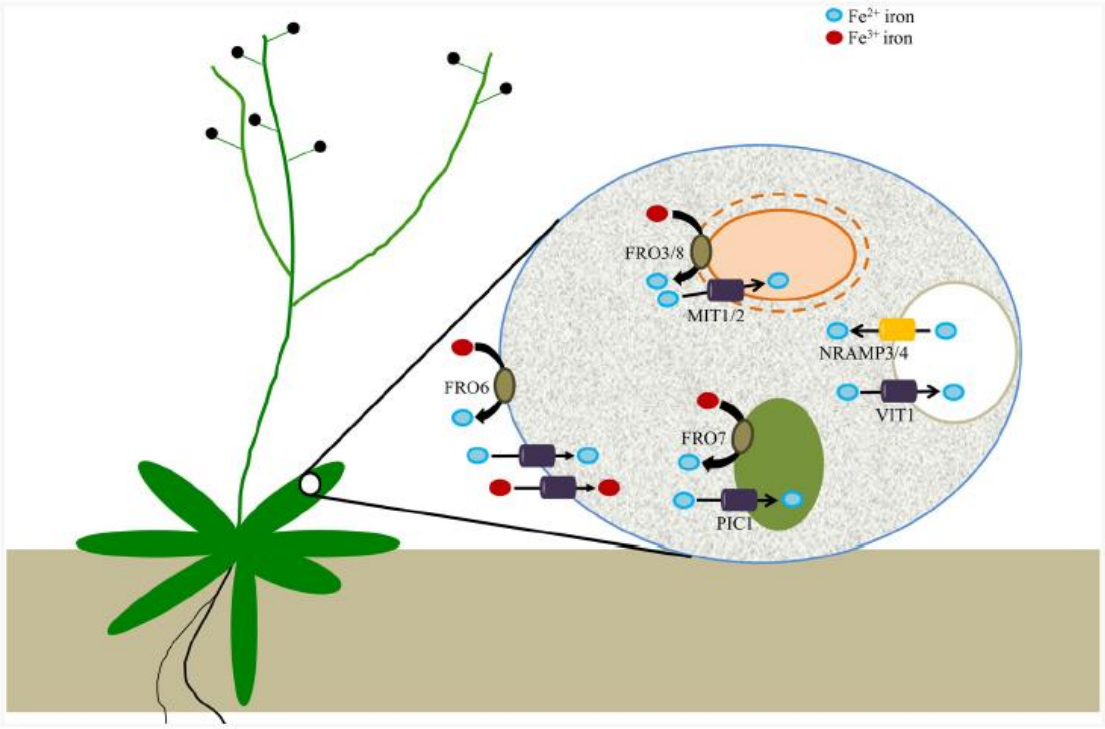

Figure 1.4: Ferric reductases and transporters that contribute to intracellular iron homeostasis.
Adapted from Jain et al, 2014

Chapter 2

A Mitochondrial Ferric Chelate Reductase, FRO3 Plays Critical Roles in Intracellular Iron Transport and Seed Production in *Arabidopsis thaliana* [2]

Abstract

Iron (Fe) is an essential nutrient for growth and development of virtually all species. Fe deficiency afflicts a significant proportion of the human population with approximately 2 billion suffering from Fe deficiency worldwide. Plants serve as the major sources of dietary Fe for many people; however, this can be problematic because most staple crops are very poor sources of dietary Fe. Thus it is important to study the pathways controlling Fe uptake, distribution, storage and regulation in plants. Although the mechanisms controlling Fe uptake from the soil are relatively well understood, considerably less is known about subcellular trafficking of Fe in plant cells. In particular, our understanding of mitochondrial iron metabolism is incomplete, despite the fact that mitochondria require significant amounts of Fe to ensure proper functioning of electron transport protein complexes. In this study, we have identified and characterized a novel pathway

[2] Portions of this chapter have been adapted from
Jain, A., Wilson, G.T., and Connolly, E.L. (2014). The diverse roles of FRO family metalloreductases in iron and copper homeostasis. *Frontiers in Plant Science* 5:100.

for Fe acquisition in mitochondria. FRO3 (**F**erric **R**eductase **O**xidase 3), a member of the FRO family of metalloreductases localizes to the outer mitochondrial membrane and plays an important role in mitochondrial Fe uptake. The analysis of loss of function *fro3* lines shows that FRO3 plays an important role in mitochondrial Fe homeostasis. *fro3* harbors significantly elevated levels of Fe in the shoots and yet fro3 mitochondria contain 50% as much Fe as WT mitochondria. Additionally, reduced mitochondrial ferric reductase activity was measured in *fro3* in Fe limiting conditions. *fro3* demonstrates impaired activities of Fe-containing enzymes that depend on mitochondrial Fe. Our results also show that FRO3 is important for the development and reproduction of the plant under Fe limiting conditions. Overall, this study demonstrates that FRO3 plays significant roles for proper mitochondrial Fe acquisition to maintain mitochondrial and whole plant Fe homeostasis.

Introduction

Fe participates as an essential cofactor in many biochemical reactions in a cell. Its significance in processes like respiration and photosynthesis has been well documented. Its physiological relevance stems from its potential to accept and donate electrons; this attribute makes Fe a central cofactor in many cellular redox reactions. However, excessive Fe accumulation in cells can result in the production of **R**eactive **O**xygen **S**pecies (ROS) as a result of Fenton chemistry (Halliwell et al., 1992). Thus, Fe metabolism is carefully regulated to ensure adequate supply of Fe while avoiding toxicity associated with its over-accumulation.

Despite its abundance in the Earth's crust, Fe is frequently a limiting factor in the growth and development of plants. One-third of the world's soils are considered to be Fe deficient due to the fact that Fe is poorly soluble in aerobic soils at neutral to basic pH. In the presence of oxygen, Fe precipitates as insoluble ferric-oxyhydroxy complexes. Thus, plants have employed sophisticated mechanisms for Fe uptake from such soils. When Fe is limiting, all dicots and non-grass monocots, like *Arabidopsis*, use strategy I for Fe acquisition from the soil. Strategy I plants follow a three step, reduction-based mechanism for Fe acquisition (Guerinot and Yi, 1994). In these plants, a proton pump at the root surface extrudes protons to acidify the rhizosphere, which solubilizes the precipitated Fe(III) complexes in the soil. The solubilized Fe(III) may then be reduced by a membrane-bound ferric chelate reductase, to Fe(II), which is subsequently taken up into the root cells via an iron regulated transporter. In contrast, all the grasses follow a chelation based mechanism for Fe acquisition (termed strategy II). In strategy II, **P**hyto**S**iderophores (PSs) are secreted into the rhizosphere, where they chelate Fe(III). These PS-Fe complexes are then transported into plant cells (Guerinot and Yi, 1994).

In recent years, a number of proteins have been shown to be involved in proper Fe trafficking and in the maintenance of Fe homeostasis in the plants, Among these, FRO family members have emerged as important players in acquisition of both Fe and Cu as well as subcellular trafficking of Fe. The *Arabidopsis* genome contains a total of eight *FRO* genes that likely encode ferric chelate reductases. FROs belong to a superfamily of flavocytochromes and share close homology with FRE1 in yeast and to a subunit of the human NADPH oxidase, gp91phox, which is involved in the ROS generation as a defense mechanism against invading pathogens. In *Arabidopsis*, the members of FRO

family serve as metalloreductases facilitating the reduction of metals prior to their trafficking across the membranes.

In addition to their role in Fe uptake, recent studies have demonstrated a role for FRO family members in reduction of copper (Cu) for its uptake by plants. Furthermore, emerging roles of FROs also point to their significance in trafficking of Fe to subcellular compartments.

Plasma membrane Ferric Reductases

The founding member of FRO family, FRO2 was identified based on its sequence similarity with human NADPH oxidase gp91phox and yeast **F**erric **Re**ductases (FRE1) (Robinson et al., 1999). Localized to the root plasma membrane, FRO2 functions to reduce ferric iron complexes in the rhizosphere for their further uptake into the plant. It is strongly regulated by the master regulator of Fe-deficiency responses, FIT [(**F**er like **I**ron-deficiency induced **T**ranscription factor; (Colangelo and Guerinot, 2004)]. Membrane topology studies in FRO2, have identified 10 **T**rans**M**embrane (TM) helices, an intracellular FAD and a NAD(P)H binding domain and an extracellular catalytic domain that mediate the reduction of extracellular Fe (Schagerlof et al., 2006). NAD(P)H is believed to function as the electron donor which is transferred across the membrane to reduce the rhizodermal Fe(III) ions. Like their FRE counterparts, *Arabidopsis FROs* are differentially regulated by deficiencies of Fe and/or Cu (Mukherjee et al., 2006). Studies of FRO2 have suggested that it may have a role in the reduction of Cu^{2+} to Cu^{+} at the root surface, in addition to its role in Fe reduction (Yi and Guerinot, 1996; Robinson et al., 1999). However, reduction of Cu by FRO2 is not physiologically relevant (Connolly et

al., 2003); this result opens up the possibility that other FROs function to reduce Cu at the root surface.

Recent studies have shown that FRO4 and FRO5 act redundantly to reduce Cu at the root surface (Bernal et al., 2012) . These genes are strongly induced under Cu deficiency (Mukherjee et al., 2006) and are tightly regulated by a master regulator of the copper deficiency response, SPL7 [**S**QUAMOSA **P**romoter Binding-**L**ike7;(Yamasaki et al., 2009;Bernal et al., 2012)]. At this point, it remains unclear whether FRO4/5 are involved in Fe homeostasis, however expression of *FRO5* is induced under Fe-deficiency (Wu et al., 2005;Mukherjee et al., 2006)

The role of another member of FRO family, FRO6 has been implicated in light dependent Fe-reduction in leaves (Jain et al., 2014). Although the expression of FRO6 is not regulated by the Fe status of the plant, it is controlled in a light-dependent manner (Feng et al., 2006;Mukherjee et al., 2006). *FRO6* promoter contains several light-responsive elements and etiolated *FRO6-GUS* seedlings exhibit no FRO6 promoter activity (Feng et al., 2006). Thus, FRO6 appears to play important role to reduce Fe in the presence of light, perhaps to enable the assembly of new photosynthetic complexes in the leaves.

Intracellular Ferric Reductases

The chloroplasts and mitochondria are unique organelles and they are thought to have evolved via endosymbiosis. As a result, both organelles are surrounded by two membranes; the outer membrane resembles eukaryotic membranes while the inner resembles prokaryotic membranes. Thus, these two organelles may utilize prokaryotic

and/or eukaryotic type Fe transport systems (Shimoni-Shor et al., 2010). It is usually assumed that Fe may pass freely across the outer membrane of both organelles via porins. It is also important to note that there is little known about the speciation of cytosolic Fe although it is assumed that there is very little free Fe present in the cytosol (Hider and Kong, 2013). Thus, the Fe species that are available for transport into subcellular compartments are unclear at this time. Recent studies implicate FRO family members in Fe delivery to chloroplasts [FRO7; (Jeong et al., 2008;Solti et al., 2012;Solti et al., 2014)] and speculate their role in mitochondria [FRO3 and FRO8; (Jeong and Connolly, 2009;Jain and Connolly, 2013)]. Intriguingly, although work in yeast has shown that metalloreductases are important in vacuolar metal homeostasis, to date there is no evidence to support an analogous role in plants.

Mitochondria contribute to two major iron utilization pathways in the cell: heme synthesis and Fe-S cluster biogenesis. Despite this, the mechanisms involved in Fe trafficking to this organelle are relatively unknown. The recent discovery of a **M**itochondrial **I**ron **T**ransporter (MIT) in rice provided new insight into the mechanism of Fe import into the plant mitochondria (Bashir et al., 2011). The homologs of MIT in yeast (MRS3 and MRS4) are known to transport Fe(II) across the **I**nner **M**itochondrial **M**embrane [IMM; (Froschauer et al., 2009a)]. Moreover, the high aqueous solubility of Fe(II) over Fe(III) favors this form of Fe for intracellular translocation (Hider and Kong, 2013). Although Fe(II) is believed to be the most predominant pool of Fe in the cytosol, the presence of Fe(III) iron (as a result of enzymatic reactions/ auto-oxidation/Fenton reaction) has also been proposed in the cytosol (Hider and Kong, 2013). During Fe-deprivation, it is reasonable to believe that Fe(III) iron significantly contributes to the

cytosolic pool of Fe and plays an important role in biochemical reactions such as photosynthesis and respiration. While a chelation based mechanism would be required for direct Fe(III) uptake into the organelle, a functional reductase would be required to transport Fe through the other Fe(II) translocating channels. A reduction based mechanism (mediated by FRO7) was reported for chloroplast in *Arabidopsis* and sugar beet (Jeong et al., 2008;Solti et al., 2012). The molecular mechanism for Fe acquisition in *Arabidopsis* mitochondria has not been characterized so far. It is interesting to note that although the yeast metalloreductase FRE5 localizes to mitochondria (Sickmann et al., 2003), there are no reports to date that demonstrate a role for a metalloreductase in mitochondria in any organism.

Here we report a novel mitochondrial ferric reductase, FRO3 important for mitochondrial Fe acquisition in *Arabidopsis*. FRO3 shows a ubiquitous expression pattern in both shoots and roots throughout development (Wu et al., 2005;Mukherjee et al., 2006), consistent with the idea that it is vital for mitochondrial Fe metabolism. In contrast, a second putative mitochondrial ferric reductase, FRO8 is primarily expressed in leaves during senescence (Jeong and Connolly, 2009). The non-overlapping expression patterns of FRO3 and FRO8 suggest they may function non-redundantly in mitochondrial and plant Fe homeostasis. We focused on FRO3 which appears to be the predominant ferric reductase essential for mitochondrial Fe trafficking.

Our results show that FRO3 is involved in maintaining mitochondrial Fe homeostasis in Fe-limiting conditions. *fro3* mitochondria contain 50% as much Fe as WT mitochondria and thus exhibit impaired mitochondrial metabolism, particularly for the chemical reactions that require mitochondrial Fe for their cofactors. Sub-mitochondrial

localization studies demonstrate that FRO3 is localized on the **O**uter **M**itochondrial **M**embrane (OMM). FRO3 is oriented such that it likely functions to reduce a pool of Fe(III) present in the **I**nter-**M**embrane **S**pace (IMS) of the organelle. Lastly, our results show that FRO3 is essential for seed production under Fe-limiting conditions.

Materials and Methods

Plant Lines and Growth Conditions

Wild type Arabidopsis (No-*0* or Col-*gl-1*) was used as a control in all experiments. A T-DNA insertion mutant in FRO3 (*frohc*, subsequently called fro3) was obtained from Dr. Nigel Robinson (Robinson et al., 1997). *FRO3 RNAi* lines were previously generated by a former graduate student, (Mukherjee, 2006). The seeds were surface sterilized with 25% bleach and 0.02% SDS. After a thorough washing, the seeds were imbibed in the dark for 2 days at 4°C. The plants were grown on Gamborg's B5 media (Phytotechnology Laboratories, Shawnee Mission) supplemented with 2% sucrose, 1mM MES and 0.6% agar, pH 5.8 for 2 weeks under constant light (80µmol/m^{-2}/s^{-2}) at 22°C. The plants were grown in Metro-Mix 360: perlite: vermiculite (5:1:1) in 16 h days or hydroponically in the constant light (media replaced weekly). The composition of the hydroponics nutrient solution was as follows: 0.75 mM K_2SO_4, 0.1 mM KH_2PO_4, 2.0 mM $Ca(NO_3)_2$, 0.65 mM $MgSO_4$, 0.05 mM KCl, 10 µM H_3BO_3, 1 µM $MnSO_4$, 0.05 µM $ZnSO_4$, 0. 05 µM $CuSO_4$, 0.005 µM $(NH_4)_6Mo_7O_{24}$, with 0 or 50 µM Fe(III)-EDTA (Kerkeb et al., 2008). To induce iron deficiency in plants, the plants were either transferred from B5 media to FerroZine [3-(2-pyridyl)-5,6-diphenyl-1,2,4 triazine sulfonate] for three days or they were grown on 1/2X MS media without iron for 17 days.

Cloning

35S-FRO3-GFP and *FRO3-RNAi* constructs used in this study were previously generated in our lab (Mukherjee, 2006). To generate the constructs for the self-assembling GFP assay, first strand cDNA was synthesized from the RNA extracted from the roots of No-*0* according to manufacturer's instructions (Superscript first strand cDNA synthesis kit, Life Technologies, CA). The cDNA was used as a template to amplify the *FRO3* sequence. Three truncated versions of *FRO3* (FRO3-FAD: amino acid 1- 420; FRO3-NADH: amino acid1- 452; FRO3-H7: 1-amino acid 350) were amplified from the template using a common forward primer with an additional *Kpn*I restriction site at its 5' end (5'ttGGTACCATGGCGGCGCGTGGTAGACTCGTGGT3'). Domain-specific reverse primers were designed with an additional *Spe*I site at their 5' end: *FRO3-FAD RP*: 5'ctACTAGTagaagaagaaccGGACCATTTGCCTTGGCTCT3', *FRO3-NADH RP*: 5'aaACTAGTagaagaagaaccTAGGTAATCAGTGGAAGCAGGG3', *FRO3-H7RP*: 5' ACTAGTagaagaagaaccATTGTTCCGCGACTGGAGA3'. The constructs were cloned into the *Kpn*I and *Spe*I sites of the pAVA-11C vector (kind gift from Dr. Maik Sommer, Goethe University, Germany). Other constructs with the marker proteins fused with N-terminal GFP (1^{st}-10 strands) (Cytoplasmic marker: pAVA-1-10, IMS marker: pAVA-1-10-Tim50, mitochondrial matrix marker: pAVA-1-10-F1ATPase) were also obtained from Sommer lab (Groß et al, 2011). The recombinant vectors were then transformed into *E. coli* (DH5α); subsequently they were purified using a Qiagen midiprep kit following the manufacturer's instructions (Qiagen, MD, USA).

Transformation of Onion Peel Cells by Biolistic Bombardment

1µg of the recombinant vector in which *FRO3* is fused with the C-terminal end of GFP was mixed with an equimolar concentration of each of the marker vectors fused with the N-terminal end of GFP. Plasmid mixtures were precipitated with ethanol and coated on 1.6 micron gold microcarriers (Bio-Rad, Hercules,CA,USA). The DNA-coated gold particles were used to prepare gold cartridges according to manufacturer's instructions.

The gold cartridges were used to transform onion peel epidermis via particle bombardment using the Helios Gene Gun System according to the manufacturer's instructions (Bio-Rad, Hercules, CA, USA). The transformed onion peel epidermis was allowed to recuperate in MS media for 8 hours in the dark before it was screened for fluorescence.

Subcellular Localization Studies

Root tissue of *35S-FRO3-GFP* lines was previously stained with MitoTracker Red and imaged using confocal microscopy by our collaborators at Dartmouth College. Transformed onion peel cells were stained with 150nM Mitotracker Orange (CMTMRos, Life technologies, Carlsbad, CA,USA) and visualized for fluorescence using a Zeiss LSM 700 meta confocal system. An argon laser at 488nm and 535nm provided the excitation for GFP and for the MitoTracker orange (CMTMRos), respectively. Emission of GFP was collected between 505nm and 530nm and emission of MitoTracker was collected between 585nm and 615nm. The images were analyzed using Zen lite 2011 (Zeiss microscopy).

Mitochondrial Extraction

Mitochondria were prepared from seedlings grown in either Gamborg's B5 media (Phytotechnology Laboratories, Shawnee Mission) or in Fe-sufficient or Fe-dropout 1/2X MS media for 2.5 weeks. A total of 40-50 g of tissue was ground using a blender in 100 ml of ice cold extraction buffer containing 0.3 M sucrose, 25 mM MOPS pH 7.5, 0.2% (w/v) BSA, 0.6% (w/v) polyvinyl-pyrrolidone 40, 2 mM EGTA and 4 mM L-cysteine. All procedures were carried out at 4°C. The extract was filtered through two layers of Miracloth and centrifuged at 6,500xg for 5 min. The supernatant was then further centrifuged at 18,000xg for 15 min. The pellet thus obtained was gently resuspended in extraction buffer and the aforementioned centrifugation steps were repeated. The resulting crude organelle pellet was resuspended and layered on a 32% (v/v) continuous percoll gradient solution (0.25M sucrose, 10mM MOPS, 1mM EDTA, 0.5% PVP-40, 0.1% BSA, 1mM glycine). The gradient was centrifuged at 40,000xg for 2 hours, 30 mins and the mitochondrial band, visible as a whitish/light-brown ring, was collected. The purified mitochondria were washed twice by resuspending in wash medium containing 0.3 M sucrose, 5 mM MOPS, followed by centrifugation at 18000xg for 15 min. The final mitochondrial pellet was resuspended in wash buffer containing 0.3M sucrose and 25mM MOPS (Branco-Price et al., 2005). Mitochondrial protein concentrations were determined using the BCA assay (Pierce).

To assess for the integrity of mitochondrial samples, cytochrome C oxidase assays were conducted on the isolated mitochondria using the cytochrome C oxidase kit (Sigma, St. Lois, MO) as suggested by the manufacturer. The purity of the preparation was

examined by probing the mitochondrial extracts against a mitochondrial marker antibody (α-SHMT) and a chloroplastic marker antibody [(α-PsbA; (Agrisera, Vännäs, Sweden)].

Enzymatic Assays

For the root ferric reductase activity, plants were grown on Gamborg's B5 media (Phytotechnology Laboratories, Shawnee Mission) for two weeks and then transferred to Fe sufficient (50µM Fe) and Fe deficient media (300µM ferrozine for three days) for the measurement of the reductase activity (Connolly et al., 2003). The roots of the intact seedlings were submerged in 300 µl assay solution comprised of 50µM Fe(III) EDTA and 300µM ferrozine and placed in the dark for 20 minutes. The absorbance of the assay solution was then measured at 562 nm and the activity was normalized to the fresh weight of the roots (Connolly et al., 2003). The activity of 10 biological replicates was averaged for each genotype for the assay. A student's t-test was used to perform the statistical analysis.

For mitochondrial preparations, 5µg of each sample was pre-incubated in 200 µl assay solution [1mM NADH, 1mM ATP, 10mM $MgCl_2$, 1mM **B**atho**P**henanthroline di**S**olfonic acid (BPS) (Sigma, St. Louis, MO)]. After incubation for 2 minutes at room temperature, the Fe(III) substrate was added to a final concentration of 150µM and the absorbance of the reaction was recorded every 20 seconds over 10 minutes at 535nm (Lesuisse et al., 1990). To prevent the photo-oxidation of NADH, the assay was conducted in the dark. The activity was expressed as the formation of µmol Fe(II)-BPS chelate complex using the molar extinction coefficient

22.13$mM^{-1}.cm^{-1}$. The experiment was repeated on five technical replicates to obtain the mean value. A student's t-test was used to perform the statistical analysis.

For copper (Cu) reductase assays on purified mitochondria, BPS was replaced by 1mM Na_2-2,9-dimethyl-4,7-diphenyl-1.10-bathophenanthrolinedisulfonic acid (BCDS; Sigma, St. Louis, MO) in the assay solution and 150µM CuSO4 was used as the substrate. The absorbance of the reaction was measured every 20 seconds over 10 minutes at 483nm. To prevent the photo-oxidation of NADH, the assay was conducted in the dark. The activity was expressed as the formation of µmol Cu(II)-BCDS chelate complex using the molar extinction coefficient 12.25$mM^{-1}.cm^{-1}$ The experiment was repeated on three technical replicates to obtain the mean value. (Welch et al., 1993;Robinson et al., 1999). A student's t-test was used to perform the statistical analysis.

Catalase enzyme assays on whole seedling extract were carried out as described by Maliandi et al, 2011 with minor modifications. The reduction in absorbance was measured at 300nm (Maliandi et al., 2011).

Elemental Analysis

For the plant tissue and seeds, separate biological replicates were analyzed in the Purdue University Ionomics Laboratory by Dr. David Salt at Purdue University (Lahner et al., 2003). For the mitochondrial preparations, three biological replicates were analyzed in the Trace Elemental Analysis Core Laboratory lab by Dr. Brian Jackson at Dartmouth College.

Protein Blot Analysis

Proteins were extracted and 25µg of the samples were separated by SDS-PAGE and transferred to **p**oly**v**inyl **dif**luride (PVDF; Fisher Scientific, Waltham, MA) membrane by electroblotting. Membranes were labeled with antibodies and chemiluminescence detection was carried out as described (Connolly et al., 2002). Western blot analysis for IRT1 was conducted as described (Connolly et al., 2002;Kerkeb et al., 2008). 25 µg of total protein extract and 2 µg of mitochondrial proteins were separated for aconitase antibody. Antibodies against aconitase were a kind gift from Dr. Janneke Balk (Luo et al., 2012).

Results

Subcellular Localization of FRO3

Previous data from our lab has shown that *FRO3* is expressed in both roots and shoots and that FRO3 is strongly induced under Fe deficiency (Mukherjee et al., 2006;Buckhout et al., 2009;Rodriguez-Celma et al., 2013b). GUS histochemical assay of *proFRO3-GUS* lines show that the gene is most strongly expressed in the vasculature of the plant (Mukherjee et al., 2006).

The first- 23 amino acids of FRO3 have been putatively determined to serve as mitochondrial signal peptide (ARAMEMNON). Additionally, phylogenetic studies have shown close homology of FRO3 with yeast mitochondrial FRE, FRE5. (Sickmann et al., 2003). To test the hypothesis that FRO3 is a mitochondrial FRO, our first objective was to confirm its subcellular localization. Root tissue of stable transgenic *35S-FRO3-GFP* lines generated by former graduate student, Indrani Mukherjee were co-stained with a

mitochondrial stain, Mitotracker Red and examined using a confocal microscope by our collaborators (Jeeyon Jeong and Mary Lou Guerinot, Dartmouth College). The resulting fluorescence images showed a punctate pattern of widely distributed GFP signal which colocalized with MitoTracker (Figure 2.1A-C). This data confirms that FRO3 is localized to the mitochondria.

Analysis of FRO3-Knockout (*fro3*) and RNAi (*FRO3-RNAi*) Lines

To study the role of FRO3 in metal homeostasis *in planta*, two types of loss-of-function lines were characterized. An insertion mutant of FRO3 was identified in No-*0* background with an insert in the last exon (Figure 2.2A). The precise location of the insert at position 2958 relative to position 1 of FRO3 ORF nucleotide sequence was determined via PCR and sequencing using gene specific primers and primers specific to the Basta resistance marker in the insert (Figure 2.2B). Additionally, *FRO3-RNAi* lines constructed by former graduate student (Indrani Mukherjee) were characterized to examine *fro3* phenotypes. Both the mutant lines (*fro3* and *FRO3-RNAi*) exhibit dramatically reduced transcript abundance as observed by qRT-PCR (Figure 2.3A, 2.3B) (figure from Indrani Mukherjee; Mukherjee, 2006).

Based on its subcellular localization, we hypothesized that FRO3 plays an essential role in Fe reduction and its acquisition at the mitochondrial surface. To investigate FRO3's role in Fe trafficking to mitochondria, we determined the elemental profile of *fro3* and *FRO3-RNAi* lines. Interestingly, *fro3* mutants exhibit small but significantly elevated levels of Fe in the shoot tissue (Figure 2.4A), while mitochondrial Fe levels were reduced by ~50% (Figure 2.5A, Figure 2.5B). In addition to altered Fe

levels, *fro3* mutants also harbor elevated Cu levels in their shoots (Figure 2.4B) and depleted Cu levels in their mitochondria (Figure 2.5 C, Figure 2.5D). These results are consistent with a role for FRO3 in the acquisition of mitochondrial Fe and Cu.

Loss of FRO3 affects Iron Homeostasis in Plants

Since metal content of the *fro3* mutants was significantly altered, we wanted to test the expression levels of various Fe homeostasis markers in *fro3*. Loss of FRO3 resulted in reduced mitochondrial Fe content but elevated whole shoot Fe content. These data promoted us to speculate that loss of FRO3 results in reduced mitochondrial Fe content, which, in turn, leads to up-regulation of the root Fe uptake machinery. To test this hypothesis, we measured root ferric reductase activity in WT, *fro3* and *FRO3-RNAi* mutant plants. In Fe-deficient conditions, the roots of both *fro3* and *FRO3-RNAi* lines show significantly enhanced ferric reductase activity as opposed to their corresponding WT (Figure 2.6A, Figure 2.6B). Similarly, increased abundance of IRT1 protein was observed in *fro3* and *FRO3-RNAi* mutants (Figure 2.6C). These data show that loss of FRO3 up-regulates the root surface Fe uptake machinery, which, in-turn, leads to elevated Fe levels in the shoots. We also measured the expression of a Fe storage gene (*FER1*) by semi quantitative RT-PCR. FER1 expression is known to be induced by increases in Fe content (Lescure et al., 1991). *FER1* expression was elevated in the roots and shoots of *fro3* mutants (Figure 2.6D), which is consistent with our observations of elevated levels of Fe in *fro3* mutant.

We also observed impaired Fe-dependent biochemical processes in the mitochondria of *fro3*. We measured the levels of a Fe-S cluster requiring protein, aconitase (ACO) (Figure

2.6E). Reduced ACO levels were observed in both the total as well as mitochondrial protein extract isolated from plants grown in Fe deficient conditions. Additionally, we determined the effect of loss of FRO3 on a heme-requiring protein, catalase (CAT). Three isoforms of catalase are found in a eukaryotic cell; While CAT1 and CAT2 can be found in the peroxisome, CAT3 localizes to mitochondria. A 60% reduction in total catalase activity was measured in *fro3* mutants grown in Fe-deficient conditions (Figure 2.6F). Mitochondria are believed to supply Fe-S clusters and possibly heme for cytosolic and nuclear demands. Thus, a reduction in the extra-mitochondrial proteins which depend on these cofactors is observed in the absence of FRO3. Together, these results indicate that in Fe deficient conditions, the absence of FRO3 limits the Fe content of the mitochondria, thus affecting the Fe-utilization pathways of *fro3* mitochondria.

FRO3 Functions as Mitochondrial Fe(III) Reductase

To test the function of FRO3 as a mitochondrial Fe(III) reductase, we isolated mitochondria from 2.5 week old seedlings of WT, *fro3* and *FRO3-RNAi* grown in Fe sufficient and Fe dropout MS media. The quality of mitochondrial preparations were investigated using a cytochrome C oxidase assay, which measured the integrity of the mitochondrial membranes. In addition, western blots were run using antibodies against mitochondrial (SHMT) and the chloroplastic marker (PsbA) to assess the purity of the samples. The mitochondrial preparations were highly intact (data not shown) with little to no chloroplast contamination (Figure 2.5E). Ferric reductase activity was measured on the surface of the isolated mitochondria. Interestingly, low basal activities were observed in Fe-sufficient conditions. However, a 3 fold induction was observed in the WT under Fe-deficiency while this induction was significantly reduced in *fro3* (Figure 2.7A).

Similar results were observed for *FRO3-RNAi* line, where the WT showed almost a two-fold induction under Fe-deficiency, while the knockout maintained the basal levels of activity (Figure 2.7B). We next wanted to test the hypothesis that FRO3 prefers a particular Fe(III)-complex over other Fe(III) sources. To test this, we assayed mitochondrial ferric reductase activity in the presence of several Fe substrates such as Fe(III)-EDTA (Connolly et al., 2003), Fe(III)-citrate, Fe(III)-NA (Schaaf et al., 2004), Fe(III)-ATP , Fe(III)-AMP (Weaver and Pollack, 1990;Weaver et al., 1990). The assay was carried out on the seedlings grown in Fe dropout MS media to induce general iron deficiency in plants, which in turn, induced FRO3 expression. Similar results were obtained with the various Fe substrates indicating that FRO3 does not distinguish between various Fe(III) substrates (data not shown).

A slight, non-significant reduction in activity was observed when we measured the cupric reductase activity in the mitochondria of the plants grown in Fe-dropout MS media (Figure 2.7C). Thus, more work is required to conclusively show if FRO3 functions similar to FRO2 and exhibits Fe deficiency-induced Cu reductase activity. Nevertheless, relatively high level of background was observed for surface reductase activity for both Fe and Cu. This activity could be due to the function of FRO8 or some other mitochondrially-localized reductase. These results clearly indicate that FRO3 functions as a mitochondrial surface metalloreductase and plays a significant role in mitochondrial Fe uptake.

Topology of FRO3

The aforementioned evidence suggests FRO3 functions as a reductase at the surface of mitochondria. To conclusively prove FRO3's role in mitochondrial iron acquisition, we set out to determine its membrane topology. FRO3 shares 60% homology with a previously characterized reductase - FRO2. Similar to FRO2, FRO3 has been predicted to possess 8-10 transmembrane (TM) helices, conserved FAD (HPFT) and NAD(P)H (GPYG) domains and four histidine residues (H232, H246, H306, H319) which are believed to anchor heme groups to the protein to facilitate the process of electron transfer [Figure 2.8A, Figure 2.8B; (Schagerlof et al., 2006)]. According to the model presented for FRO2, NAD(P)H is oxidized on the cytoplasmic side and the electrons are transferred via flavin and the two intramembraneous heme groups to ferric ions on the other side of the membrane for its reduction to Fe^{2+} (Schagerlof et al., 2006). For FRO3, there are several possible orientations that are consistent with our data. First, FRO3 could be oriented on the IMM with the FAD and NAD(P)H domains located in the matrix. Second, FRO3 could be oriented on the OMM with the FAD and NAD(P)H domains located in the cytosol. Or third, FRO3 could be oriented on OMM with the FAD and NAD(P)H domains located in the IMS.

Thus, in order to define the site of Fe(III) reduction we investigated the sub-mitochondrial localization of the FAD and NAD(P)H domains of FRO3. Additionally, we also investigated the localization of an extra domain (H7) present on the loop preceding the FAD and NADPH domains. To determine the intracellular membrane topology of FRO3 we used self-assembling GFP vectors (sa-GFP) vectors (Wiesemann et al., 2013). We constructed versions of FRO3 that were truncated at the FAD domain, the

NAD(P)H domain and at the loop preceding Helix 7 fused with C-terminal end of GFP. These constructs were co-transfected into onion peel epidermal cells with constructs in which the N-terminal end of GFP is fused with various markers specific for the different sub-compartments of the mitochondria. Targeting of both the proteins to the same compartment results in the assembly of GFP, which in-turn, results in green fluorescence in the cell (Figure 2.9). If the two co-transfected constructs encode proteins that targeted to different subcompartments, there will be no self-assembly of GFP and thus, no fluorescence will be observed. As controls, we first bombarded the matrix marker, F1-ATPase fused with N-terminal GFP by itself into the onion peel cells and no fluorescence was observed in the green channel (Figure 2.10A). Next, F1-ATPase fused with C-terminal GFP was co-transfected with the three different subcompartment markers into onion peel epidermal cells. Several fluorescent spots, colocalizing with mitochondria were observed only with the F1-ATPase marker suggesting the specificity and high efficiency of the technique (Figure 2.10B). Subsequently, the orientation of FRO3 on the mitochondrial membrane was determined. Both FAD and NAD(P)H constructs show fluorescence with the empty vector (N-terminal GFP remains in the cytosol) suggesting a cytosolic localization of the two domains (Figure 2.11A, Figure 2.11B). On the other hand, the H7 domain showed fluorescence with the IMS marker protein (Figure 2.11C). These results suggest that FRO3 is present on OMM and uses cytosolic electrons to reduce the ferric ion pool in the IMS of the mitochondria. Reduced IMS-localized Fe^{2+} may then be transported across the inner membrane of the mitochondria, perhaps by the MIT transporters. Furthermore, by sequence homology with the experimentally determined FRO2 topology (Schagerlof et al., 2006), FRO3 appears to possess 10 TM

helices with both its N-terminal and C-terminal located on the cytosolic side of the mitochondria.

fro3 shows developmental defects

The *fro3* mutant exhibits delayed flowering (Figure 2.12A) and a more robust development of the vegetative tissue as compared to WT, when germinated and grown in soil. The leaves and the stem of the mutant are bigger, thicker and darker green in color that the WT (Figure 2.12B). Infact, our former lab tech observed that *fro3* produces twice as many leaves in the rosette as produced by the WT (data not shown). Furthermore, *fro3* plants also display altered architecture (Figure 2.12C) with a significantly reduced number of branches and siliques in the soil grown mutants (Figure 2.12D). However, the number of seeds produced per plant and their Fe content is not significantly different from WT (Figure 2.12E, Figure 2.12F). These phenotypes indicate that while *fro3* reproduces normally, the transition from vegetative to reproductive phase is severely delayed. To study *fro3* phenotypes in Fe deficient growth conditions, we grew the mutants hydroponically in Fe dropout media. When grown in this media, initially, *fro3* displays a robust vegetative tissue, but later, it is evident that reproduction is severely compromised. In Fe deplete media, while the WT exhibits a shorter stature, and reduced seed content (as compared to when grown under Fe sufficient conditions) *fro3* produces a few small and shrunken siliques with no seeds (Figure 2.13A, Figure 2.13B). This phenotype is rescued by providing exogenous Fe [Fe(III)-EDDHA; (Figure 2.13C)]. Similar phenotypes were observed with *FRO3-RNAi* lines (Figure 2.14A, Figure 2.14B). This suggests that in Fe deplete conditions; FRO3 plays an indispensable role for

mitochondrial iron acquisition, which eventually results in proper growth, development and reproduction of the plants, especially under Fe deficient conditions.

Discussion

Members of the FRO family have been reported to function as metalloreductases with various localizations/functions in the plant. While most of the FROs are localized to the plasma membrane, a recent report showed that FRO7 serves as a Fe(III) reductase at the chloroplast surface (Jeong et al., 2008); none of the other intracellular reductases have been characterized to date. Targeting predictions suggest that FRO3 and FRO8 are localized to mitochondria; gene expression data and the spatio-temporal expression patterns (Wu et al., 2005;Mukherjee et al., 2006) of these two genes show that FRO3 is much more widely and ubiquitously expressed and thus may play a more predominant role in mitochondrial Fe homeostasis (Jain et al., 2014). In this study, we have characterized FRO3 which indeed functions as a metalloreductase to aid the import of Fe and Cu into the mitochondria, particularly under Fe-limiting conditions.

Loss of FRO3 Leads to Altered Iron Homeostasis

For this study, we and our collaborators confirmed the localization of FRO3 to the mitochondria in the roots of *Arabidopsis* (Figure 2.1). Loss of FRO3 results in reduced mitochondrial Fe content and elevated whole shoot Fe content, confirming FRO3's role in mitochondrial Fe acquisition (Figure2.4, Figure 2.5). Due to the loss FRO3, Fe-deficient mitochondria signal the plant to up-regulate Fe uptake at the roots which includes the up-regulation of *FRO2* and *IRT1* (Figure 2.6A-C). As a consequence of increased Fe uptake and accumulation, ferritin gene expression is also induced (include

ref for FER1 upregulation (Figure 2.6D). On the other hand, impaired Fe uptake by *fro3* mitochondria negatively affects the synthesis of Fe –S clusters and possibly heme groups in mitochondria. This results in reduced accumulation of an Fe-S cluster requiring protein (aconitase) in mitochondria as well as cytosol (Figure 2.6E). Furthermore, the activity of a heme-containing enzyme, catalase is also impaired in *fro3* (Figure 2.6F). The existence of heme biosynthetic pathways in plant mitochondria is controversial (Masuda et al., 2003); thus, this phenotype could be due to an indirect effect of altered mitochondrial Fe metabolism on chloroplast Fe homeostasis. Experiments in our lab have previously shown that the *fro3* mutant exhibits resistance to high light exposure (Mukherjee, 2006). Excessive light causes photo-oxidative stress which can be exacerbated in the presence of Fe by the production of ROS via the Fenton reaction (Noorjahan et al., 2005). The enhanced tolerance of high light displayed by fro3 supports the hypothesis that chloroplast Fe homeostasis is altered in *fro3*.

FRO3 Functions as a Mitochondrial Fe(III) Chelate Reductase

Elevated Fe content in *fro3* and reduced Fe accumulation in its mitochondria is indicative of a role for FRO3 in mitochondrial Fe acquisition. FRO3 belongs to a superfamily of flavocytochromes; the members of the ferric reductase clade of this superfamily (FREs and FROs) possess a heme-containing ferric reductase domain and an additional NAD(P)H/FAD containing domain (Zhang et al., 2013). These proteins are known to transfer electrons from NAD(P)H to ferric iron to reduce them to ferrous iron (Zhang et al., 2013). To examine the role of FRO3 as a ferric reductase responsible for mitochondrial Fe acquisition, we developed an assay to measure ferric reductase activity at the surface of intact mitochondria. In contrast to the ferric reductase activity assay at

the chloroplast surface, additional cofactors such as ATP and NADH were required to assay mitochondrial ferric reductase activity. ATP in the assay solution, helped to energize the mitochondria and create a membrane potential while NADH served as an electron donor for the reaction. Under Fe sufficient conditions, both WT and *fro3* mitochondria display low, background levels of ferric reductase activity. Under Fe-deficient conditions, while WT shows a strong induction of ferric reductase activity, *fro3* mitochondria maintain the basal levels of activity indicating its role as a surface mitochondrial reductase (Figure 2.7) . Several sources of ferric iron complexes such as Fe(III)-citrate, Fe(III)-NA, Fe(III)-EDTA, Fe(III)-ATP, Fe(III)-AMP were used to test for the substrate specificity of FRO3. However all the substrates yielded similar results with in the activity by mutant mitochondria. The high level of basal activity as observed in the mutant and WT is probably a result of either FRO8 activity or another reductase(s) that functions constitutively at the mitochondrial surface.

FRO3 is an OMM Protein and Likely Reduces a Fe(III) Pool in the IMS

To further substantiate the role of FRO3 as a mitochondrial ferric reductase and to identify the pools of ferric iron being reduced by FRO3, we set out to study the orientation and the precise localization of the protein. To achieve this goal, we used the HMMTOP predicted topology of FRO3 (http://proteinformatics.charite.de/rhythm/index.php?site=helix) [Figure 2.8; (Punta et al., 2007)] and the self-assembling GFP technique [Figure 2.9; (Wiesemann et al., 2013)] to study the suborganellar localization and orientation on the mitochondrial membrane. The members of FRO family are thought to transfer electron from cytosolic donors (NAD(P)H) to FAD and then through two consecutive heme groups to the electron

acceptors (ferric ions) at the other side of the membrane. Using the sa-GFP technology, we showed that the NAD(P)H and FAD domains are located on the cytosolic side of the membrane while the preceding soluble domain was found in the IMS (Figure 2.11). This suggested that FRO3 was located at the OMM with its catalytic, ferric reductase domain localizing to the IMS. The OMM is typically enriched in β-barrel proteins, so whether it can place/accommodate such a large polytopic integral membrane protein with 8-10 TM helices, was our next concern.

The origin of the OMM has been a controversial topic for over a decade now; whether it is a remnant of the eukaryotic endosomal membrane or the outer membrane of gram-negative bacteria is still an open question. The resemblance of its lipid composition with a eukaryotic membrane supports the endosomal theory (Alberts et al., 2002). Conversely, some researchers believe for it to be of the prokaryotic origin (Cavalier-Smith, 1987). It has been reasoned that the outer membrane of gram negative bacteria was an integral part of its energy production pathway that became important for the host cell. Thus, they suggest that it is unreasonable to believe that the outer membrane in the modern day mitochondria is a result of endocytosis (Morgan et al., 2012). Nevertheless, its proteome is believed to be a chimera with both prokaryotic and a eukaryotic-derived components. Thus, as opposed to the outer membrane of gram-negative bacteria, which is primarily composed of B-barrel proteins, the OMM of plants harbors several proteins that are comprised of multiple TM-spanning domains; these proteins are involved in trafficking, signaling, metabolism and maintenance of membrane morphology (Duncan et al.;Duncan et al., 2011). Thus, our data, which support the OMM localization FRO3, are

supported by previous report of OMM localizations for other polytopic TM spanning proteins.

The endosymbiotic theory for mitochondrial evolution supports the aforementioned orientation of FRO3, according to which the membrane containing the epidermal ferric reductase formed the endocytotic vescicle to engulf a proteobacterium to form a mitochondria. This rendered the NAD(P)H and FAD domain on the cytosolic side of the membrane and the catalytic site for the reduction of ferric ions in the IMS. The high sequence homology (62% identity, 72% similarity) between FRO2 and FRO3 further supports this orientation. In contrast, the sub-organellar localization of chloroplastic FRO7 is different from our results. FRO7 was recently placed on inner chloroplast envelope; it was hypothesized that FRO7 reduces ferric iron in the IMS (Solti et al., 2014). It is important to note that FRO3 is more closely related to FRO2 than it is to FRO7 (Mukherjee et al., 2006); FRO3 and FRO7 share a lower sequence homology (~30%). The fact that *in vitro* chloroplastic ferric reductase activity assays work in the absence of an electron donor corroborates the reported orientation of FRO7 (or corroborates the stromal orientation of the NAD(P)H domain of FRO7) (Jeong et al., 2008). However the requirement for external NADH for mitochondrial ferric reductase activity assays, supports the cytosolic orientation of the NAD(P)H domain of FRO3 (Figure 2.11).

FRO3 Plays Important Role in Cu Transport in *Arabidopsis*

While *FRO3* expression has been previously shown to respond to the Cu status of the plant, (Mukherjee et al., 2006;Yamasaki et al., 2009) in this work we have reported

that FRO3 does not appear to be capable of Cu reduction (Figure 2.7C). The importance of cross-talk between Fe and Cu in maintenance of cellular metal homeostasis is an emerging area of research. In times of nutrient depletion, plants feature the use of alternate cofactor by switching the enzymes to carry out the same biochemical reaction [such as Cu/Zn superoxide dismutase (Cu/ZnSOD) vs FeSOD]. The first evidence of this interplay between Fe and Cu homeostasis was provided when anemia in rats was rescued by Cu fortification (Hart et al., 1928; Klevay, 1997). Similarly, Fe uptake in yeast is mediated, in part, by a multicopper ferroxidase, FET3 (Askwith et al., 1994;Dancis et al., 1994). Such a direct connection in plants was first demonstrated in C. *reinhardtii*, in which the Cu containing plastocyanin is replaced by the haem-containing cytochrome c_6 (Quinn and Merchant, 1995;Kropat et al., 2005). While several studies have indicated a switch to Fe cofactors during Cu deficiency, recent work has also suggested the potential for Fe deficiency-induced Cu reduction by FRO2 (Robinson et al., 1999). While Cu uptake by FRO2 was found to be physiologically irrelevant (Connolly et al., 2003), FRO3-mediated Cu uptake in mitochondria may play significant roles in the cofactor switch. Indeed, we showed here that *fro3* mutants show alterations in Cu content (Figure 2.4B). Regulation of FRO3 by SPL7, the master regulator of Cu-homeostasis genes, supports the importance of FRO3 in Cu metabolism (Yamasaki et al., 2009), however, further studies are required to characterize the significance of FRO3 in Cu uptake and metabolism.

FRO3 is Essential for Growth, Development and Reproduction of *Arabidopsis*

In addition to the molecular phenotypes, *fro3* exhibits several developmental defects (Figure 2.12). Just like many other mitochondrial mutants (Han et al.,

2010;Nechushtai et al., 2012) , *fro3* exhibits delayed flowering time. The robust appearance of the vegetative tissue along with the delayed transition into reproductive growth appears to be a consequence of altered mitochondrial metabolism and perhaps inefficient nutrient distribution within the plant. Similarly, altered plant architecture with significantly reduced number of branches and siliques suggests an impaired translocation of nutrients from source to sink tissues. Despite this, the total amount of seeds produced and the nutrient content of the seeds in *fro3* did not differ from the WT when plants were grown in standard soil.

Fe deficiency has been reported to induce auxin production in plants (Römheld and Marschner, 1981), which is responsible for the phenomenon of apical dominance (Wickson and Thimann, 1958). Loss of FRO3 results in altered Fe homeostasis which induces the Fe deficiency response in the plant and thus may induce the production of hormones such as auxin. An increase in auxin production in the plant may be responsible for the apical dominance exhibited by *fro3* mutants. This effect is more pronounced when the plants are grown hydroponically in Fe drop-out nutrient solution (Figure 2.12, Figure 2.13). Under Fe limitation, the *fro3* mutant produces very few branches and siliques, and fails to produce any seeds. Thus, while FRO3 seems to be important for maintaining Fe homeostasis under normal conditions its role is indispensable for seed production in Fe-limiting conditions.

Conclusion

FRO3 is expressed most highly in the vasculature of young seedlings and its expression is strongly induced under iron deficiency; for this reason, *FRO3* has been

widely used as an iron deficiency marker (Mukherjee et al., 2006; Tarantino et al., 2010). Interestingly, *FRO3* expression is negatively regulated by the basic helix-loop-helix (bHLH) transcription factor PYE and positively by another bHLH transcription factor-bHLH101 (Sivitz et al., 2012). Whereas PYE appears to control a pericycle-specific Fe deficiency response in roots (Dinneny et al., 2008; Long et al., 2010), bHLH101 has been recently discovered to regulate the genes involved in Fe distribution in the plant (Sivitz et al., 2012). Thus, it is tempting to speculate that this co-expression/regulatory network might be indicative of a role of FRO3 in long distance signaling in addition to its intracellular iron transport (Figure 2.15).

Taken together, we show that FRO3 localizes to the OMM and likely reduces an IMS-localized pool of ferric iron to facilitate its import into the matrix (Figure 2.16). Additional work is required to investigate whether it works in tandem with mitochondrial iron transporters located on the IMM. Based on the current understanding of its regulatory network and its co-expression with other genes (NAS4, ZIF1, OPT3) involved in Fe sensing and Fe distribution, it appears to play important roles in Fe signaling and Fe translocation; however, further work will be required to investigate its role in these processes. Nevertheless, FRO3 is absolutely essential for proper development and seed production under Fe-limiting conditions.

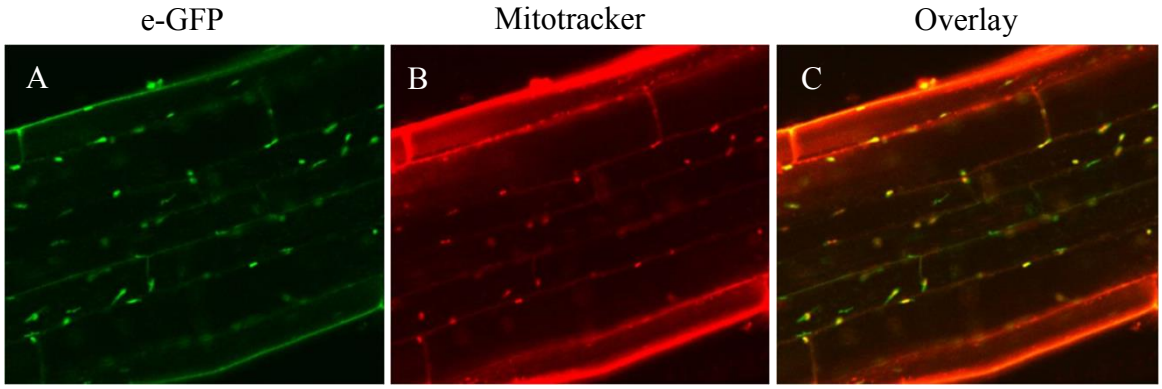

Figure 2.1: Mitochondrial localization of FRO3. Confocal optical Z-sections of root tissues of *35S-FRO3-GFP* plants co stained with MitoTracker observed in (A) green channel (B) red channel to produce the (C) merged image showing mitochondrial localization of FRO3.

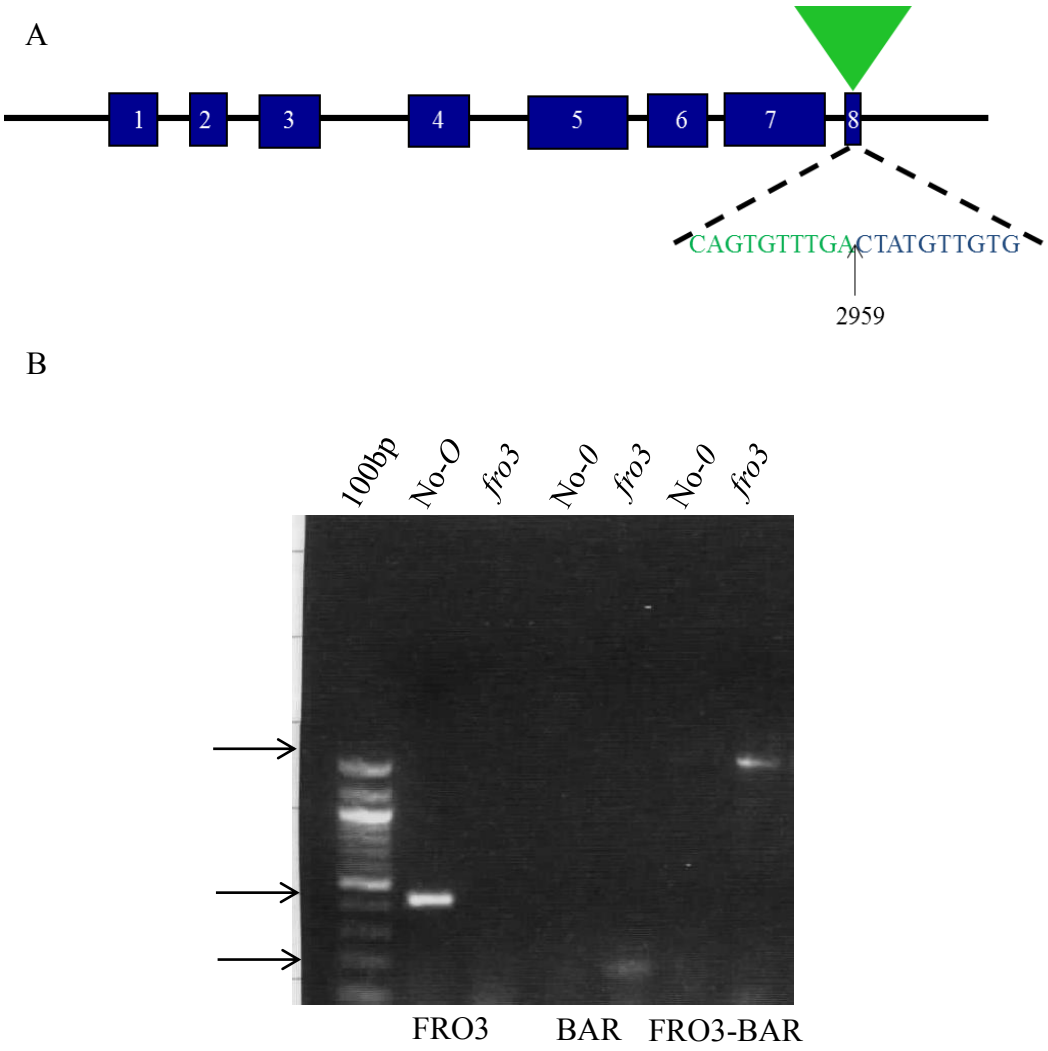

Figure 2.2: Genetic analysis of *fro3* mutants. (A) Gene structure of *fro3* insertion mutant. 8 exons (blue boxes) are interspersed by 7 introns (black line) The green triangle represents the insertion in the last exon. (Adapted from Mukherjee, 2006) (B) Determination of the insertion site in *fro3* mutant by genotyping. Top panel depicts the genotypes and the bottom panels characterize the amplicon obtained in the PCR.

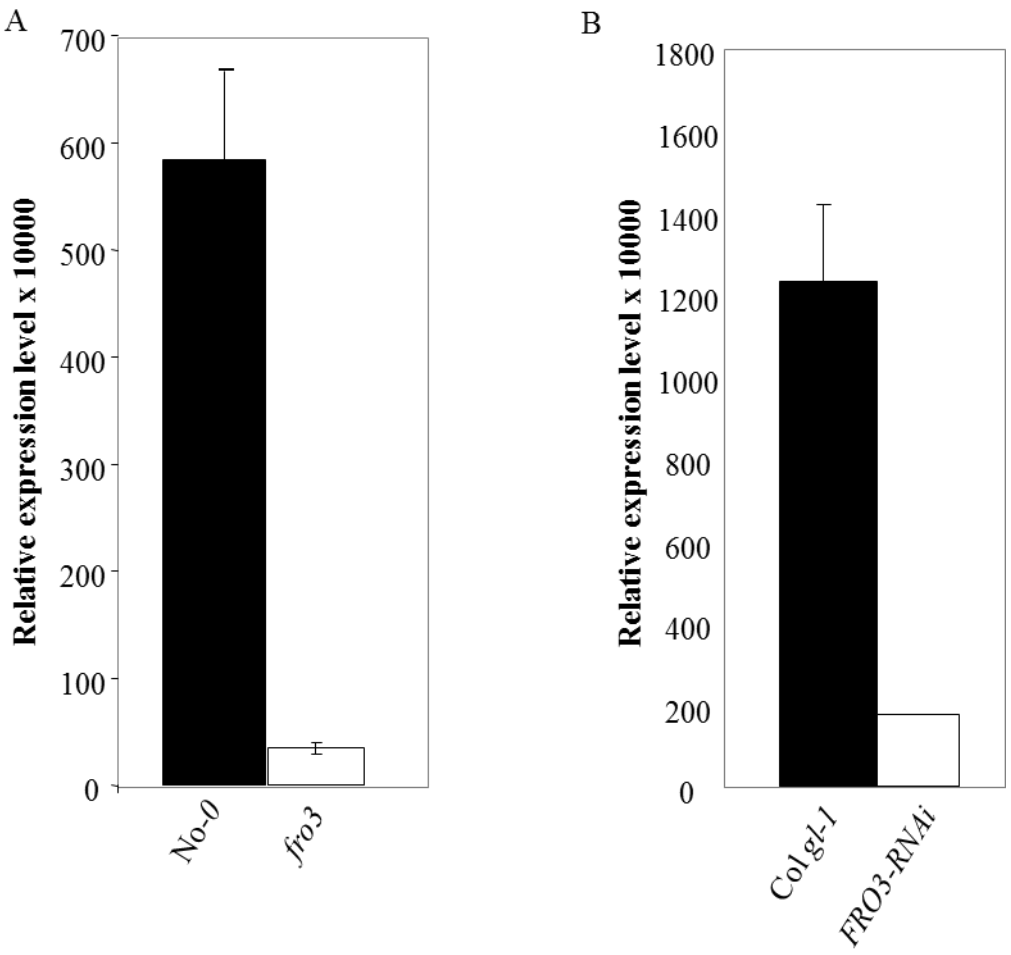

Figure 2.3: *FRO3* transcript abundance in *fro3* and *FRO3-RNAi* lines. Quantitative PCR analysis was conducted on the RNA obtained from the roots of (A) *fro3* and (B) *FRO3-RNAi* lines. The plants were grown in B5 media for 2-weeks and then transferred to ferrozine plates for additional 3 days. Ubiquitin was used as a control. (Adapted from Mukherjee, 2006)

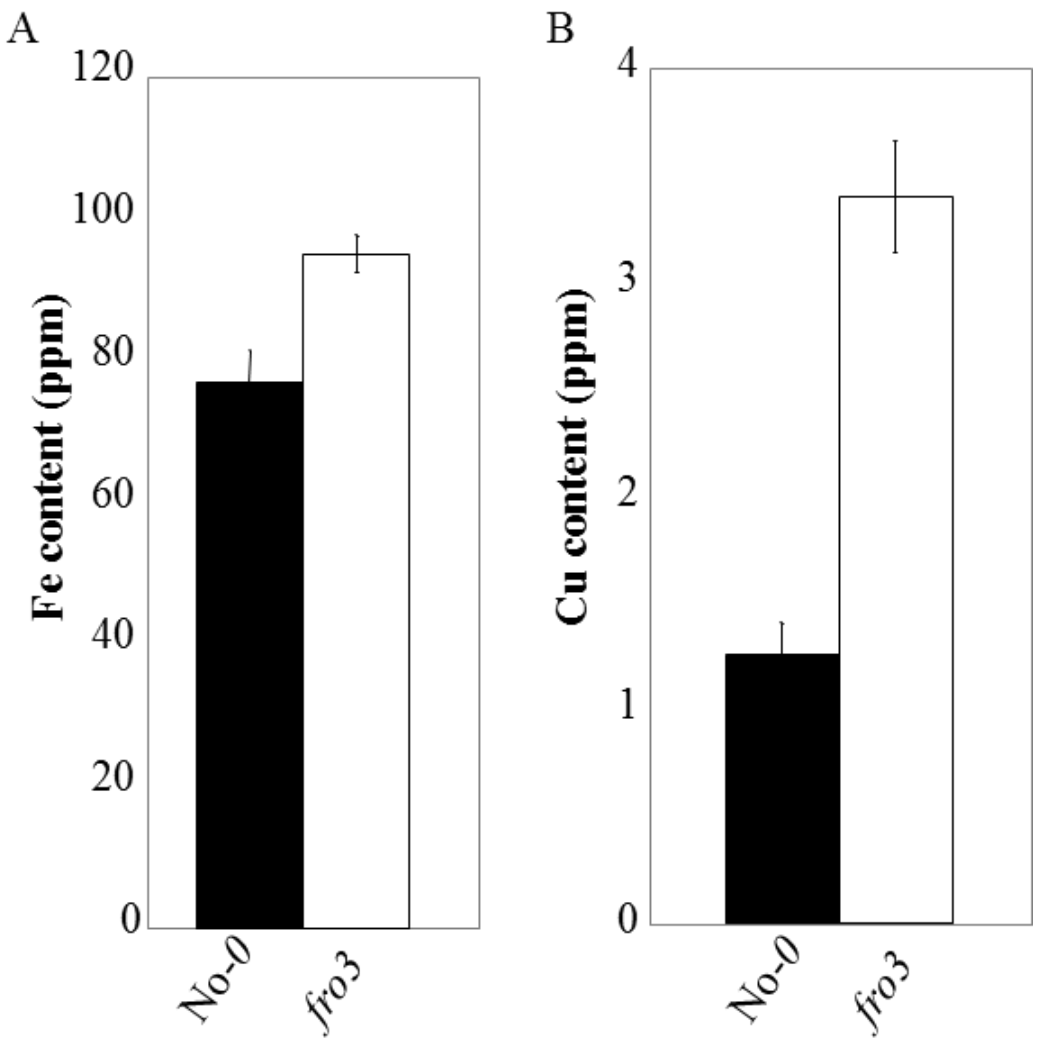

Figure 2.4: ICP-elemental analysis of WT and *fro3* mutant. The aerial part of the plants frown in soil was harvested and analyzed for (A) Fe content and (B) Cu content in the shoots. The graphs represent an average of approximately 20 plants and the error bars represent the standard error.
ppm indicates parts per million. Adapted from Mukherjee, 2006

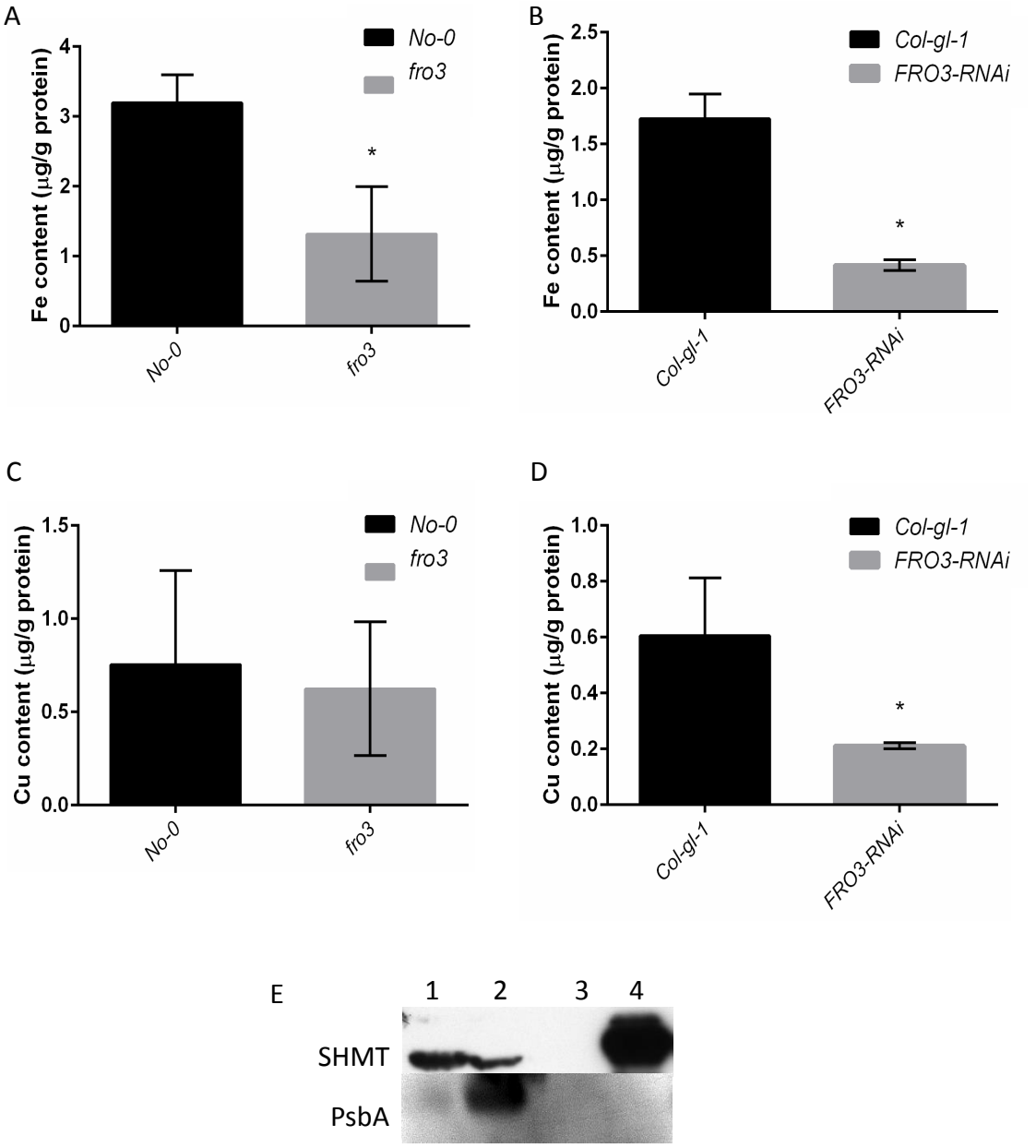

Figure 2.5: Mitochondrial ICP elemental analysis. Fe content in the total mitochondria extracted from (A) WT and *fro3* (B) WT and *FRO3-RNAi*. Cu content in the total mitochondria extracted from (C) WT and *fro3* (D) WT and *FRO3-RNAi*. (E) Western blot to assess the purity of the isolated mitochondria using anti SHMT (mitochondrial matrix marker), anti-PsbA (chloroplast marker. Lane1- Total plant extract, Lane 2. Crude mitochondrial pellet, Lane 3- Crude mitochondrial supernantant, Lane4- Purified mitochondrial pellet. The plants were grown for 2 weeks in B5 media. The bars represent the average of three technical replicates; error bars represent standard error)

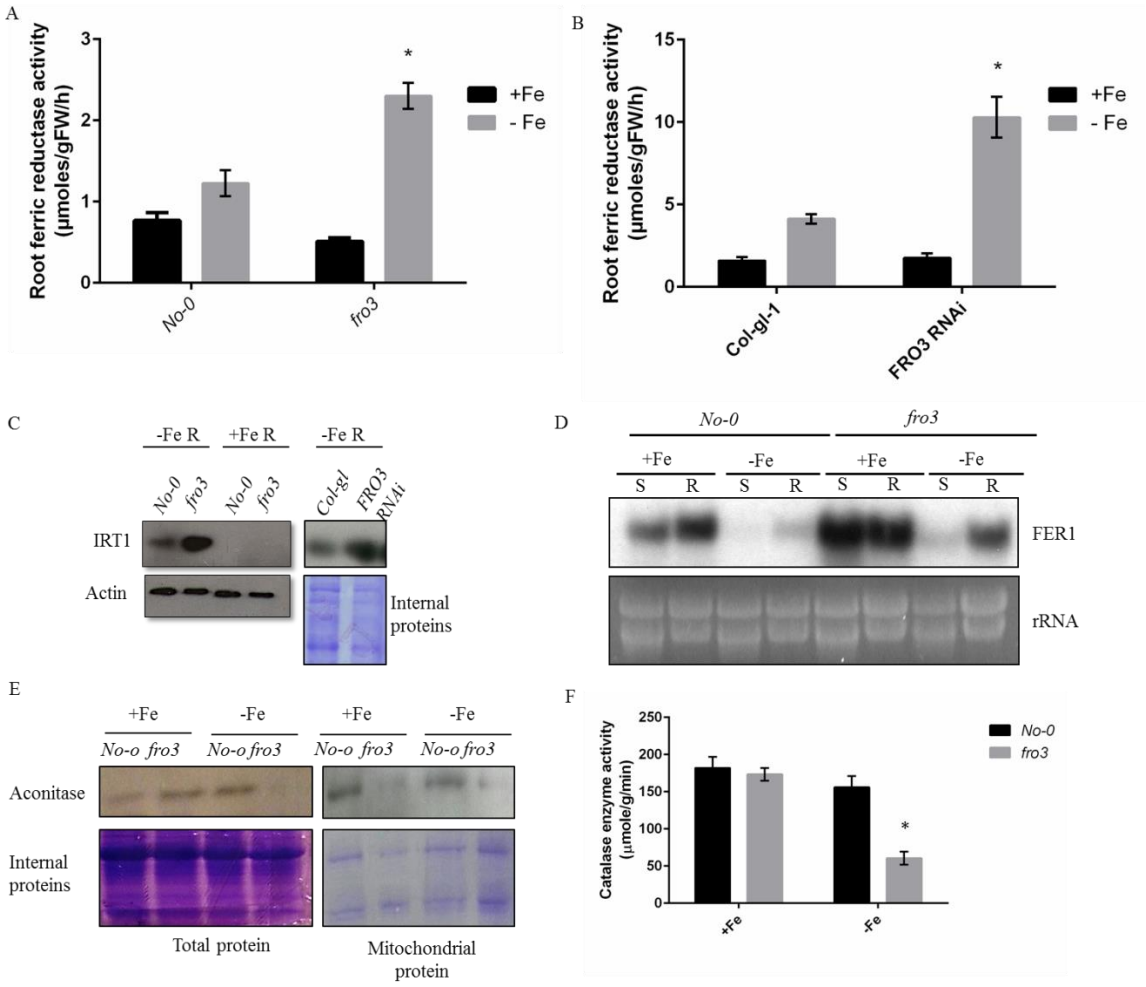

Figure 2-6: Loss of FRO3 leads to altered iron homeostasis in plants. Root ferric reductase activity in Fe-sufficient and Fe-deficient seedlings in (A) WT and *fro3* mutants, (B) WT and *FRO3-RNAi* mutants. (C) IRT1 protein levels in Fe-sufficient and Fe-deficient roots. (D) Ferritin1 transcript levels. (E) Levels of aconitase in total and mitochondrial protein extract (F) Enzymatic activity of catalase in WT and *fro3* . The plants were grown in B5 media for 2 weeks and then transferred to Fe-sufficient/Fe-deficient media for 3 days. The graphs represent an average of approximately 10 biological replicates and the error bars represent the standard error. S: Shoots; R: Roots

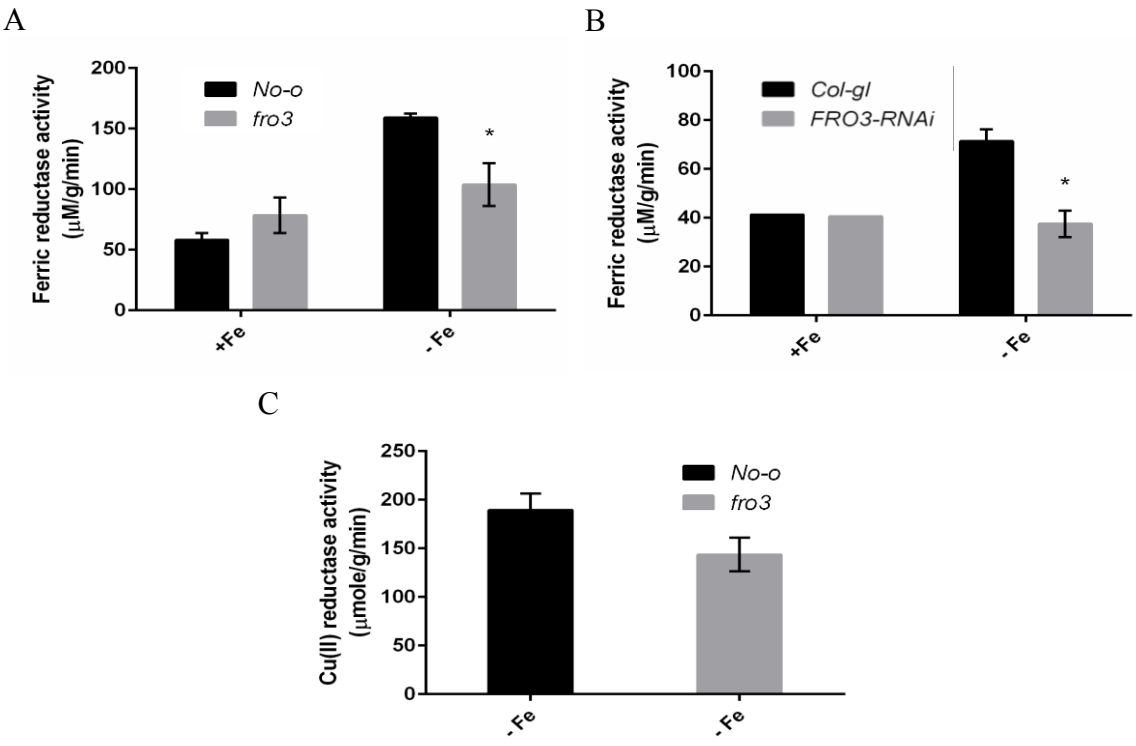

Figure 2.7: Analysis of mitochondrial surface reductase activity. Ferric reductase activity on (A) WT, *fro3* (B) WT, *FRO3-RNAi*. (C) Cupric reductase activity on WT, *fro3*. Loss of FRO3 leads to altered iron homeostasis in plants. The plants were grown for 17 days in either Fe-replete or Fe-deplete MS media. The graphs represent an average of approximately 4 technical replicates and the error bars represent the standard error.

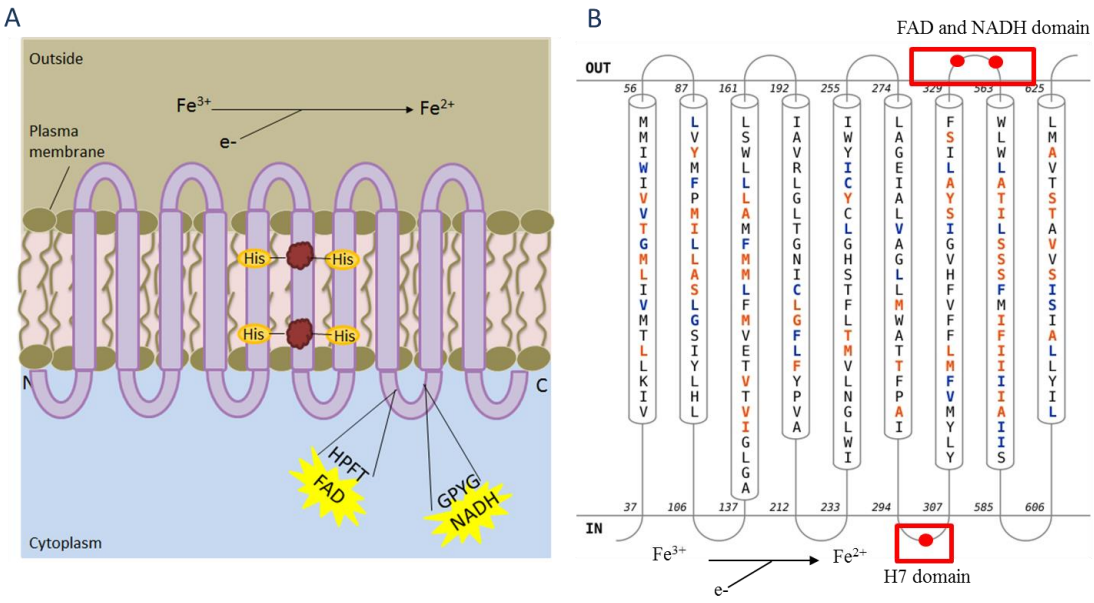

Figure 2.8: Predicted membrane topology of (A) FRO2; Adapted from Buchanan, Gruissem and Jones, 2002. (B) FRO3 (Topology determined using HMMTOP software- http://proteinformatics.charite.de/rhythm/index.php?site=helix)

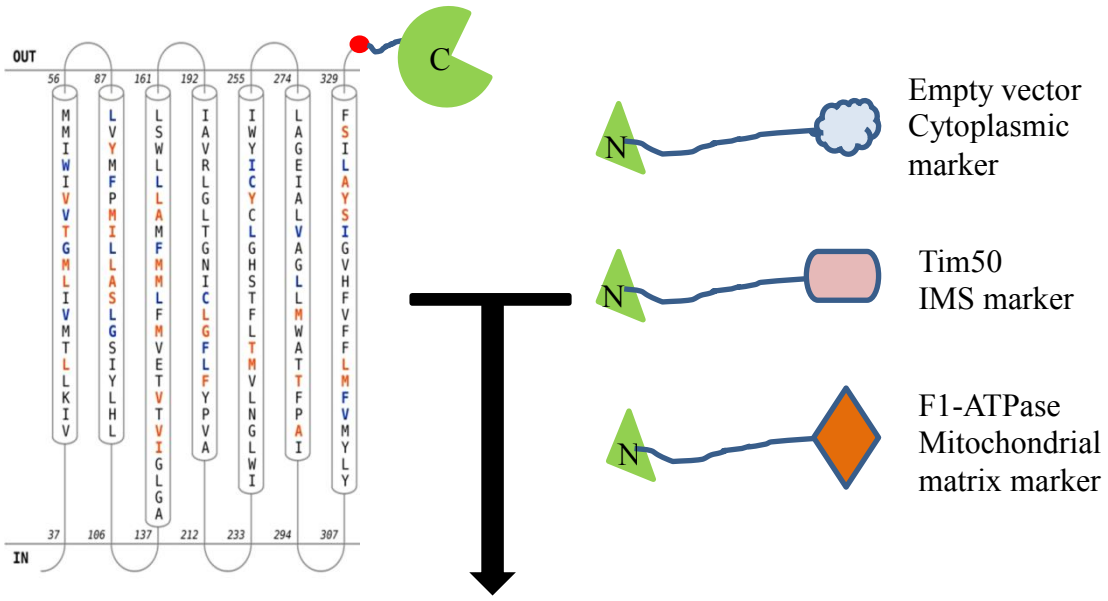

Figure 2.9: Schematic diagram representing the methodology used for the determination of the membrane topology of FRO3 by self-assembling GFP (sa-GFP). Truncated versions of FRO3 fused with C-terminal end of GFP were co-transfected with markers specific for the different sub-compartments of the mitochondria fused with N-terminal end of GFP in onion peel epidermis. Targeting of both the proteins to the same compartment results in the assembly of GFP; which in-turn results in green fluorescence in the cell.

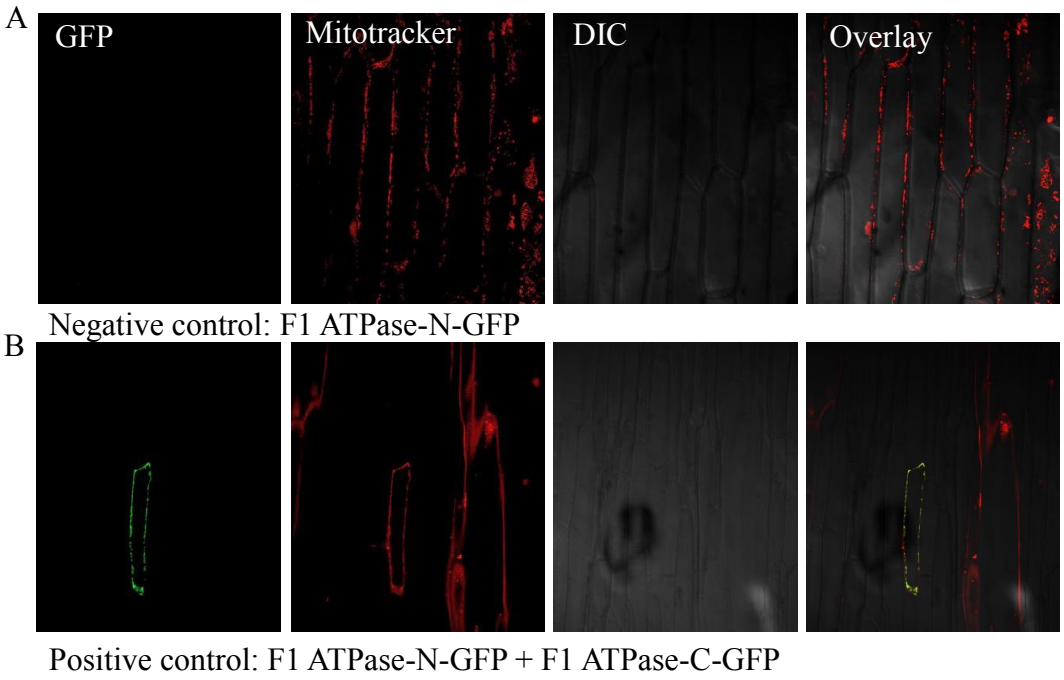

Figure 2.10*:* Confocal images of the controls used in sa-GFP technique. Matrix targeted F1-ATPase fused with N-terminus of GFP was (A) transfected alone and (B) co-transfected with the matrix targeted F1-ATPase fused to C-terminus of GFP. Targeting of both constructs into the same compartment results in fluorescent signal. Mitotracker stains for mitochondria in the cell.

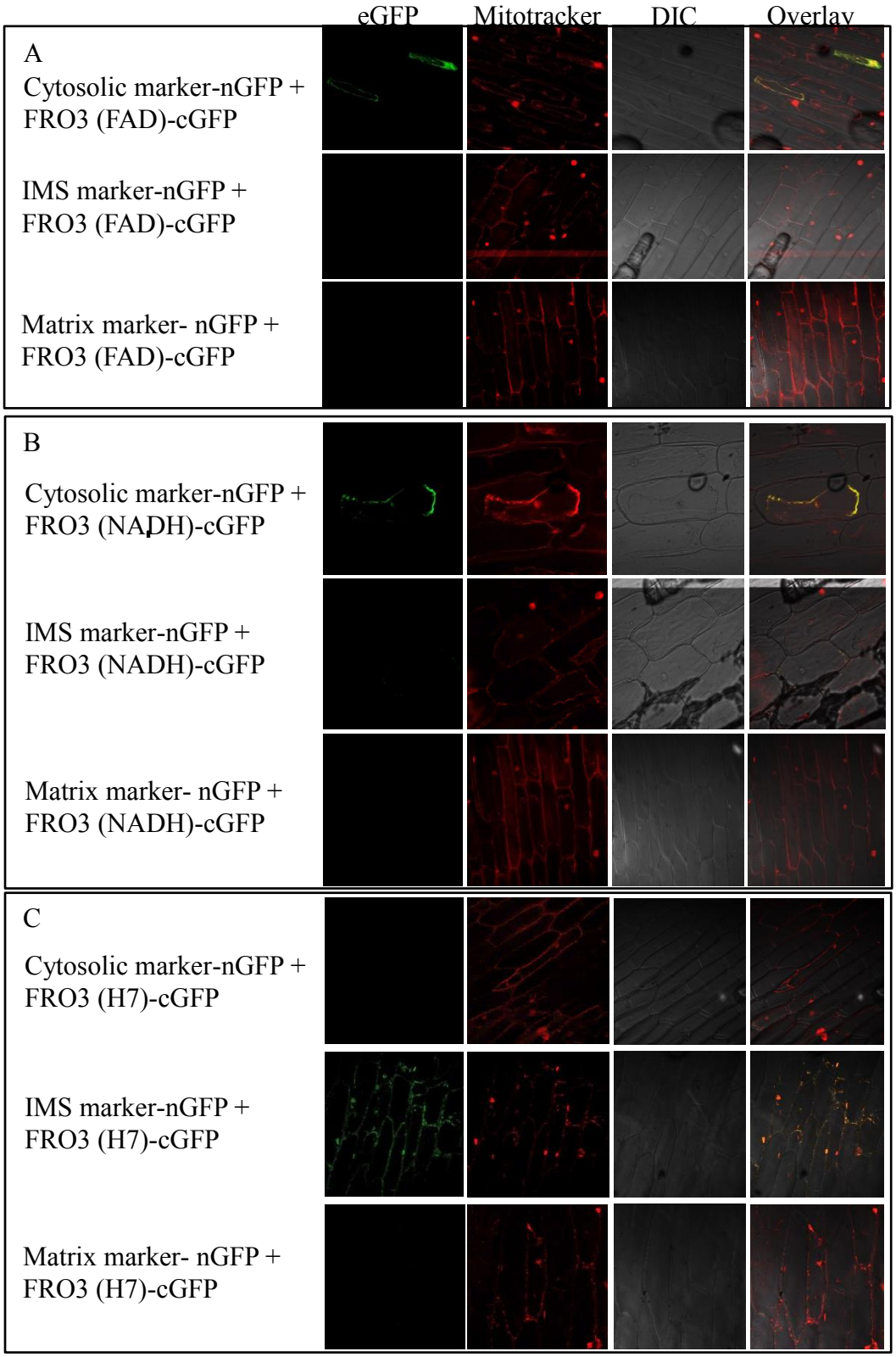

Figure 2.11: Determination of FRO3 topology by sa-GFP. FRO3 protein truncated at a) the FAD domain, b) the NADH domain and c) the end of Helix7 and fused with C-terminal half of GFP, co-transfected with constructs in which N-terminus GFP is fused with various markers specific for mitochondrial sub-compartments.

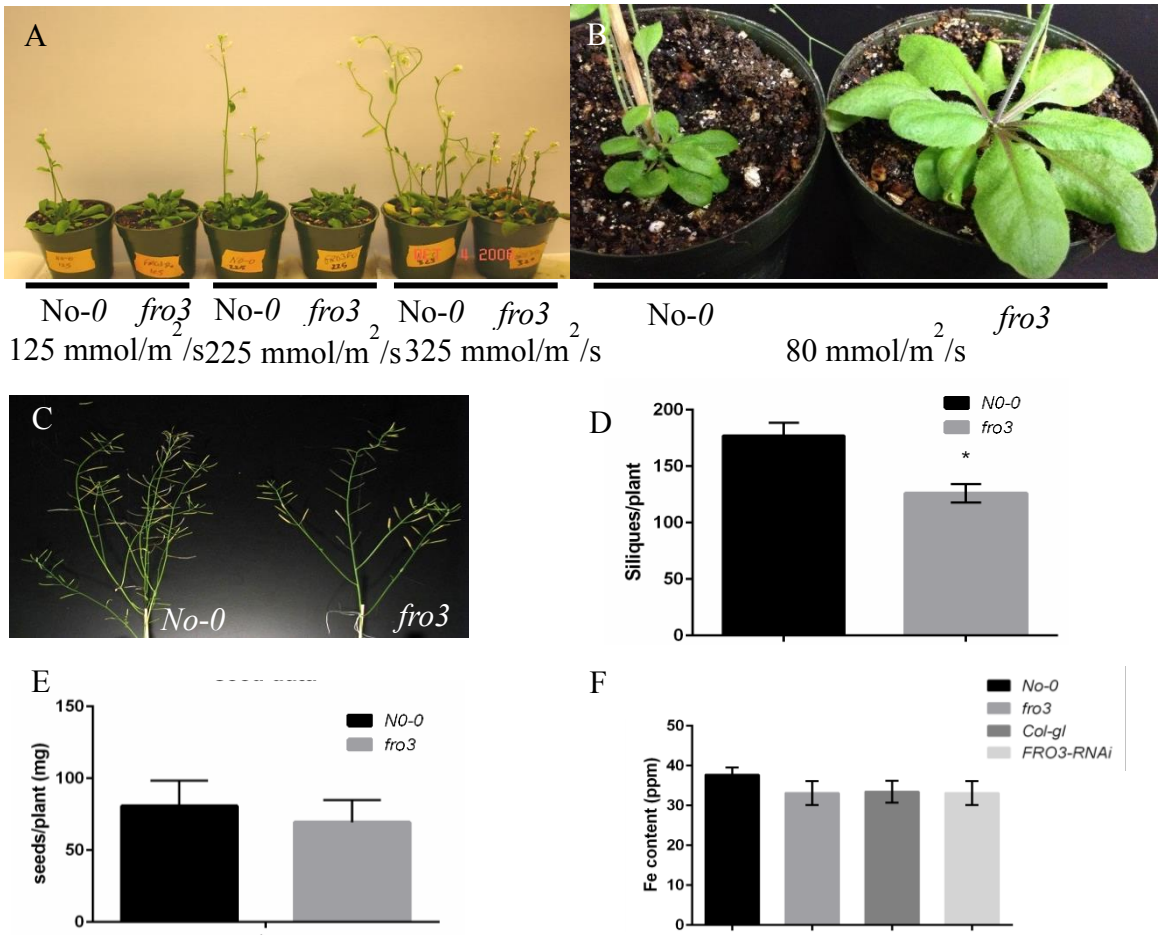

Figure 2.12: *fro3* phenotypes. (A) Late flowering phenotype of *fro3* in different light in three different light intensities. (B) Altered leaf and stem morphology in *fro3*. (C) Altered plant architecture. (D) Number of siliques per plant. (E) Seed weight per plant. (F) Fe-content measured in seeds by ICP-MS. The bars represent an average of approximately 12 plants grown in soil under standard light intensity of 80 mmol/m^2/s. The error bars indicate standard error.

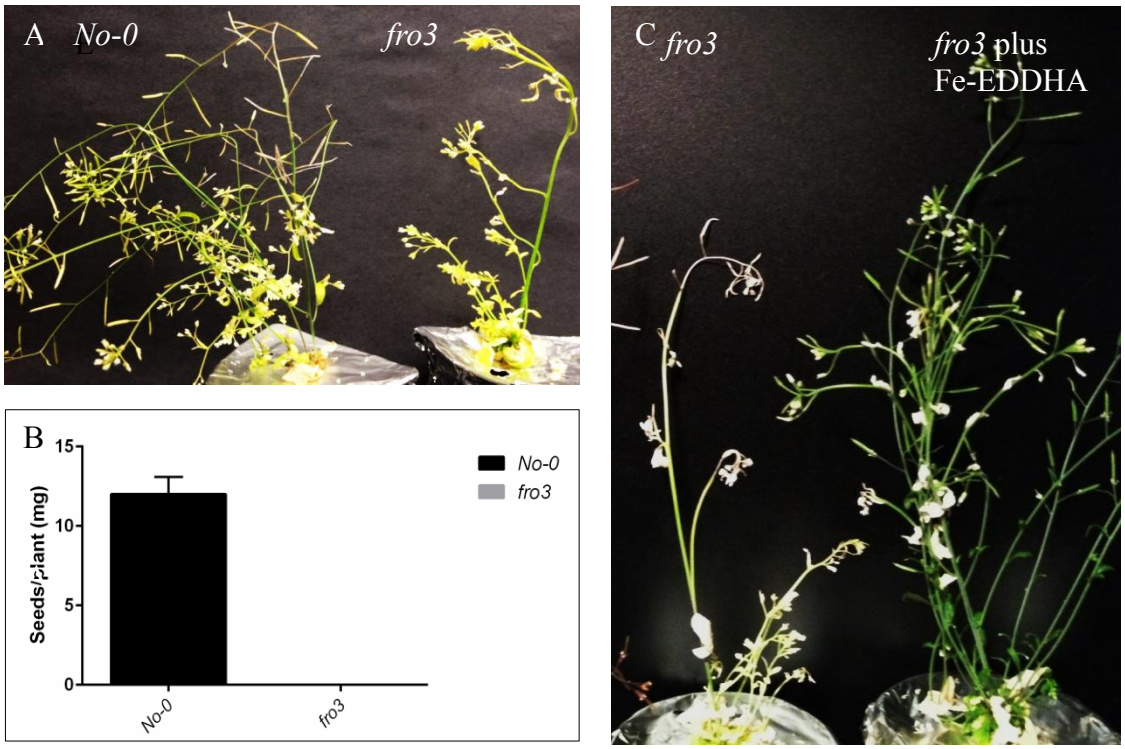

Figure 2.13: *fro3* phenotypes in Fe-limited conditions. (A) Altered plant architecture. (B) Reduced seed production in *fro3*. (C) *fro3* phenotype can be rescued by supplementing with soluble iron.

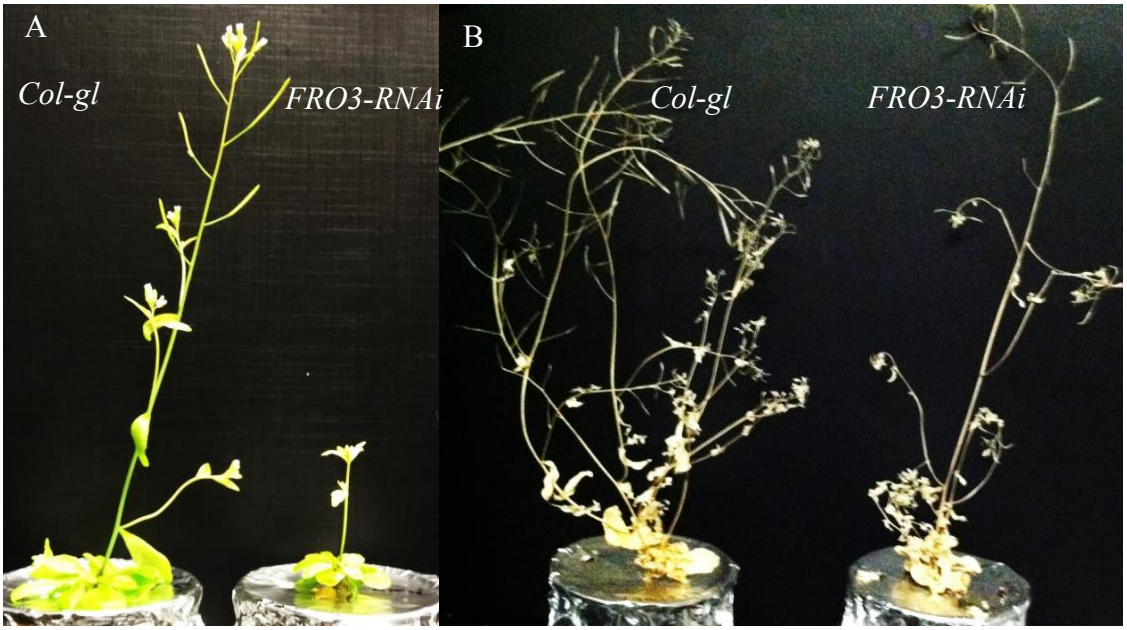

Figure 2.14: Altered plant architecture of *FRO3-RNAi* lines in Fe-limited conditions. (A) Growth phenotype at 35 day stage (B) Growth phenotype at 70 day stage

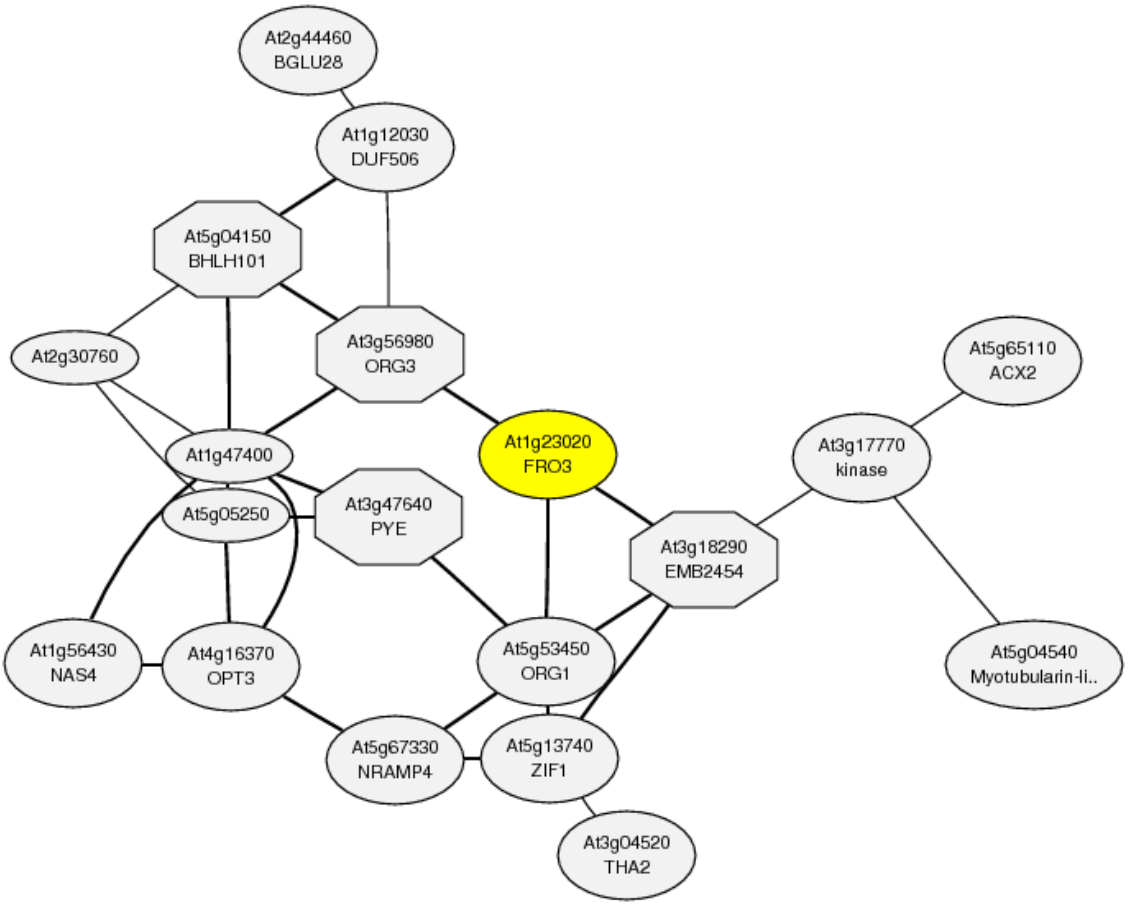

Figure 2.15: Regulatory network of FRO3
Adapted from http://atted.jp/cgi-bin/locus.cgi?loc=At1g23020

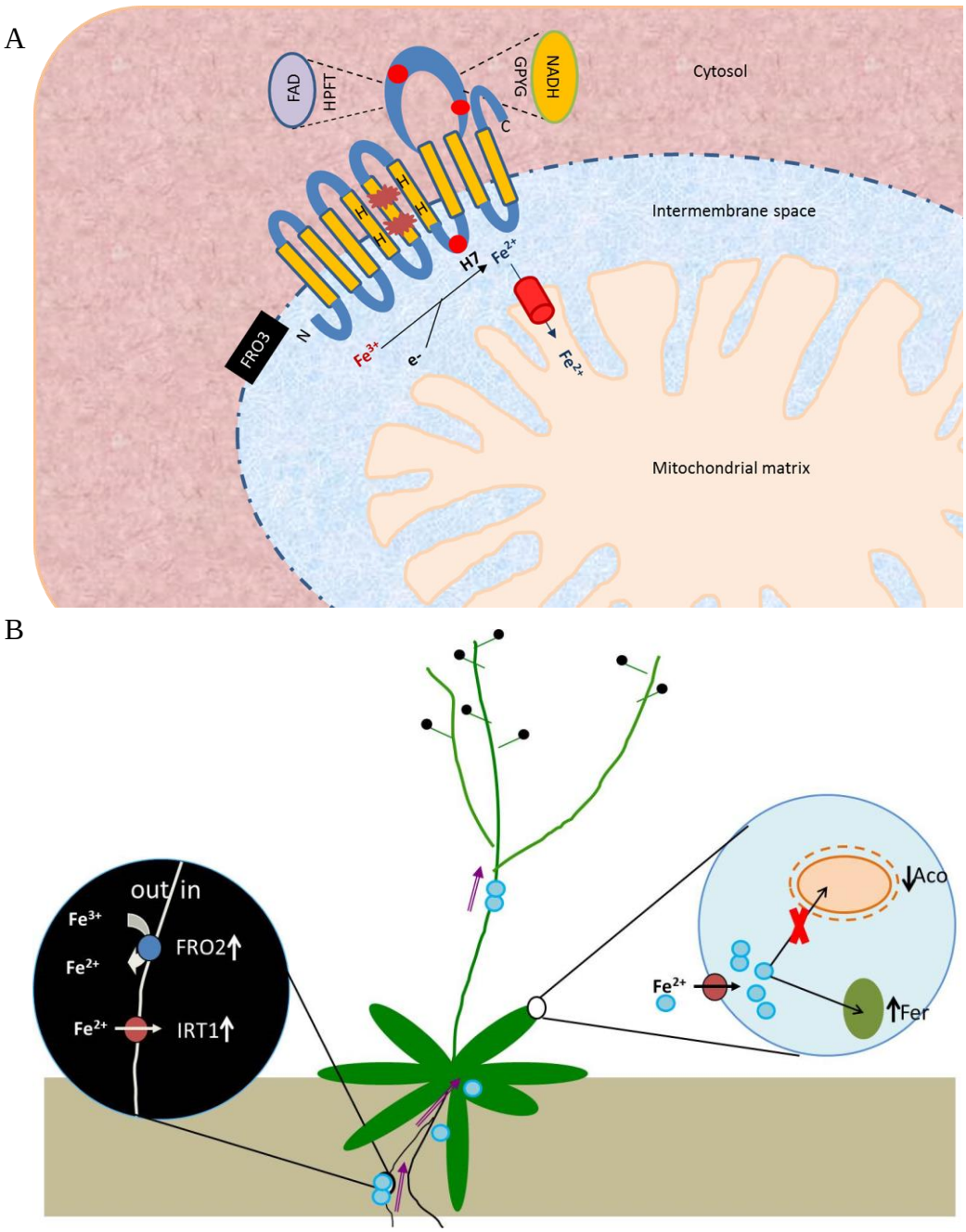

Figure 2-18: FRO3 is important to maintain Fe homeostasis in *Arabidopsis*. A) Membrane topology of FRO3 in the outer mitochondrial membrane. Our data are consistent with a model in which FRO3 reduces a ferric iron pool in the IMS that is subsequently transported into the matrix via MIT1 and MIT2. B) Loss of *FRO3* results in reduced mitochondrial Fe content and accumulation of ferritin in the chloroplast. Mis-localization of Fe in *fro3* results in up-regulation of the Fe uptake machinery at the root surface.

Chapter 3

Mitochondrial Iron Transporters, MIT1 and MIT2 are Essential for Embryogenesis in *Arabidopsis thaliana*

Abstract

Iron plays important roles for various biochemical processes in cells. It is particularly important as a cofactor for the enzymes required in respiration and photosynthesis. Thus, Fe trafficking into these subcellular organelles is imperative for the proper function of plants. While several reports have shed light on the mechanisms involved in Fe transport into the chloroplast, our understanding of mitochondrial iron transport is incomplete. Here, we report the identification of two *Arabidopsis* genes (*MIT1 and MIT2*) that belong to the **M**itochondrial **C**arrier **F**amily (MCF) and display considerable homology with mitochondrial Fe transporters of yeast and zebrafish. *proMIT1/2-GUS* lines analyses show that *MIT1/2* are expressed throughout the plant. MIT1 and MIT2 partially rescue the phenotype of a yeast *mrs3/4* mutant that is defective in mitochondrial iron transport. Although the *Arabidopsis mit* single mutants do not show any significant phenotypes, the double mutant *mit1mit2* displays embryo lethality. Analysis of a *mit1/mit1, MIT2/mit2* line has revealed that MIT1 and MIT2 are essential for iron acquisition and proper mitochondrial function. The loss of MITs results in reduced Fe accumulation in the

mitochondria which results in the upregulation of the Fe uptake machinery in the roots. Thus, in this chapter, we show that MIT1 and MIT2 are required for maintaining mitochondrial and whole plant Fe homeostasis, which in turn, is important for the proper growth and development of the plant.

Introduction

Iron (Fe) is an essential element that is required for numerous biochemical processes in cells. Due to its ability to accept and donate electrons, it functions as a part of redox centers where it serves as a cofactor for various enzymes. Mitochondria, which house the respiratory complexes of the cell, have a high Fe requirement. Various respiratory complex subunits utilize Fe (Fe-S clusters, heme and/or non-heme iron) as their cofactors (Philpott and Ryu, 2014). Mitochondria are also believed to be sites for biosynthesis of Fe-S clusters and heme groups (in addition to chloroplasts in plants) (Yoon and Cowan, 2004;Balk and Pilon, 2011). Despite its importance, subcellular trafficking of iron to/from the mitochondria is not fully understood. While Fe export out of the mitochondria is an open question in all living systems, several pathways have been reported for iron import in the literature.

Yeast mitoferrins, MRS3 and MRS4 (**M**itochondrial **R**NA **S**plicing proteins) were first shown to function in mitochondrial iron uptake (Foury and Roganti, 2002). These high affinity iron transporters were shown to transport ferrous ions across the mitochondrial inner membrane during iron limitation, in a pH and concentration dependent manner (Froschauer et al., 2009b). Using overexpression lines, the accumulation of Fe, heme and Fe-S clusters in yeast mitochondria were shown to be

directly proportional to the expression levels of *MRS3* and *MRS4* (Foury and Roganti, 2002;Muhlenhoff et al., 2003). Subsequently, homologs of yeast mitoferrins were identified in zebrafish (Shaw et al., 2006;Paradkar et al., 2009), Drosophila (Metzendorf et al., 2009) and rice (Bashir et al., 2011). The *frascatii* (*mfrn1*) mutant identified in zebrafish displays impaired heme synthesis which leads to severe defects in erythropoiesis, which, in turn, results in the death of the embryo (Shaw et al., 2006). Mfrn1 and a related protein Mfrn2 are responsible for Fe transport in the mitochondria of nonerythroid cells as well (Paradkar et al., 2009). Similarly, Drosophila Mitoferrin (Dmfrn) was shown to be essential for mitochondrial Fe import and loss of Dmfrn affects spermatogenesis and causes male sterility (Metzendorf et al., 2009).

Recently a mitoferrin ortholog, **M**itochondrial **I**ron **T**ransporter (MIT), responsible for mitochondrial iron acquisition was identified in rice (Bashir et al., 2011). While *mit* knockout mutants were embryo lethal, the knock-down mutants exhibited a poor growth phenotype, reduced mitochondrial Fe content and increased total Fe content in the shoots, indicating mislocalization of Fe in cells. In addition, the expression level of the gene encoding for the **V**acuolar **I**ron **T**ransporter1 (*VIT1*) was up-regulated in the *mit* mutant, which likely directed excess cytosolic Fe into the vacuole (Bashir et al., 2011). Thus, the mutants for mitoferrins in each of these species exhibited severely retarded growth and/or embryo lethal phenotypes, underscoring the importance of proper Fe import to the mitochondria (Muhlenhoff et al., 2003;Shaw et al., 2006;Paradkar et al., 2009;Bashir et al., 2011).

Arabidopsis is an important model organism for genetic studies in dicot plants. Like all other dicots and non-grass monocots, *Arabidopsis* follows strategy I for Fe

acquisition from the soil (Guerinot and Yi, 1994). At the root surface, Fe uptake is facilitated by a group of three proteins. A root plasma membrane proton pump, AHA2 (**A**rabidopsis **H**$^{+}$ **A**TPase) acidifies the rhizosphere via proton extrusion (Santi and Schmidt, 2009b). Soluble ferric iron chelates are then reduced by **F**erric **R**eductase **O**xidase 2 [FRO2; (Robinson et al., 1999;Connolly et al., 2003)], to ferrous iron, which is subsequently taken up across the plasma membrane of root cells via IRT1 [**I**ron **R**egulated **T**ransporter; (Eide et al., 1996;Yi and Guerinot, 1996;Robinson et al., 1999;Vert et al., 2002;Santi and Schmidt, 2009b)]. Following uptake from soil, iron must be shuttled into various organelles for specific biochemical purposes. While the mechanisms involved in delivery of Fe to subcellular compartments are not yet completely clear, a few key players involved in subcellular Fe trafficking have been reported in *Arabidopsis*. Relative to the proteins involved in Fe transport into chloroplasts (Duy et al., 2007;Jeong et al., 2008) and vacuoles (Lanquar et al., 2005;Kim et al., 2006), very little is known about delivery of Fe to mitochondria in *Arabidopsis*.

Here we report the first mitochondrial Fe transporters in dicots. In this study we cloned and characterized two mitochondrial iron transporters (MIT1 and MIT2) from *Arabidopsis* and demonstrate their importance for mitochondrial iron acquisition. Loss of MIT1 and MIT2 results in impaired mitochondrial functions as evidenced by the changes in the relative abundance of various respiratory subunits and aconitase (ACO) levels. Our results also show that MIT1 and MIT2 function redundantly and are essential for embryogenesis.

Materials and Methods

Plant lines and Plant growth conditions

Wild type *Arabidopsis* (Col-0 or Col-*gl-1*) was used as a control in all the experiments. T-DNA insertion mutants (SALK_013388 for MIT1 and SALK_096697 for MIT2) were obtained from the **A**rabidopsis **B**iological **R**esearch **C**enter (ABRC). *mit1mit2* double mutant was generated using artificial microRNA technology (Schwab et al., 2006). The seeds were surface sterilized with 25% bleach and 0.02% SDS. After thorough washes, the seeds were imbibed in the dark for 2 days at 4°C. The plants were grown on Gamborg's B5 media (Phytotechnology Laboratories, Shawnee Mission) supplemented with 2% sucrose, 1mM MES and 0.6% agar, pH 5.8 for 2 weeks under constant light (80mmol/m^{-2}/s^{-2}) at 22°C. The plants were grown in Metro-Mix 360: perlite:vermiculite (5:1:1) in 16 h days or hydroponically in the constant light (media replaced weekly). The composition of the hydroponics nutrient solution was as follows: 0.75 mM K_2SO_4, 0.1 mM KH_2PO_4, 2.0 mM $Ca(NO_3)_2$, 0.65 mM $MgSO_4$, 0.05 mM KCl, 10 μM H_3BO_3, 1 μM $MnSO_4$, 0.05 μM $ZnSO_4$, 0.05 μM $CuSO_4$, 0.005 μM $(NH_4)_6Mo_7O_{24}$, with 0 or 50 μM Fe(III)-EDTA (Kerkeb et al., 2008). To induce iron deficiency in plants, the plants were either transferred from B5 media to FerroZine [3-(2-pyridyl)-5,6-diphenyl-1,2,4 triazine sulfonate] for three days or they were grown on 1/2X MS media without iron for 17 days.

Cloning

For the generation of 35S-MIT1/2.YFP constructs, the full length cDNAs for *MIT1* and *MIT2*, already cloned in an entry vector (D-TOPO, Invitrogen) were ordered

from **T**he **A**rabidopsis **I**nformation **R**esource (TAIR). In order to obtain MIT-YFP fusion constructs, full length CDS without the stop codon of *MIT1* and *MIT2* were amplified using gene specific primers (MIT1: 5'- CACCATGGCAACAGAAGCAACAACC-3', MIT1 RP: 5'- AGCTGCGTTTGCTTCACCATTGAG-3', MIT2 FP: 5'- CACCATGGCTACGGAGGCTACAAC-3', MIT2 RP: 5'- GGCAGAGTTTGAATCGACATTGAAG-3'). The amplicons thus obtained were subcloned into pENTER/D-TOPO and further transformed in pEARLY Gateway101 (Gateway cloning, Life Technologies, Carsbald, CA). The recombinant destination vectors isolated using Qaigen miniprep kit following the manufacturers' instruction (Qiagen, MD) were then transformed in *Agrobacterium tumefaciencs GV3101* using standard cloning techniques (Koncz and Schell, 1986).

Primers were designed to amplify a 1.5 kb region upstream of *MIT1* and a 0.75 kb region upstream of *MIT2* from the genomic DNA
(pMIT1 FP: 5'-GGTACCCTTTAGTTTAACCGCCGCAT-3',
pMIT1 RP: 5'-GAATTCTTTCTCTATCAATGCAAACCAGAA-3',
pMIT2 FP: 5'- GGTACCTTGTGGAAGAAAGATCAAATCTTG-3',
pMIT2 RP: 5'- GAATTCATCATCAACACAAACCTGGAAA-3'). pMIT1 was cloned into *HindIII* and *EcoRI* sites and similarly pMIT2 was cloned into *HindIII/BamH1*sites of pCAMBIA1381Xa. These clones were further transformed into *Agrobacterium GV3101*. A positive *Agrobacterium* colony was screened and used to transform wild type *Arabidopsis* (Col *gl*-1) using floral dip protocol (Clough and Bent, 1998).

Artificial microRNA lines for *mit1mit2* were using the Web MicroRNA Designer (Schwab et al., 2006) and transformed as previously published (Bernal et al., 2012). The

targeting microRNA (TATATAGTAGCGAAAACGCCG) was chosen by the website and following primers were designed for its amplification from the plant:mit1/2miR-sense:5'GATATATAGTAGCGAAAACGCCGTCTCTCTTTTGTATTCC3', mit1/2miR-antisense: 5'GACGGCGTTTTCGCTACTATATATCAAAGAGAATCAATGA3', mit1/2miR*sense:5'GACGACGTTTTCGCTTCTATATTTCACAGGTCGTGATATG3', mit1/2miR*antisense: 5'GAAATATAGAAGCGAAAACGTCGTCTACATATATATTCCT3'. The fragment was amplified by overlapping PCR using a template plasmid (pRS300), a kind gift from Dr. Detlef Weigel [http://www.weigelworld.org; (Schwab et al., 2006)]. The amplicon was further cloned into the *Not*1 and *Xho*1 sites of pBARN (LeClere and Bartel, 2001).

For the yeast complementation assay, *MIT1*, *MIT2* cDNAs were amplified from *Col-0* cDNA and cloned into *BamHI* and *XhoI* sites of pRS426 (a kind gift from Dr. Jerry Kaplan) using following sets of primers. MIT1 FP: 5'-CGCGGATCCATGGTAGAAAACTCGTCGAGTAATAATTCAACAAGGCCAATTCCAGCAATACCTATGGATCTACCCTTTCATCCAGCAATCATCGTT-3', MIT1 RP: 5'-CCGCTCGAGTTATCACTTGTCATCGTCATCCTTGTAATCACCACCAGCTGCGTTTGCTTCACCATT -3', MIT2 FP: 5'-CGCGGATCCATGGTAGAAAACTCGTCGAGTAATAATTCAACAAGGCCAATTCCAGCAATACCTATGGATCTACCCCCGGATTTCAAACCGGAAATC-3', MIT2 RP: 5'-

CCGCTCGAGTTATCACTTGTCATCGTCATCCTTGTAATCACCACCGGCAGTGT TTGAATCGACATT -3’

Subcellular localization

The Agrobacterium cultures of 35S-MIT1-YFP and 35S-MIT2-YFP were transformed into the onion peel epidermis as described (Sun et al., 2007) . The transformed onion peels were rinsed with water and stained with 150nM mitoTracker orange (CMTMRos, Life technologies, Carsbald, CA). The fluorescent images were screened using Zeiss LSM 700 meta confocal system. An argon laser at 488nm provided the excitation for YFP and 535nm for the mitotracker orange (CMTMRos). Emission of YFP was collected between 505 and 530nm and emission of mitotracker was collected between 585nm and 615nm. Zen lite 2011 was used to analyze the fluorescent images.

GUS histochemical staining

2 weeks old seedlings of the homozygous T4 generation were used for GUS histochemical staining using X-Gluc (5-bromo-4-chloro-3-indonyl B-D-glucoronide; Thermo Scientific, Waltham, MA) as a substrate as described in (Jefferson et al., 1987;Divol et al., 2013) . The staining was performed on five independent lines and a representative line (N5E for MIT1 and M12A for MIT2 were chosen for the further experiments).

RNA isolation and Transcript analysis

Total RNA was extracted from 100mg frozen tissue of two-week old seedlings grown on standard Gamborg’s B5 media using TRIzol reagent (Sigma, St. Lois, MO).

DNAse1 (New England Biolabs, Ipswich, MA) was conducted on 3.5µg of the total RNA for 15 minutes. Superscript First strand Synthesis system (Life Technologies, Carsbald, CA) was used to prepare the cDNA from total RNA according to the manufacturer's instructions (Mukherjee et al., 2006). Quantitative real-time PCR was performed as described (Fraga et al., 2008). Gene-specific primers are as follows: MIT1 FP: 5'-AGACGCAGTTGCAATGTCAG-3', MIT1 RP: 5'- AGCCATCCTCTAGCAAGTCCT-3', MIT2 FP: 5'-CGCTTGATGTTGTCAAGACG-3', MIT2 RP: 5'-AGGAGCATGGAAGAGCATTCT-3', Actin FP: 5'-CCTTTGTTGCTGTTGACTACGA-3', Actin RP: 5'-GAACAAGACTTCTGGGCATCT-3'. Semi-quantitative PCR was performed using the primers to amplify the full length CDS of the specific gene. The primer sequence is as follows. MIT1: 5'- CACCATGGCAACAGAAGCAACAACC-3', MIT1 RP: 5'-AGCTGCGTTTGCTTCACCATTGAG-3', MIT2 FP: 5'-ATGGCTACGGAGGCTACAAC-3', MIT2 RP: 5'-GGCAGAGTTTGAATCGACATTGAAG-3'

Yeast complementation assay

The primers were designed to substitute the first- 22 amino acids with the yeast MRS3 amino acids adding the yeast leader peptide to the clones. Δ*mrs3*Δ*mrs4* mutant yeast was transformed with empty vector (pRS426) or the vector containing the *MRS4* ORF or the vector containing *AtMIT1* or *AtMIT2* (Pan et al., 2004). The yeast strains were grown on synthetic defined (SD-URA) medium as described (Li and Kaplan 2004). Yeast strains were grown in liquid SD-URA medium, and serial dilutions were prepared

(OD600) as 0.1, 0.01 and 0.001 and plated onto SD-URA plates. The plates were incubated at 30 °C for 4 days.

Ferric reductase assay

For the ferric reductase activity, plants were grown on Gamborg's B5 media for two weeks and then transferred to Fe sufficient (50µM Fe) and Fe deficient media supplemented with 300µM ferrozine for three days (Connolly et al., 2003). For the measurement of the reductase activity, the roots of the intact seedlings were submerged in 300 µl assay solution comprising 50µM Fe(III) EDTA and 300µM ferrozine and placed in the dark for 20 minutes. The absorbance of the assay solution was then measured at 562nm and the activity was normalized to the fresh weight of the roots (Robinson et al., 1999;Connolly et al., 2003). The activity of 10 biological replicates was averaged for each genotype for the assay. A student's t-test was used to perform the statistical analysis.

Mitochondrial fractionation and purification

Mitochondria were prepared from seedlings grown in Fe dropout MS media for 2.0 weeks. A total of 40-50 g of tissue was ground in 100 ml of ice-cold extraction buffer containing 0.3M sucrose, 25mM MOPS pH 7.5, 0.2% (w/v) BSA, 0.6% (w/v) polyvinyl-pyrrolidone 40, 2mM EGTA and 4mM L-cysteine. All procedures were carried out at 4°C. The extract was filtered through two layers of Miracloth and centrifuged at 6500xg for 5 min. The supernatant was then further centrifuged at 18000xg for 15 min. The pellet thus obtained, was gently resuspended in extraction buffer and the aforementioned centrifugation steps were repeated again. The resulting crude organelle pellet was purified and resuspended and layed on a 32% (v/v) continuous percoll gradient solution

(0.25M sucrose, 10mM MOPS, 1mM EDTA, 0.5% PVP-40, 0.1% BSA, 1mM glycine). The gradient was centrifuged at 40,000xg for 2 hours 30 mins and the mitochondria, visible as a whitish/light-brown ring, were collected. The purified mitochondria were washed twice by resuspending in wash medium containing 0.3 M sucrose, 5 mM MOPS followed by centrifugation at 18000xg for 15 min. The final mitochondrial pellet was resuspended in wash buffer containing 100mM PMSF (Branco-Price et al., 2005). Mitochondrial proteins concentrations were determined using BCA assay (Pierce).

Elemental analysis

For the plant tissue and seeds, separate biological replicates were analyzed in the Purdue University Ionomics Laboratory by Dr. David Salt at Purdue University (Lahner et al., 2003). For mitochondria, samples were digested overnight in 250µl concentrated HNO_3 and 50µl concentrated HCl at 60°C. Subsequently, 50µl hydrogen peroxide was added and the samples were re-heated at 60°C for 5-6 hours. The digested samples were centrifuged and the supernatatnt was diluted to obtain a final concentration of 2.5% HNO_3.Samples were analyzed at Center for Elemental Mass Spectrometry, USC on a Thermo Elemental PQ ExCell ICP-MS using a glass conical nebulizer drawing 1 ml per min. The activity of 3 biological replicates was averaged for each genotype for the assay. A student's t-test was used to perform the statistical analysis.

Protein blot analysis

Proteins were extracted and 25µg of the samples were separated by SDS-PAGE and transferred to **p**oly**v**inyl **dif**luoride (PVDF; Fisher Scientific, Waltham, MA) membrane by electroblotting. Membranes were labeled with antibodies and

chemiluminescence detection was carried out as described (Connolly et al., 2002). Western blot analysis for IRT1 was conducted as described (Connolly et al., 2002;Kerkeb et al., 2008). 25µg of total protein extract and 2 µg of mitochondrial proteins were separated for aconitase antibody. Antibodies against aconitase were a kind gift from Dr. Janneke Balk (Luo et al., 2012).

Blue Native PolyAcrylamide Gel Electrophoresis (BN-PAGE) and in-gel assay

The resuspended mitochondrial fraction enriched in respiratory complexes was subjected to BN-PAGE according to (Schagger and von Jagow, 1991) and the in-gel assay was carried out for Complex-1 according to (Sabar et al., 2005). The relative intensities of the complex-I bands were calculated using ImajeJ software (Schneider et al., 2012).

Results

MIT1 and MIT2 localize to mitochondria

A homology-based search for yeast mitoferrin (*MRS3 and MRS4*) orthologs in the *Arabidopsis* genome yielded two proteins with ~38% identity to yeast and zebrafish mitoferrins: At2g30160 (MIT1) and At1g07030 (MIT2). These proteins belong to the mitochondrial substrate carrier family (MCF) and exhibit signature Fe binding residues, GXXXAHXXY, MN and A on transmembrane helices II, IV and V1 respectively (Figure 3.1). These residues have been previously characterized as substrate specific residues required for mitochondrial Fe transport in yeast (Walker, 1992;Kunji and Robinson, 2006).

To further confirm their role as MITs, we first determined their subcellular localization *in planta*. MIT1 and MIT2 overexpressing transgenic lines fused in frame with YFP tag (35S-MIT1-YFP and 35S-MIT2-YFP) were generated and transformed into the onion peel epidermis. The epidermis peels were costained with MitoTracker Orange and were further analyzed for fluorescence with the confocal microscope. Both MIT1 and MIT2 proteins colocalized with the mitochondrial marker thus confirming their localization to mitochondria (Figure 3.2A, Figure 3.2B).

Expression pattern analysis of MIT1 and MIT2

Publically available datasets show that *MIT1* and *MIT2* are ubiquitously expressed throughout the plants' development. However, the highest expression levels were detected in young developing seedlings (http://bar.utoronto.ca/efp/cgi-bin/efpWeb.cgi). Thus, we tested the expression levels of *MIT1* and *MIT2* in the roots and shoots of *Col-0* seedlings under Fe-deficient and Fe-sufficient conditions. Based on the expression pattern analysis obtained by semi-qRT-PCR, *MIT1* seems to be the predominant mitochondrial iron transporter in *Arabidopsis* (Figure 3.3). Additionally, although the expression of these genes did not show a stark regulation by the Fe status in the roots, *MIT1* appears to be positively regulated by the presence of Fe in the shoots as observed previously for MIT in rice (Bashir et al., 2011) (Figure 3.3). Subsequently, to study the spatial expression patterns of *MIT1* and *MIT2* we generated stable transgenic lines transformed with β-glucuronidase (GUS) reporter constructs driven by either MIT1 or MIT2 promoters. GUS histochemical staining was primarily observed in both shoots and roots of young seedlings (Figure 3.4A-Figure 3.4F) and the promoters were predominantly active in the vascular cylinder (Figure 3.4G).

MIT1 and MIT2 functionally complement yeast mitoferrin mutants

In order to assess their functionality in yeast, chimeric versions of *MIT1* and *MIT2* were constructed in which the endogenous targeting sequences were substituted with a yeast leader sequence in order to ensure proper targeting of the *Arabidopsis* proteins to the mitochondria in yeast. These constructs were used to transform the yeast *Δmrs3Δmrs4* mutant. Both MIT1 and MIT2 were able to partially rescue the Fe-limited growth phenotype of *Δmrs3Δmrs4* (Figure 3.5). These results show that MIT1 and MIT2 function as mitochondrial Fe transporters in yeast.

Characterization of mutant of *mit1* and *mit2* lines

To investigate the role of *MIT1* and *MIT2 in vivo*, T-DNA insertion mutants (SALK_013388 for MIT1 and SALK_096697 for MIT2) were obtained from the **A**rabidopsis **B**iological **R**esearch **C**enter [ABRC; https://abrc.osu.edu; (Figure 3.6A)]. Single homozygous mutants, (*mit1 and mit2*) were backcrossed and then identified via genotyping. Both *mit1* and *mit2* exhibit suppressed expression of *MIT1* and *MIT2* respectively (Figure 3.6B, Figure 3.6C). Visible phenotypes of the single mutants were indistinguishable from the wild type (data not shown) and therefore the individual T-DNA lines were crossed to obtain a double knockout line *mit1mit2*. However, we failed to obtain a line homozygous for both *mit1 and mit2*. Dissection of the siliques of self-crossed $mit1^{--}/mit2^{+-}$ to look for the embryonic phenotypes revealed an embryo lethal phenotype caused due to the loss of *MIT1* and *MIT2* (Figure 3.6D- Figure 3.6I). Similar results were observed for $mit1^{+-}/mit2^{--}$ (data not shown). The exogenous supply of Fe(III)-EDDHA to the roots was unable to rescue the embryo lethal phenotype suggesting that

MIT1 and *MIT2* are essential during embryogenesis (Figure 3.6J, Figure 3.6K). We analyzed the individual embryos in the mutant lines; while approximately 6% aborted embryos were observed in *mit1*$^{+-}$*/mit2*$^{+-}$, approximately 20% aborted embryos were observed in the self-crossing lines *mit1*$^{--}$*/mit2*$^{+-}$ or *mit1*$^{+-}$*/mit2*.$^{-}$ (Figure 3.6L). The statistical significance of these ratios was confirmed by chi-square test. Since *mit1*$^{--}$ */mit2*$^{+-}$ or *mit1*$^{+-}$*/mit2*$^{--}$ lines exhibited similar phenotypes, it appears that the two genes function redundantly. *mit1*$^{--}$*/mit2*$^{+-}$ exhibits stronger transcript suppression as compared to *mit1*$^{+-}$*/mit2*$^{--}$ (Figure 3.6C) and therefore, all further experiments were performed on *mit1*$^{--}$*/mit2*$^{+-}$ to investigate the role of *MIT1* and *MIT2*. Additionally artificial micro RNA lines targeting both MIT1 and MIT2 (*amiRmit1mit2)* were constructed in order to confirm the double mutant phenotypes. Out of the five independent lines, Line A17 showed the lowest transcript abundance (approximately 50% reduction) of *MIT1* and *MIT2,* and therefore it was chosen for all further experiments (Figure S3.1A).

mit mutants exhibit altered iron homeostasis in plant

The complementation of yeast *mrs3/4* mutant by *MIT1* and *MIT2* suggests their role in mitochondrial Fe trafficking. To investigate their significance on Fe homeostasis in plants, we first examined the elemental profile of the mutants. The aerial portion of *mit1* and *mit2* single mutants and the double knockdown mutants (*mit1*$^{--}$*/mit2*$^{+-}$, *mit1*$^{+-}$ */mit2*$^{--}$ *and amiRmit1/2*) were subjected to **I**nductively-**C**oupled **P**lasma **M**ass **S**pectrometry (ICP-MS) for their elemental analysis. Although Fe levels in the shoot tissue of the soil grown plants were largely unchanged in the mutant lines, *mit1* and *mit*$^{+-}$ */mit2*$^{--}$ exhibited reduced Fe levels as compared to the WT (Figure 3.7A, S3.1B). However, all the mutants exhibited the Fe deficiency signature phenotype (Baxter et al.,

2008). The shoots of the *mit* mutants accumulated significantly elevated levels of Cu, Mn, Zn, and Co (Figure 3.7B- Figure 3.7E). This elemental profile of the mutant lines suggests a sensing of severe Fe deficiency by the mutants which in turn results in increased uptake of Cu and other divalent metals.

Furthermore, since mitoferrins are believed to function predominantly under low Fe conditions, we investigated the effect on Fe accumulation/ Fe homeostasis in response to Fe deficiency in the *mit* mutants. We grew our plants for two weeks on the regular B5 media and then transferred them to Fe-sufficient (50µM Fe(III)-EDTA) or Fe-deficient (300µM ferrozine) media for three days. Subsequently, we measured the elemental profile on the roots and the shoots of these plants by ICP-MS. The mutant plants exhibited general Fe deficiency in their shoots and roots (Figure 3.8A, Figure 3.8B). Based on the aforementioned elemental profile, the Fe uptake machinery at the root surface is expected to be upregulated in order to maintain the Fe homeostasis. Thus, to test this hypothesis, we studied the effect on two Fe-deficiency markers in *Arabidopsis*. We measured the ferric reductase activity and probed for the IRT1 at the root surface of the WT and the mutant plants. While the single *mit1* and *mit2* mutants did not show a significant difference from the WT, *mit1*$^{--}$*/mit2*$^{+-}$ *and amiRmit1/2* lines displayed an approximate three-fold and two-fold induction, respectively, in ferric reductase activity under Fe limitation (Figure 3.8C, Figure S3.1C). Similarly, IRT1 protein levels were also significantly higher in in the mutant lines. (Figure 3.8D, Figure S3.1D). These results suggest that Fe homeostasis is altered in *mit* mutants as compared to the WT and that loss of MITs enhances the Fe deficiency response in the plants.

To further investigate the effect of loss of MIT1 and MIT2 on mitochondrial Fe homeostasis, we first investigated the elemental profile of the organelle using mitochondrial preparations from 2 weeks old seedlings grown in Fe-deplete media. Fe levels in *mit1*$^{--}$*/mit2*$^{+-}$ mutant mitochondria were approximately 43% reduced as compared to the wild type (Figure 3.9A). *mit1* and *mit2* single mutants also exhibited reduced mitochondrial Fe content (Figure S3.2A). Interestingly, these mutant mitochondria harbor increased levels of other metals like Zn (Figure S3.2B). Based on the reduced Fe content in the mutant mitochondria, it is reasonable to predict an adverse effect on the Fe-dependent biochemical processes in the organelle. Since mitochondria are known to be the major site for Fe-S cluster biogenesis, we probed for the levels of a [4Fe-4S] cluster requiring protein- aconitase (ACO) (Balk and Pilon, 2011). One isoform of this protein is present in cytosol, while the other two can be found in the mitochondria (Bernard et al., 2009). While the transcript level of *ACO3* (mitochondria ACO) was constant (data not shown), reduced ACO protein levels were observed both in the mitochondrial as well as in total cellular protein extract of *mit* mutants (Figure 3.9B, Figure S3.2C). This suggests a post transcriptional or a post translational defect in the synthesis of aconitase protein. It could possibly be a result of either defective translation of the transcript or a rapid turnover of the synthesized protein due to depleted levels of Fe. Additionally, Fe depletion may also affects the integrity and the function of the electron transport chain in mitochondria. To investigate the effect on the mitochondrial respiratory complexes, the mitochondrial preparations were separated as native complexes by BN-PAGE and in-gel complex-I activity was assayed. The activity of complex-I, which has the highest demand of approximately 20 Fe atoms (Ohnishi, 1998)

in its core was severely compromised in *mit1*$^{--}$*/mit2*$^{+-}$ mutant mitochondria (Figure 3.9C). The complex-1 band was reduced by approximately 50% in the mutant while the other supercomplexes harboring Complex-I also showed a reduction by ~30 %. These results indicate that in the absence of MITs, Fe cannot be properly imported into the mitochondria resulting in significant alterations in Fe requiring protein abundance and their biochemical activities.

In addition to these molecular phenotypes, the lines mutant for both MIT1 and MIT2 show a bushy and stunted growth phenotype when grown hydroponically in an Fe drop-out media. This phenotype can be rescued via exogenous supply of Fe(III)-EDDHA, indicating the that these growth phenotypes are due to alterations in Fe uptake/trafficking (Figure 3.10, Figure S3.3).

In summary, these results suggest that mitochondrial Fe transporters are essential for embryogenesis and proper biochemical operation in young seedlings under iron limiting conditions.

Discussion

Mitochondrial Fe is known to be required for two major biochemical pathways: Fe-S cluster biogenesis and heme synthesis. Despite its importance, Fe uptake across the mitochondrial membrane is still not fully understood. Our studies in *Arabidopsis* have identified two putative mitochondrial metalloreductases (FRO3 and FRO8), of which FRO3 was shown to reduce Fe to aid in Fe trafficking across the membrane (as described in Chapter 2). It has been widely accepted that mitochondria export Fe-S clusters to meet the requirements of cytosolic and nuclear Fe-S containing proteins, Although the Fe

exporting protein in the mitochondria is still unidentified, a recent study has shown that ATM3 (member of **A**TP **B**inding **C**assette (ABC) family) exports glutathione polysulphide for the assembly of cytosolic Fe-S clusters (Schaedler et al., 2014). In this chapter, we provide evidence that yeast MRS3/4 orthologs, MIT1 and MIT2 function redundantly as mitochondrial iron transporters in *Arabidopsis thaliana*.

Mitochondrial **C**arrier **F**amily (MCF) proteins are small 30kDa proteins that localize to the inner mitochondrial membrane (IMM) and are involved in solute transport from the inner membrane space (IMS) into the mitochondrial matrix (Walker, 1992). The outer mitochondrial membrane (OMM) possesses porin proteins which allow a free movement of many types of molecules across the membrane. The IMM, on the other hand, is selectively permeable, and therefore requires transporters to shuttle various solutes into the matrix. MCF proteins have a tripartite structure, with six transmembrane domains (Kunji and Robinson, 2006). Three major motifs at these proteins serve as the contact points which together form the central cavity of the carrier for the substrate recognition and binding (Kunji and Robinson, 2006). *Arabidopsis* MIT1 and MIT2 belong to the MCF protein family and are believed to reside at the IMM of mitochondria (Picault et al., 2004). Similar to other MCF proteins, MIT1 and MIT2 possess 6 transmembrane helices, with their substrate specific residues on helix 2, 4 and 6. We identified the conserved residues for iron specificity on these two proteins suggesting their potential as mitochondrial Fe transporters [Figure 3.1; (Kunji and Robinson, 2006)]. Expression of 35S-MIT-YFP constructs in onion peel epidermal cells allowed us to show that MIT1 and MIT2 are indeed localized to mitochondria (Figure 3.2).

Furthermore, both *MIT1 and MIT2* are ubiquitously expressed, consistent with an essential role in Fe metabolism. Additionally, they show strong expression in the vasculature of the plant, which is indicative of their role in long distance metal transport into the stele (Figure 3.4).

In a recent study, the largest group of genes coordinately expressed in response to Fe deficiency were found to reside in the pericycle (Long et al., 2010). According to this study, while MITs were expressed in pericycle along with the stele, they were not much modulated by Fe availability (Dinneny et al., 2008;Long et al., 2010). Our expression pattern fits well in the data set with what was presented for the same genes in previous microarray datasets which suggested slight to no regulation of *MIT1* and *MIT2* by Fe availability [Figure 3.3; (Dinneny et al., 2008;Long et al., 2010)]. This might be important in order to prevent toxicity by Fe-overload and maintain a constant influx of iron into the organelle.

The role of MIT1 and MIT2 as mitochondrial Fe transporters was confirmed by complementation of the yeast mitoferrin mutants (Δ*mrs3* Δ*mrs4*); both MIT1 and MIT2 partially rescued the Fe-limited growth phenotype of Δ*mrs3* Δ*mrs4* (Figure 3.5). In order to ensure a proper localization of the *Arabidopsis* MITs in the heterologous yeast system, the first-22 amino acids in MIT1 and MIT2 were substituted with the yeast leader sequence.

To better understand the molecular function of *MIT1* and *MIT2 in planta*, we identified T-DNA insertion mutants of *MIT1* and *MIT2* (Figure 3.6A). While the double mutant was embryo lethal (Figure 3.6 D-K), no obvious growth defects were noted when

the single mutants were grown in soil or on MS agar plates (data not shown). Thus, lines homozygous for either *mit1* or *mit2* and heterozygous for the other gene were used for further characterization (*mit1*$^{--}$*/mit2*$^{+-}$, *mit*$^{+-}$*/mit2*$^{--}$). We also constructed artificial microRNA lines (*amiRmit1/2*) in which expression of both genes were targeted. Reduced transcript levels were observed in all the knockdown and knockout mutants (Figure 3.6B, 3.6C, S3.1A). Since both *mit1*$^{--}$*/mit2*$^{+-}$, *mit*$^{+-}$*/mit2*$^{--}$ mutants exhibit similar phenotypes and no differences in growth or appearance were identified, we concluded that *MIT1* and *MIT2* function redundantly to each other and therefore, the mutants (*mit1*, *mit1*$^{--}$*/mit2*$^{+}$) showing stronger transcript suppression were used for most of the investigations.

As noted above, 20% aborted embryos were found in self-crossed *mit1*$^{--}$*/mit2*$^{+-}$, *mit*$^{+-}$*/mit2.*$^{-}$, indicating that loss of both genes results in embryo lethality. The slight deviation from the expected 3:1 ratio may have been the result of impenetrance of the trait. The *amiRmit1/2* lines did not display the embryo lethal phenotype, likely due to the fact that expression of *MIT1* and *MIT2* was only partially reduced in these lines (Figure S3.1A). Similar to the *mit1mit2* double mutant, the frataxin mutant (*atfh*) also exhibits an embryo lethal phenotype (Vazzola et al., 2007). Despite being accumulation of excess mitochondrial Fe, *atfh* mutants are unable to direct their Fe reserves for proper Fe-S cluster and heme synthesis, resulting in compromised Fe-requiring biochemical reactions in the cell (Maliandi et al., 2011;Jain and Connolly, 2013). Thus, during embryogenesis, adequate supply of Fe and its proper utilization are obligatory for survival.

To further investigate the role of MIT1 and MIT2 in metal homeostasis, we analyzed the elemental content of the mutants. In contrast to rice *mit*, where the mutant exhibited elevated levels of Fe and normal levels of Zn in the shoot (Bashir et al., 2011),

In *Arabidopsis*, while *mit1* and *mit*$^{+-}$*/mit2*$^{--}$ show slightly reduced Fe content, *mit2* and *mit1*$^{--}$*/mit2*$^{--}$ mutants show normal levels of Fe in the shoots. However, all the *mit* mutants exhibited the Fe deficiency signature phenotype (Baxter et al., 2008) as manifested by elevated levels of Zn, Mn and Co (Figure 3.7). This can be explained by the different Fe-acquisition strategies employed by the two species (Walker and Connolly, 2008). Rice acquires its Fe via phytosiderophores and *Arabidopsis* via a non-specific divalent metal transporter - IRT1. IRT1 responds to Fe deficiency; however it non-specifically transports various other metals such as Mn, Co, Zn and Cd along with Fe (Eide et al., 1996;Korshunova et al., 1999;Rogers et al., 2000;Connolly et al., 2002). Thus, similar to rice, onset of Fe-deficiency in *Arabidopsis mit* mutants is demonstrated by up-regulation of Fe-uptake machinery (FRO2 and IRT1; Figure 3.8 S3.1); however, different elemental profiles can be expected /are observed due to the difference in the Fe-uptake strategies followed by the two species. In addition to this, *mit* mutants also exhibit a significantly elevated Cu content in their shoots. This is presumably because Fe deficiency is known to up-regulate a high affinity **COP**per **T**ransporter (COPT2), which in turn leads to accumulation of Cu in the shoots (Perea-Garcia et al., 2013). This elevated Cu uptake is thought to aid in maintaining metal homeostasis as it allows the plant to switch from Fe-utilization to Cu-utilization pathways, which in turn, helps in the prioritization of Fe and eventually recovery from Fe deficiency (Yamasaki et al., 2009).

To validate their role in mitochondrial Fe transport *in planta*, we studied the effect of loss of MITs on mitochondrial Fe homeostasis. Loss of MIT1 and MIT2 results in reduced mitochondrial Fe content (Figure 3.9A S3.2A). The Fe deficiency in the mitochondria is further corroborated by elevated Zn levels in *mit* mutant mitochondria

(Figure S3.2B). In the recent past, a few regulators have emerged which function to sense Fe availability based on the ratio of Fe to other metals such as Zn in the cell (Kobayashi et al., 2013). The Fe and Zn binding sites on these regulators sense the mis-coordination between the two elements to trigger the Fe-deficiency response. (Kobayashi et al., 2013). Although mitochondrial Fe sensors are still unknown, the aforementioned mechanism may explain the up-regulation of the Fe deficiency pathways in response to the altered elemental profile of *mit1*$^{-}$*/mit2*$^{+-}$ mitochondria. Reduced complex–I activity and depleted mitochondrial and cytosolic aconitase levels in the mutants further substantiate the significance of MITs in mitochondrial iron trafficking (Figure 3.9B-E, S3.2C, S3.2D).

Although the types of Fe species in the various subcellular compartments of cells are not yet clear, it is generally accepted that Fe is transported across the mitochondrial inner membrane in the ferrous form (Froschauer et al., 2009a;Jain and Connolly, 2013). This suggests a role for reductases in reducing a ferric ion pool in the IMS to facilitate Fe transport into the matrix. Putative mitochondrial reductases have been identified in *Arabidopsis* (FRO3 and FRO8) and yeast (FRE5), however our work on FRO3 is the first to demonstrate a role for a mitochondrial ferric reductase in Fe import to the mitochondria (Jain et al, 2014).

Iron transporters have been well characterized in several species. While mitoferrins/MITs seem to be the major carriers, they are not the sole transporters of Fe into the mitochondrial matrix. These proteins however, seem indispensable during early stages of development in all species (Figure 3.6) (Muhlenhoff et al., 2003;Shaw et al., 2006;Bashir et al., 2011). A siderophore-mediated pathway for Fe transport has been reported in mammals and similar pathways proposed in other species may serve as

alternative mechanisms for mitochondrial Fe acquisition (Devireddy et al., 2010;Jain and Connolly, 2013). However, the existence of these pathways remains controversial in the cell. On the contrary, the presence of other low affinity mitochondrial Fe transporters or non-specific divalent metal transporters is also plausible; such transporters may be responsible for Fe import under normal to high cytosolic Fe conditions (Jain and Connolly, 2013). Whether MIT1 and MIT2 can shuttle other ions apart from Fe is not clear at this point but a role of their homologs, MRS3/4 in transporting other cations has been reported in the past (Muhlenhoff et al., 2003;Froschauer et al., 2009b;Froschauer et al., 2009a). These proteins play a crucial role in heme and Fe-S cluster biosynthesis in yeast, zebrafish and mammals, however their role in plants may be limited to Fe-S synthesis, since heme synthesis in a plant mitochondria is still a controversy (Muhlenhoff et al., 2003;Shaw et al., 2006;Paradkar et al., 2009;Bashir et al., 2011;Jain and Connolly, 2013). Nevertheless, MITs seem to be the major mitochondrial Fe transporters during Fe-deficiency and their significance in mitochondrial and cellular Fe homeostasis is clear.

To conclude, we identified two functionally redundant mitochondrial Fe transporters in *Arabidopsis* which are crucial to maintain cellular and mitochondrial Fe homeostasis. These proteins play a significant role for proper growth and development of the plant, specifically during reproduction. This study is significant as it contributes to a comprehensive understanding of Fe homeostasis in plants which may, in turn, help in formulation of strategies to develop Fe fortified food crops.

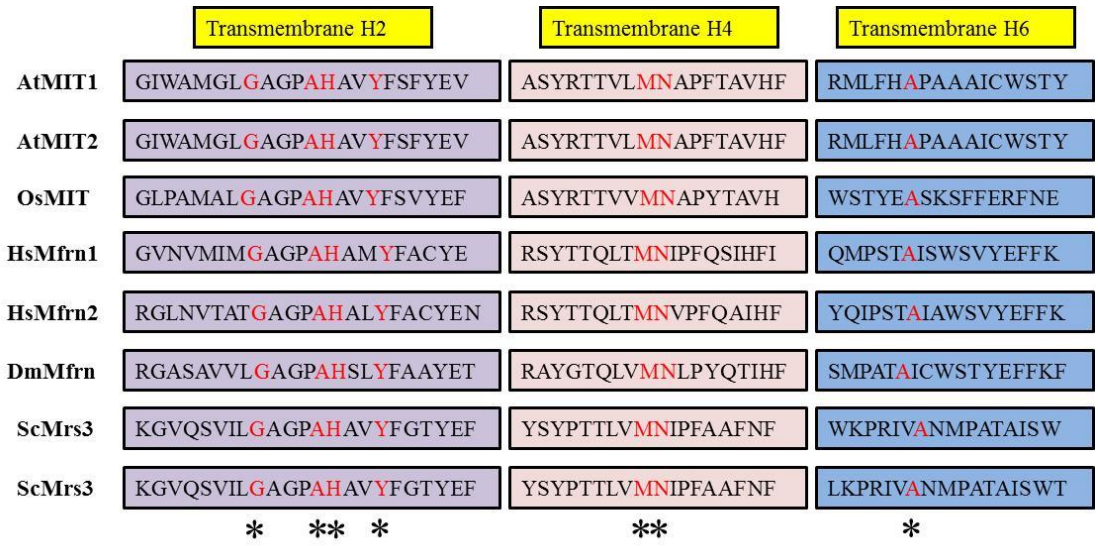

Figure 3.1: Partial alignment of amino acid sequence of mitochondrial Fe transporters in five species. Amino acid residues critical (*marked in red) for mitochondrial iron transport (Kunji and Robinson, 2005) are conserved across species.

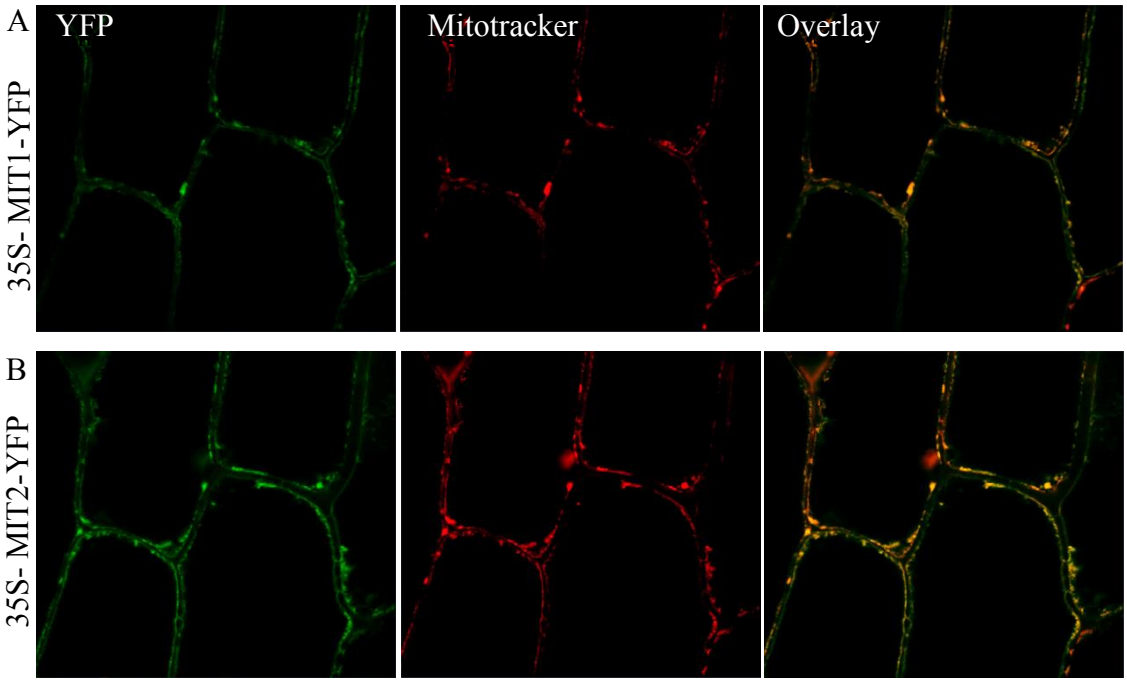

Figure 3.2: Mitochondrial localization of MIT proteins. (A) 35S-MIT1-YFP and (B) 35S- MIT2-YFP were transiently expressed in onion peel epidermis. The cells were co-stained with the organelle specific marker- Mitotracker orange. YFP fluorescence (left panel), mitotracker staining (middle pannel), merged images (right panel).

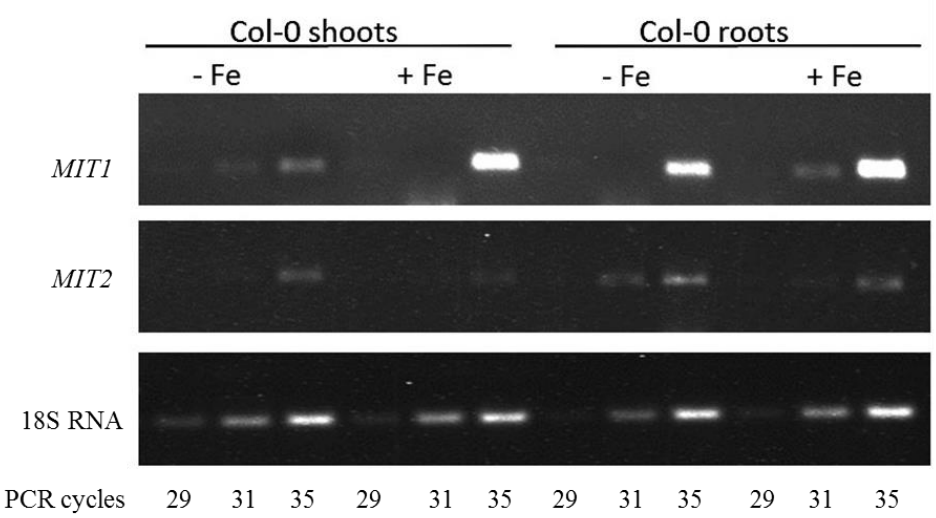

Figure 3.3: Response of *MIT1* and *MIT2* to the Fe status of the plant. Semi-quantitative RT-PCR expression analysis of *MIT1* and *MIT2* in roots and shoots of Col-0 seedlings grown in standard B5 media for 2 weeks and then transferred to Fe-sufficient or Fe-deficient for 3 days.

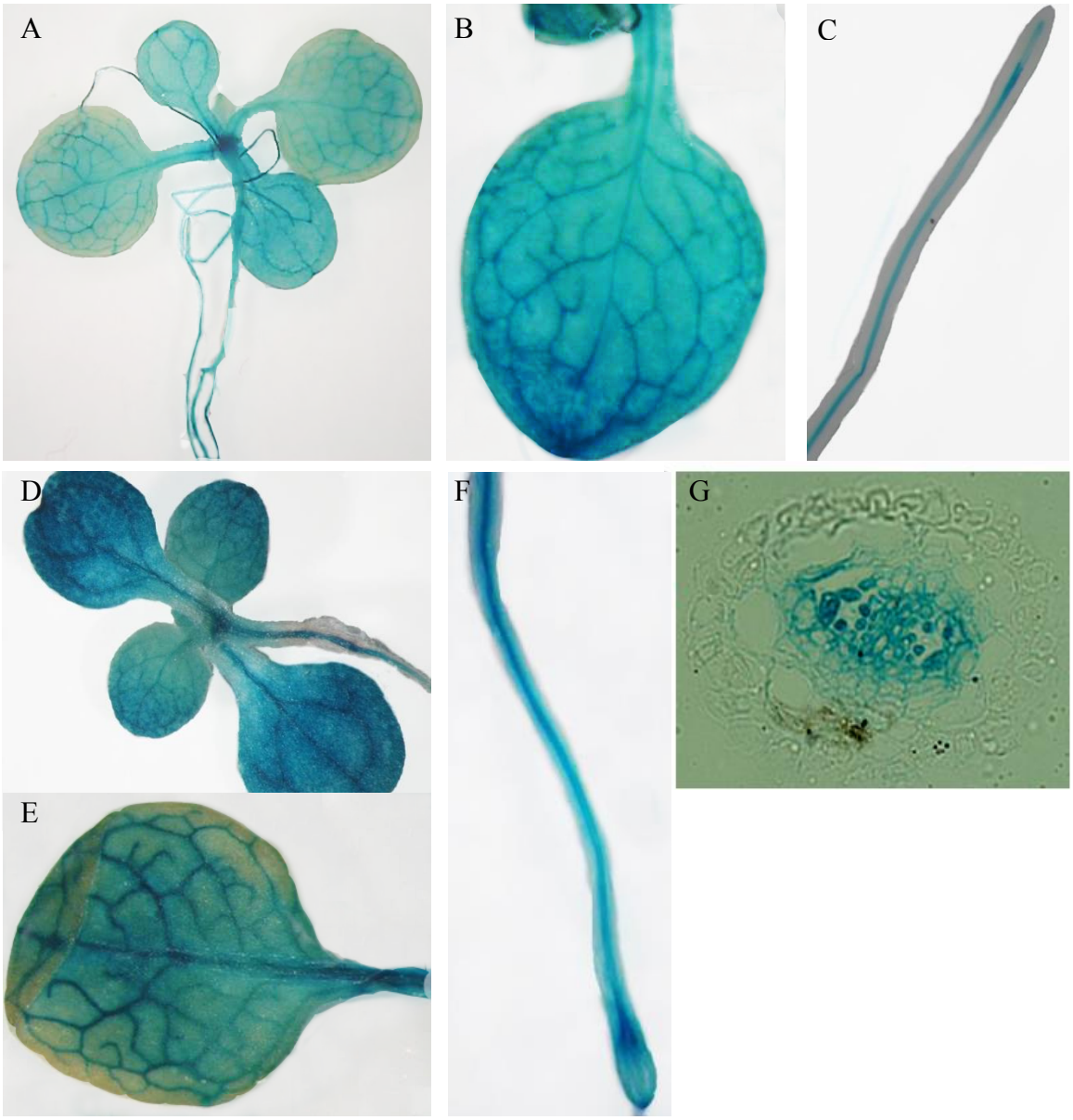

Figure 3.4: Spatio-temporal expression pattern of MIT1 and MIT2. GUS histochemical staining of 2 week old seedlings of (A-C) *proMIT1-GUS* and (D-F) *proMIT2-GUS*. (G) Root cross-section of *proMIT2-GUS*.

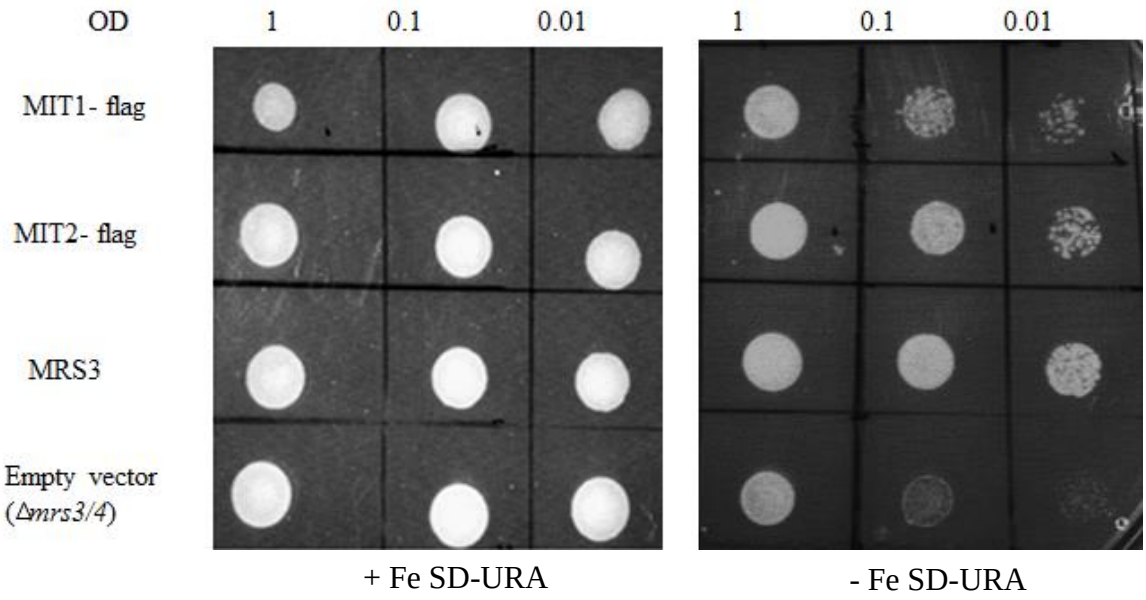

Figure 3.5: AtMIT1 and AtMIT2 complement the defective growth phenotype of *mrs3/4* on iron deficient media. *mrs3/4* was transformed with *AtMIT1-flag, AtMIT2.flag, MRS3* (positive control) and pRS300 (empty vector) and were assayed for growth complementation on +Fe SD-URA and –Fe SD-URA plates

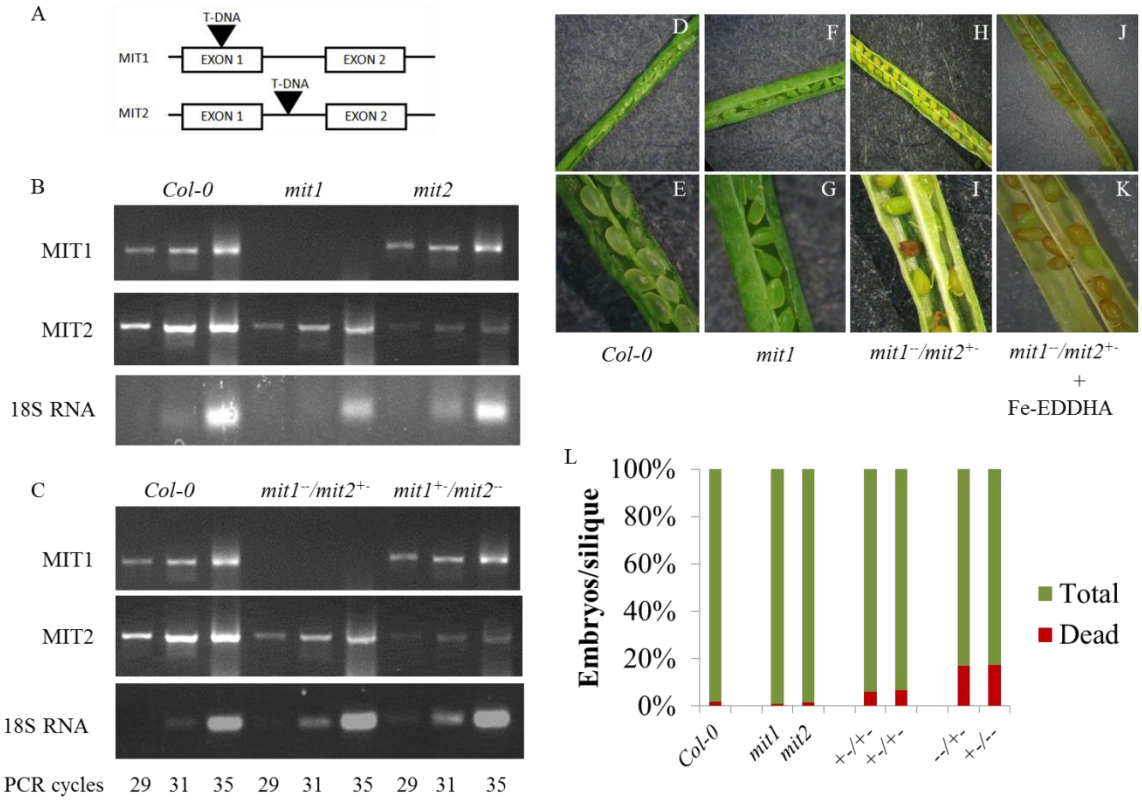

Figure 3.6: Genetic analysis of *mit1* and *mit2* mutants. (A) Gene structure of *mit1* and *mit2* T-DNA insertion mutants. (B) Semi-qRT-PCR expression analysis of *MIT1* and *MIT2* in B) *mit1* , *mit2* mutants and C) $mit1^{--}/mit2^{+-}$, $mit1^{+-}/mit2^{--}$ mutants. (D-K) Siliques of *Col-0* (D, E), *mit1* (F,G), $mit1^{--}/mit2^{+}$ (H,I) and $mit1^{--}/mit2^{+}$ supplemented with Fe-EDDHA (J, K) The red embryos and empty spaces in the siliques depict the embryo lethal phenotype. (L) Quantitative analysis of aborted embryos in *mit* mutants. N=500

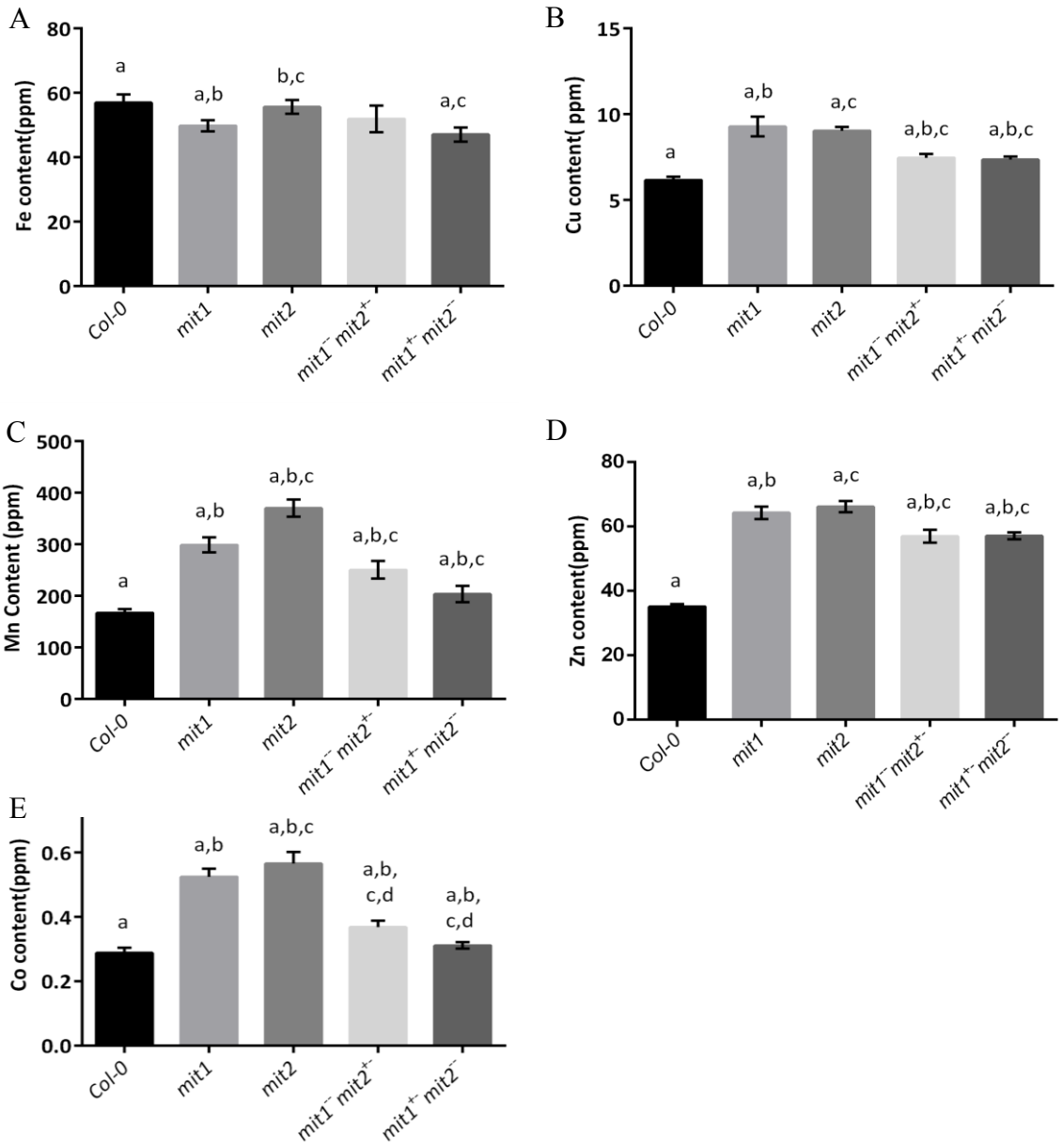

Figure 3.7: *mit* mutants exhibit iron deficiency phenotype. Levels of (A) Fe, (B) Cu, (C) Mn, (D) Zn, (E) Co in the shoots of plants grown in soil in short day conditions for 44 days. Values shown are an average of 13 biological replicates, error bars represent standard error.

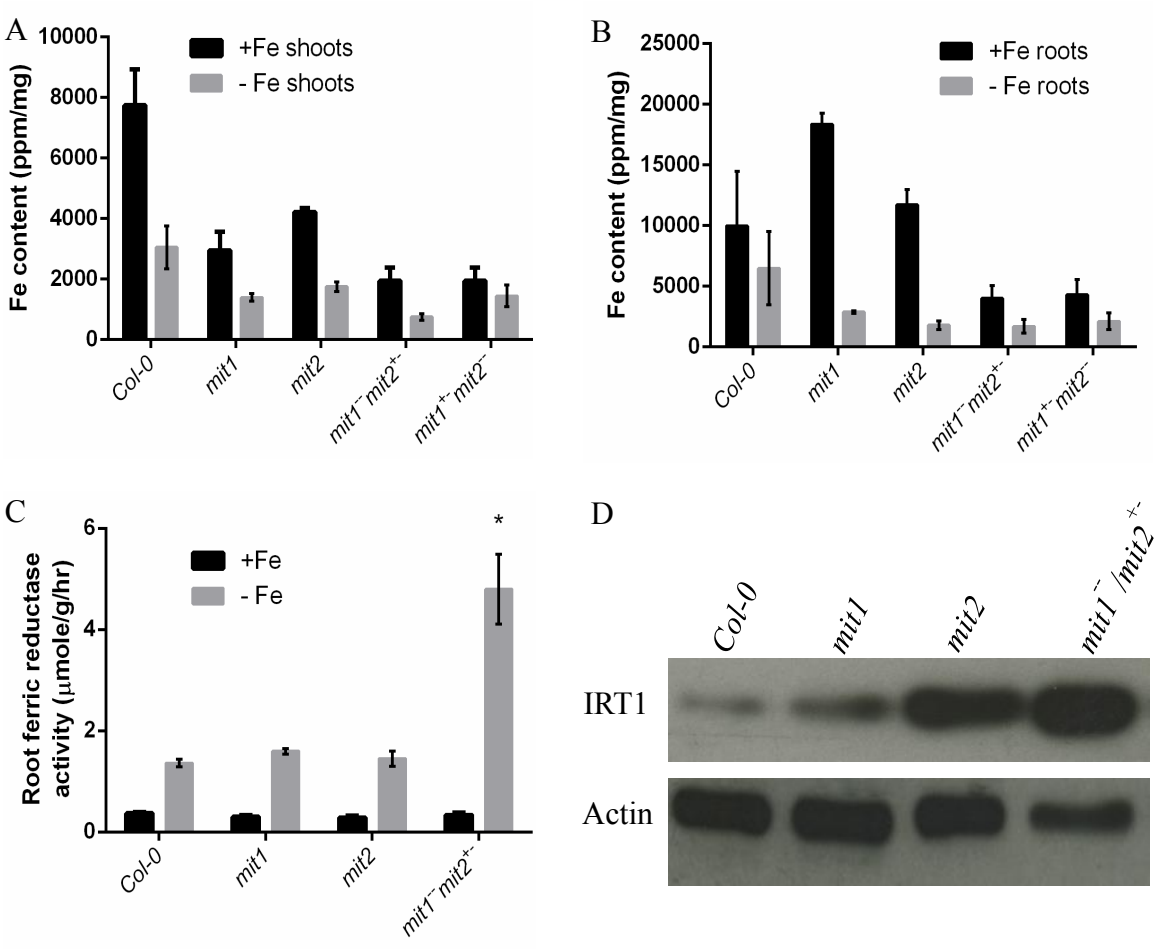

Figure 3.8: *mit* mutants exhibit altered Fe homeostasis under Fe deficiency. Levels of Fe in (A) shoots and (B) roots from seedlings grown in Fe sufficient or Fe deficient media. Shown are an average of 3 biological replicates (C) Root ferric reductase activity assay on the seedlings grown in Fe-sufficient or Fe-deficient media. Values shown are an average of 10 biological replicates. Error bars in all the graphs indicate standard error value.(G) Immunoblot representing IRT1 levels in *mit* mutants grown in Fe-deficient conditions. Actin was used as a control. All the seedlings were grown on standard B5 media for two weeks and then transferred to Fe-sufficient (50µM Fe(III)-EDTA) or Fe-deficient (300µM ferrozine) for three days.

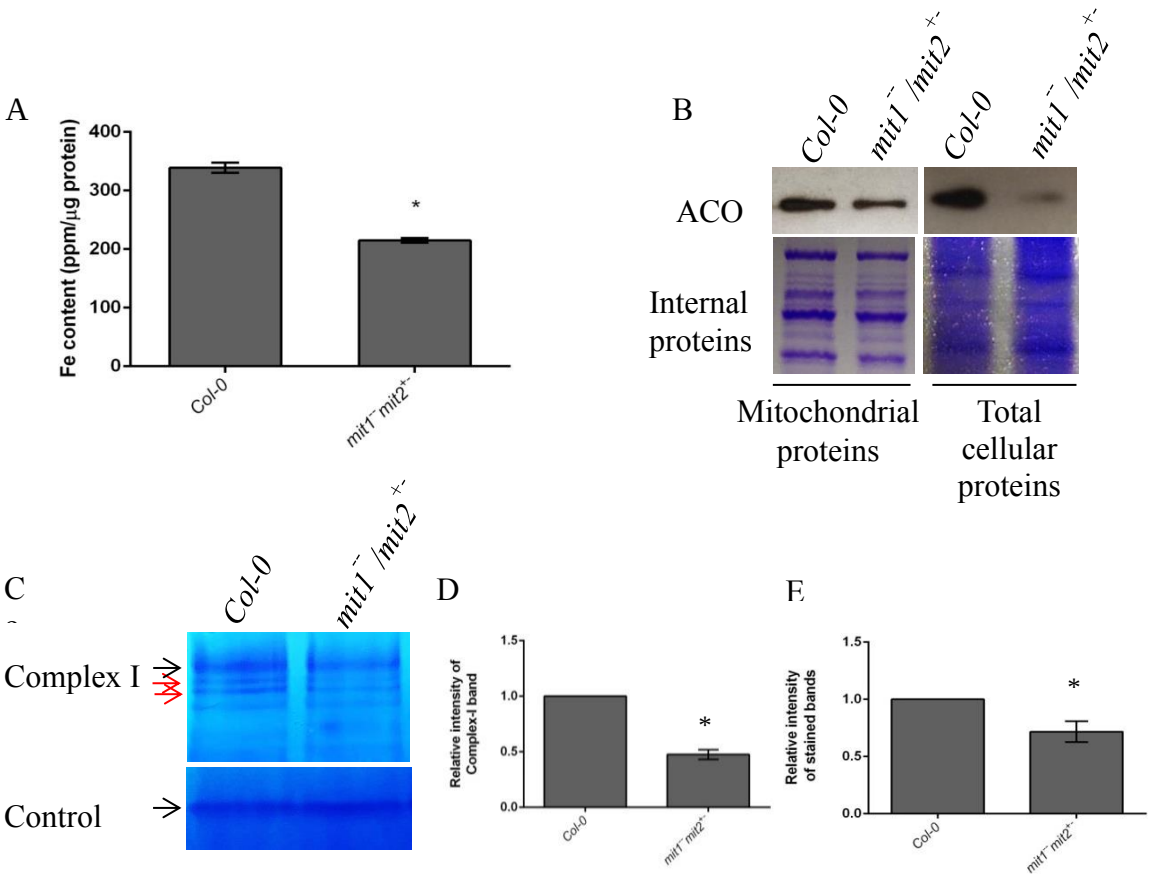

Figure 3.9: MITs are important for mitochondrial iron acquisition/import. (A) Total mitochondrial Fe content measured by ICP-MS (shown is the mean of 3 technical replicates; error bars represent standard errror) (B) Immunoblots showing aconitase protein levels in mitochondrial and total protein extracts. (C) In-gel enzyme activity staining for Complex-1 on mitochondrial extract separated by BN-PAGE. Red arrows indicate supercomplexes comprised of complex 1. Quantification of (D) complex-I band and (E) all stained bands as a results of complex-I in-gel assay. Images were quantified using Imaje J software. The bars represent the average of 3 technical replicates normalized to the reference band shown in the lower panel of (C); error bars represent standard error. The mitochondria for all the experiments were isolated from 2.weeks old seedlings grown in Fe-deplete media.

Figure 3.10: Poor growth phenotype of *mit* mutants in Fe-deficient conditions. The plants were grown vertically on B5 media for 2.5 weeks and then they were transferred to Fe-dropout hydroponics media (replaced weekly)

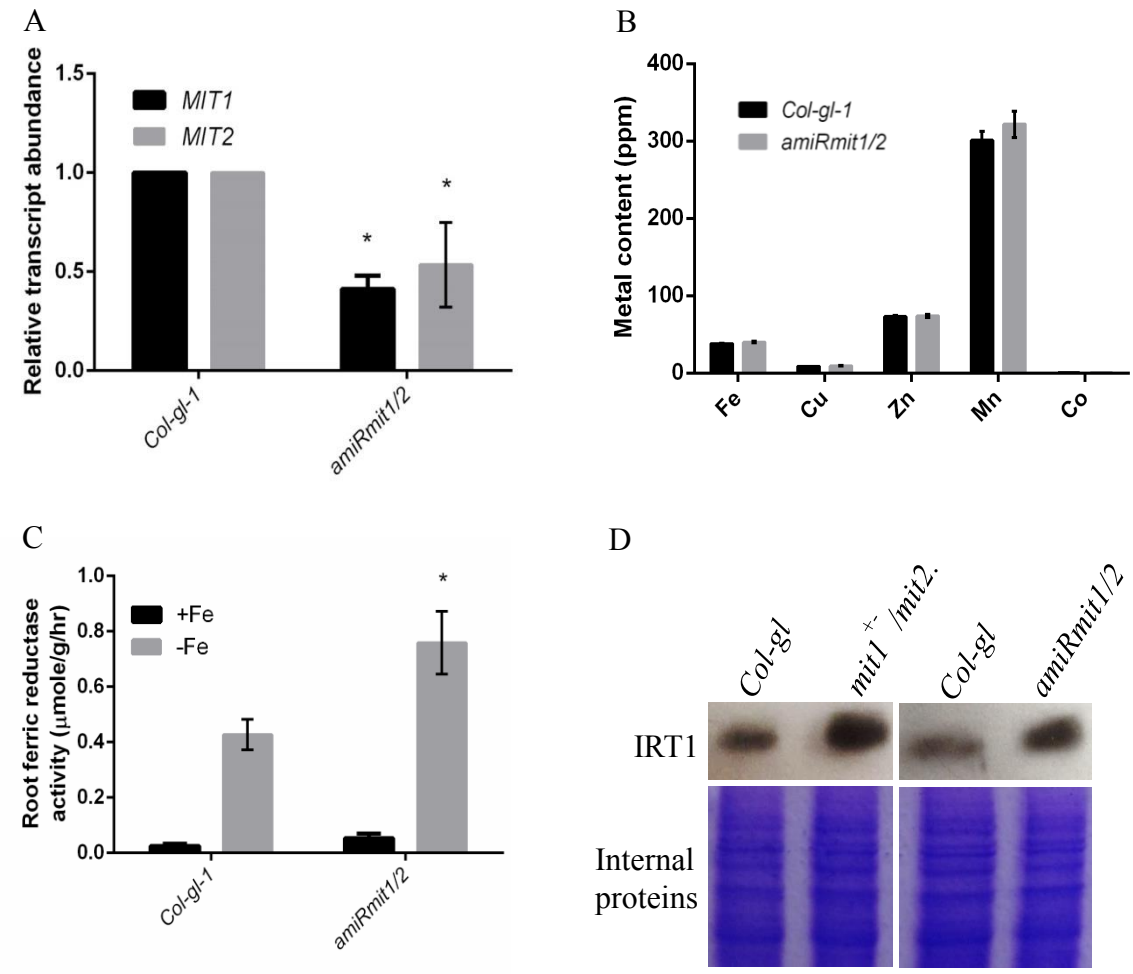

Figure S3.1: Altered Fe homeostasis in *amiRmit1/2* double mutant. (A) Expression levels of *MIT1* and *MIT2* in Col-*gl-1* and *amiRmit1/2* by qRT-PCR . (B) ICP-MS elemental analysis of Col-*gl-1* and *amiRmit1/2* grown in soil (Values shown are an average of 10 biological replicates). (C) Root ferric reductase activity assay on the seedlings grown in Fe-sufficient or Fe-deficient media. Values shown are an average of 5 biological replicates. Error bars in all the graphs indicate standard error value. (D) Immunoblot representing IRT1 levels in *mit* mutants grown in Fe-deficient conditions.

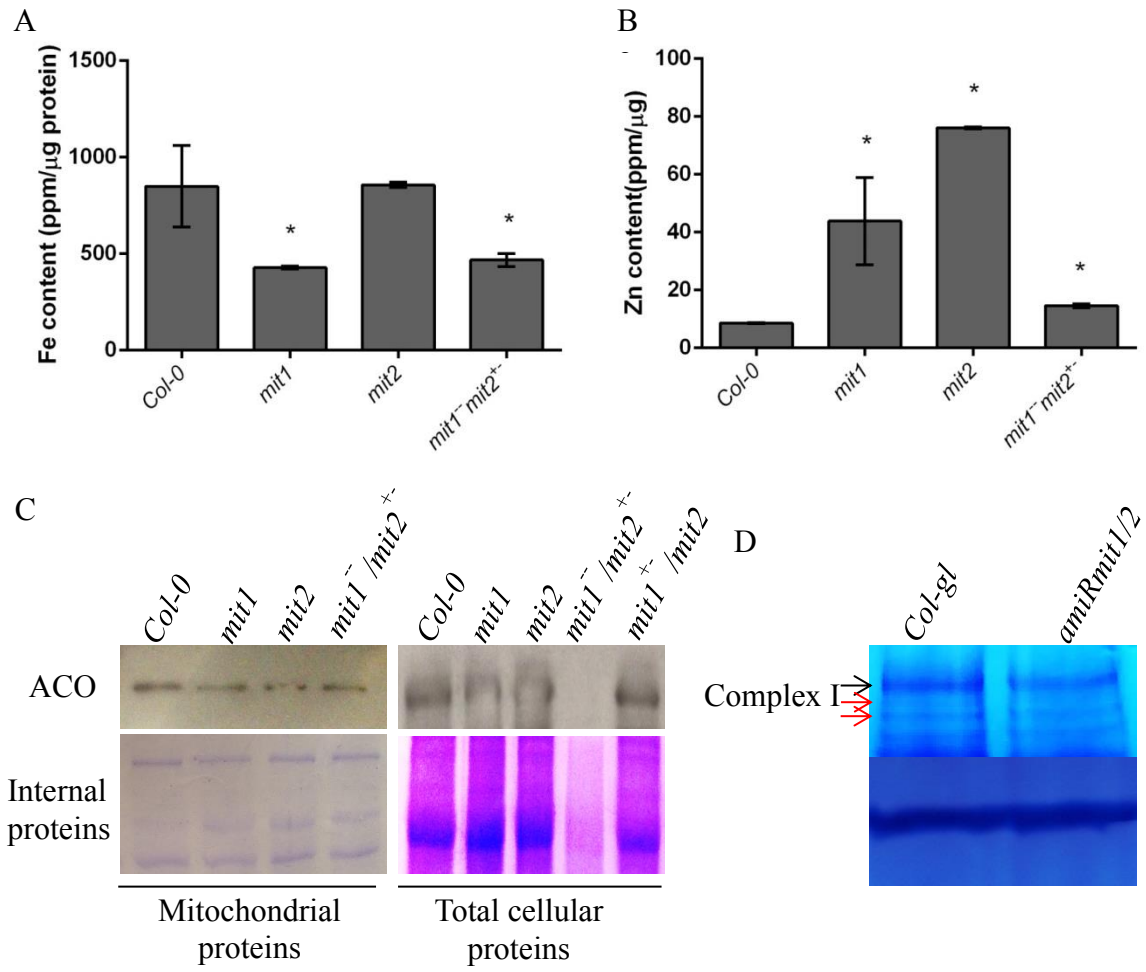

Figure S3.2: Altered mitochondrial iron homeostasis in *mit* mutants. (A) Total Fe content in the mitochondria isolated from 2 weeks old seedlings (B) Total Zn content in the mitochondria isolated from 2 weeks old seedlings (C) Immunoblots showing aconitase protein levels in mitochondrial and total protein extracts. (D) In-gel enzyme activity staining for Complex-1 on mitochondrial extract separated by BN-PAGE. Red arrows indicate supercomplexes comprised of complex 1.

Figure S3.3: Growth phenotype of *mit* in Fe-deficient conditions. (A) Stunted growth phenotype of *mit1*$^{+-}$*/mit2.* and *amiR mit1/2* double mutant grown hydroponically in Fe-drop out media. (B) Plants grown hydroponically in Fe (III)-EDDHA supplemented media

References

Alberts, B., Johnson A., Lewis, J., Raff, M., Roberts, K. and Walter, P. (2002). *Molecular Biology of the cell*, 4th Edition. New York: Garland Science

Arosio, P., Ingrassia, R., and Cavadini, P. (2009). Ferritins: a family of molecules for iron storage, antioxidation and more. *Biochim Biophys Acta* 7**,** 589-599.

Askwith, C., Eide, D., Van Ho, A., Bernard, P.S., Li, L., Davis-Kaplan, S., Sipe, D.M., and Kaplan, J. (1994). The FET3 gene of S. cerevisiae encodes a multicopper oxidase required for ferrous iron uptake. *Cell* 76**,** 403-410.

Balk, J., and Pilon, M. (2011). Ancient and essential: the assembly of iron-sulfur clusters in plants. *Trends Plant Sci* 16**,** 218-226.

Barberon, M., Dubeaux, G., Kolb, C., Isono, E., Zelazny, E., and Vert, G. (2014). Polarization of IRON-REGULATED TRANSPORTER 1 (IRT1) to the plant-soil interface plays crucial role in metal homeostasis. *Proceedings of the National Academy of Sciences* 111**,** 8293-8298.

Barberon, M., Zelazny, E., Robert, S., Conéjéro, G., Curie, C., Friml, J., and Vert, G. (2011). Monoubiquitin-dependent endocytosis of the IRON-REGULATED TRANSPORTER 1 (IRT1) transporter controls iron uptake in plants. *Proceedings of the National Academy of Sciences* 108**,** E450–E458.

Bashir, K., Inoue, H., Nagasaka, S., Takahashi, M., Nakanishi, H., Mori, S., and Nishizawa, N.K. (2006). Cloning and characterization of deoxymugineic acid synthase genes from graminaceous plants. *J Biol Chem* 281**,** 32395-32402.

Bashir, K., Ishimaru, Y., Shimo, H., Nagasaka, S., Fujimoto, M., Takanashi, H., Tsutsumi, N., An, G., Nakanishi, H., and Nishizawa, N.K. (2011). The rice mitochondrial iron transporter is essential for plant growth. *Nat Commun* 2.

Baxter, I., Tchieu, J., Sussman, M.R., Boutry, M., Palmgren, M.G., Gribskov, M., Harper, J.F., and Axelsen, K.B. (2003). Genomic comparison of P-type ATPase ion pumps in Arabidopsis and rice. *Plant Physiol* 132**,** 618-628.

Baxter, I.R., Vitek, O., Lahner, B., Muthukumar, B., Borghi, M., Morrissey, J., Guerinot, M.L., and Salt, D.E. (2008). The leaf ionome as a multivariable system to detect a plant's physiological status. *Proceedings of the National Academy of Sciences* 105**,** 12081-12086.

Bernal, M., Casero, D., Singh, V., Wilson, G.T., Grande, A., Yang, H., Dodani, S.C., Pellegrini, M., Huijser, P., Connolly, E.L., Merchant, S.S., and Kramer, U. (2012). Transcriptome sequencing identifies SPL7-regulated copper acquisition genes FRO4/FRO5 and the copper dependence of iron homeostasis in Arabidopsis. *Plant Cell* 24**,** 738-761.

Bernard, D.G., Cheng, Y., Zhao, Y., and Balk, J. (2009). An allelic mutant series of ATM3 reveals its key role in the biogenesis of cytosolic iron-sulfur proteins in Arabidopsis. *Plant Physiol* 151**,** 590-602.

Bienfait, H.F., and Van Den Briel, M.L. (1980). Rapid mobilization of ferritin iron by ascorbate in the presence of oxygen. *Biochim Biophys Acta* 631**,** 507-510.

Branco-Price, C., Kawaguchi, R., Ferreira, R.B., and Bailey-Serres, J. (2005). Genome-wide analysis of transcript abundance and translation in Arabidopsis seedlings subjected to oxygen deprivation. *Ann Bot* 96**,** 647-660.

Briat, J.-F., Duc, C., Ravet, K., and Gaymard, F. (2010). Ferritins and iron storage in plants. *Biochimica et Biophysica Acta (BBA) - General Subjects* 1800**,** 806-814.

Brown, J.C., and Chaney, R.L. (1971). Effect of iron on the transport of citrate into the xylem of soybeans and tomatoes. *Plant Physiol* 47**,** 836-840.

Buchanan, B., Gruissem, W. and Jones, R. (2002). *Biochemistry and Molecular Biology of Plant.s*

Buckhout, T., Yang, T., and Schmidt, W. (2009). Early iron-deficiency-induced transcriptional changes in Arabidopsis roots as revealed by microarray analyses. *BMC Genomics* 10**,** 147.

Busi, M.V., Maliandi, M.V., Valdez, H., Clemente, M., Zabaleta, E.J., Araya, A., and Gomez-Casati, D.F. (2006). Deficiency of Arabidopsis thaliana frataxin alters activity of mitochondrial Fe-S proteins and induces oxidative stress. *Plant J* 48**,** 873-882.

Carrondo, M.A. (2003). Ferritins, iron uptake and storage from the bacterioferritin viewpoint. *EMBO J* 22**,** 1959-1968.

Cavalier-Smith, T. (1987). The simultaneous symbiotic origin of mitochondria, chloroplasts, and microbodies. *Ann N Y Acad Sci* 503**,** 55-71.

Chollangi, S., Thompson, J.W., Ruiz, J.C., Gardner, K.H., and Bruick, R.K. (2012). Hemerythrin-like domain within F-box and leucine-rich repeat protein 5 (FBXL5)

communicates cellular iron and oxygen availability by distinct mechanisms. *J Biol Chem* 287**,** 23710-23717.

Clough, S.J., and Bent, A.F. (1998). Floral dip: a simplified method forAgrobacterium-mediated transformation ofArabidopsis thaliana. *The Plant Journal* 16**,** 735-743.

Colangelo, E.P., and Guerinot, M.L. (2004). The Essential Basic Helix-Loop-Helix Protein FIT1 Is Required for the Iron Deficiency Response. *The Plant Cell Online* 16**,** 3400-3412.

Connolly, E., Campbell, N., Grotz, N., Prichard, C., and Guerinot, M. (2003). Overexpression of the FRO2 ferric chelate reductase confers tolerance to growth on low iron and uncovers posttranscriptional control. *Plant Physiol* 133**,** 1102 - 1110.

Connolly, E.L., Fett, J.P., and Guerinot, M.L. (2002). Expression of the IRT1 metal transporter is controlled by metals at the levels of transcript and protein accumulation. *Plant Cell* 14**,** 1347-1357.

Conte, S., Stevenson, D., Furner, I., and Lloyd, A. (2009). Multiple antibiotic resistance in Arabidopsis is conferred by mutations in a chloroplast-localized transport protein. *Plant Physiol* 151**,** 559-573.

Curie, C., Panaviene, Z., Loulergue, C., Dellaporta, S.L., Briat, J.F., and Walker, E.L. (2001). Maize yellow stripe1 encodes a membrane protein directly involved in Fe(III) uptake. *Nature* 409**,** 346-349.

Dancis, A., Yuan, D.S., Haile, D., Askwith, C., Eide, D., Moehle, C., Kaplan, J., and Klausner, R.D. (1994). Molecular characterization of a copper transport protein in S. cerevisiae: an unexpected role for copper in iron transport. *Cell* 76**,** 393-402.

Dell'orto, M., Pirovano, L., Villalba, J., González-Reyes, J., and Zocchi, G. (2002). Localization of the plasma membrane H+-ATPase in Fe-deficient cucumber roots by immunodetection. *Plant and Soil* 241**,** 11-17.

Devireddy, L.R., Hart, D.O., Goetz, D.H., and Green, M.R. (2010). A mammalian siderophore synthesized by an enzyme with a bacterial homolog involved in enterobactin production. *Cell* 141**,** 1006-1017.

Didonato, R.J., Jr., Roberts, L.A., Sanderson, T., Eisley, R.B., and Walker, E.L. (2004). Arabidopsis Yellow Stripe-Like2 (YSL2): a metal-regulated gene encoding a plasma membrane transporter of nicotianamine-metal complexes. *Plant J* 39**,** 403-414.

Dinneny, J.R., Long, T.A., Wang, J.Y., Jung, J.W., Mace, D., Pointer, S., Barron, C., Brady, S.M., Schiefelbein, J., and Benfey, P.N. (2008). Cell identity mediates the response of Arabidopsis roots to abiotic stress. *Science* 320**,** 942-945.

Divol, F., Couch, D., Conejero, G., Roschzttardtz, H., Mari, S., and Curie, C. (2013). The Arabidopsis YELLOW STRIPE LIKE4 and 6 Transporters Control Iron Release from the Chloroplast. *Plant Cell* 25**,** 1040-1055.

Dix, D., Bridgham, J., Broderius, M., and Eide, D. (1997). Characterization of the FET4 protein of yeast. Evidence for a direct role in the transport of iron. *J Biol Chem* 272**,** 11770-11777.

Dix, D.R., Bridgham, J.T., Broderius, M.A., Byersdorfer, C.A., and Eide, D.J. (1994). The FET4 gene encodes the low affinity Fe(II) transport protein of Saccharomyces cerevisiae. *J Biol Chem* 269**,** 26092-26099.

Duncan, O., Taylor, N.L., Carrie, C., Eubel, H., Kubiszewski-Jakubiak, S., Zhang, B., Narsai, R., Millar, A.H., and Whelan, J. (2011). Multiple lines of evidence localize signaling, morphology, and lipid biosynthesis machinery to the mitochondrial outer membrane of Arabidopsis. *Plant Physiol* 157**,** 1093-1113.

Duncan, O., Van Der Merwe, M.J., Daley, D.O., and Whelan, J. The outer mitochondrial membrane in higher plants. *Trends in Plant Science* 18**,** 207-217.

Durrett, T.P., Gassmann, W., and Rogers, E.E. (2007). The FRD3-mediated efflux of citrate into the root vasculature is necessary for efficient iron translocation. *Plant Physiol* 144**,** 197-205.

Duy, D., Wanner, G., Meda, A.R., Von Wiren, N., Soll, J., and Philippar, K. (2007). PIC1, an ancient permease in Arabidopsis chloroplasts, mediates iron transport. *Plant Cell* 19**,** 986-1006.

Eckhardt, U., and Buckhout, T.J. (1998). Iron assimilation in Chlamydomonas reinhardtii involves ferric reduction and is similar to Strategy I higher plants. *Journal of Experimental Botany* 49**,** 1219-1226.

Eide, D., Broderius, M., Fett, J., and Guerinot, M.L. (1996). A novel iron-regulated metal transporter from plants identified by functional expression in yeast. *Proc Natl Acad Sci U S A* 93**,** 5624-5628.

Eng, B.H., Guerinot, M.L., Eide, D., and Saier, M.H., Jr. (1998). Sequence analyses and phylogenetic characterization of the ZIP family of metal ion transport proteins. *J Membr Biol* 166**,** 1-7.

Feng, H., An, F., Zhang, S., Ji, Z., Ling, H.Q., and Zuo, J. (2006). Light-regulated, tissue-specific, and cell differentiation-specific expression of the Arabidopsis Fe(III)-chelate reductase gene AtFRO6. *Plant Physiol* 140**,** 1345-1354.

Fourcroy, P., Siso-Terraza, P., Sudre, D., Saviron, M., Reyt, G., Gaymard, F., Abadia, A., Abadia, J., Alvarez-Fernandez, A., and Briat, J.F. (2014). Involvement of the ABCG37 transporter in secretion of scopoletin and derivatives by Arabidopsis roots in response to iron deficiency. *New Phytol* 201**,** 155-167.

Foury, F., and Roganti, T. (2002). Deletion of the mitochondrial carrier genes MRS3 and MRS4 suppresses mitochondrial iron accumulation in a yeast frataxin-deficient strain. *J Biol Chem* 277**,** 24475-24483.

Fraga, D., Meulia, T., and Fenster, S. (2008). "Real-Time PCR," in *Current Protocols Essential Laboratory Techniques*. John Wiley & Sons, Inc.).

Froschauer, E.M., Schweyen, R.J., and Wiesenberger, G. (2009a). The yeast mitochondrial carrier proteins Mrs3p/Mrs4p mediate iron transport across the inner mitochondrial membrane. *Biochimica et Biophysica Acta (BBA) - Biomembranes* 1788**,** 1044-1050.

Froschauer, E.M., Schweyen, R.J., and Wiesenberger, G. (2009b). The yeast mitochondrial carrier proteins Mrs3p/Mrs4p mediate iron transport across the inner mitochondrial membrane. *Biochim Biophys Acta* 5**,** 11.

Grillet, L., Mari, S., and Schmidt, W. (2014). Iron in seeds - loading pathways and subcellular localization. *Front Plant Sci* 4**,** 535.

Gro ß, L.E., Machettira, A.B., Rudolf, M., Schleiff, E. and Sommer, M.S. (2011) GFP-based in vivo protein topology determination in plant protoplast. *J. Endocytobiosis and Cell Res.* 89-97

Grossoehme, N.E., Akilesh, S., Guerinot, M.L., and Wilcox, D.E. (2006). Metal-binding thermodynamics of the histidine-rich sequence from the metal-transport protein IRT1 of Arabidopsis thaliana. *Inorg Chem* 45**,** 8500-8508.

Guerinot, M.L., and Yi, Y. (1994). Iron: Nutritious, Noxious, and Not Readily Available. *Plant Physiol* 104**,** 815-820.

Halliwell, B., Gutteridge, J.M., and Cross, C.E. (1992). Free radicals, antioxidants, and human disease: where are we now? *J Lab Clin Med* 119**,** 598-620.

Han, L., Qin, G., Kang, D., Chen, Z., Gu, H., and Qu, L.J. (2010). A nuclear-encoded mitochondrial gene AtCIB22 is essential for plant development in Arabidopsis. *J Genet Genomics* 37**,** 667-683.

Hart EB, Steenbock H, Waddell J *et al.* 2001 Iron in nutrition. VII. Copper as a supplement to iron for hemoglobin building in the rat. *J Trace Elements Exp Med* **14**, 195–206.

Hassett, R.F., Romeo, A.M., and Kosman, D.J. (1998). Regulation of high affinity iron uptake in the yeast Saccharomyces cerevisiae. Role of dioxygen and Fe. *J Biol Chem* 273**,** 7628-7636.

Heazlewood, J.L., Tonti-Filippini, J.S., Gout, A.M., Day, D.A., Whelan, J., and Millar, A.H. (2004). Experimental analysis of the Arabidopsis mitochondrial proteome highlights signaling and regulatory components, provides assessment of targeting

prediction programs, and indicates plant-specific mitochondrial proteins. *Plant Cell* 16**,** 241-256.

Hell, R., and Stephan, U.W. (2003). Iron uptake, trafficking and homeostasis in plants. *Planta* 216**,** 541-551.

Henriques, R., Jasik, J., Klein, M., Martinoia, E., Feller, U., Schell, J., Pais, M.S., and Koncz, C. (2002). Knock-out of Arabidopsis metal transporter gene IRT1 results in iron deficiency accompanied by cell differentiation defects. *Plant Mol Biol* 50**,** 587-597.

Hider, R.C., and Kong, X. (2013). Iron speciation in the cytosol: an overview. *Dalton Transactions* 42**,** 3220-3229.

Higuchi, K., Suzuki, K., Nakanishi, H., Yamaguchi, H., Nishizawa, N.K., and Mori, S. (1999). Cloning of nicotianamine synthase genes, novel genes involved in the biosynthesis of phytosiderophores. *Plant Physiol* 119**,** 471-480.

Hindt, M.N., and Guerinot, M.L. (2012). Getting a sense for signals: regulation of the plant iron deficiency response. *Biochim Biophys Acta* 1823**,** 1521-1530.

Ichikawa, Y., Bayeva, M., Ghanefar, M., Potini, V., Sun, L., Mutharasan, R.K., Wu, R., Khechaduri, A., Jairaj Naik, T., and Ardehali, H. (2012). Disruption of ATP-binding cassette B8 in mice leads to cardiomyopathy through a decrease in mitochondrial iron export. *Proceedings of the National Academy of Sciences* 109**,** 4152-4157.

Inoue, H., Kobayashi, T., Nozoye, T., Takahashi, M., Kakei, Y., Suzuki, K., Nakazono, M., Nakanishi, H., Mori, S., and Nishizawa, N.K. (2009). Rice OsYSL15 is an iron-regulated iron(III)-deoxymugineic acid transporter expressed in the roots and

is essential for iron uptake in early growth of the seedlings. *J Biol Chem* 284**,** 3470-3479.

Ivanov, R., Brumbarova, T., Blum, A., Jantke, A.M., Fink-Straube, C., and Bauer, P. (2014). SORTING NEXIN1 is required for modulating the trafficking and stability of the Arabidopsis IRON-REGULATED TRANSPORTER1. *Plant Cell* 26**,** 1294-1307.

Jain, A., and Connolly, E.L. (2013). Mitochondrial Iron Transport and Homeostasis in Plants. *Frontiers in Plant Science* 4.

Jain, A., Wilson, G.T., and Connolly, E.L. (2014). The diverse roles of FRO family metalloreductases in iron and copper homeostasis. *Frontiers in Plant Science* 5.

Jefferson, R.A., Kavanagh, T.A., and Bevan, M.W. (1987). GUS fusions: beta-glucuronidase as a sensitive and versatile gene fusion marker in higher plants. *EMBO J* 6**,** 3901-3907.

Jeong, J., Cohu, C., Kerkeb, L., Pilon, M., Connolly, E.L., and Guerinot, M.L. (2008). Chloroplast Fe(III) chelate reductase activity is essential for seedling viability under iron limiting conditions. *Proc Natl Acad Sci U S A* 105**,** 10619-10624.

Jeong, J., and Connolly, E.L. (2009). Iron uptake mechanisms in plants: Functions of the FRO family of ferric reductases. *Plant Science* 176**,** 709-714.

Katoh, H., Hagino, N., and Ogawa, T. (2001). Iron-binding activity of FutA1 subunit of an ABC-type iron transporter in the cyanobacterium Synechocystis sp. Strain PCC 6803. *Plant Cell Physiol* 42**,** 823-827.

Kerkeb, L., Mukherjee, I., Chatterjee, I., Lahner, B., Salt, D.E., and Connolly, E.L. (2008). Iron-induced turnover of the Arabidopsis IRON-REGULATED

TRANSPORTER1 metal transporter requires lysine residues. *Plant Physiol* 146**,** 1964-1973.

Kim, S.A., Punshon, T., Lanzirotti, A., Li, L., Alonso, J.M., Ecker, J.R., Kaplan, J., and Guerinot, M.L. (2006). Localization of iron in Arabidopsis seed requires the vacuolar membrane transporter VIT1. *Science* 314**,** 1295-1298.

Klevay LM. 1997 Paper 10: copper as a supplement to iron for hemoglobin building in the rat (Hart *et al.* 1928). *J Nutr* **127**, 1034S–1036S.

Kobayashi, T., Nagasaka, S., Senoura, T., Itai, R.N., Nakanishi, H., and Nishizawa, N.K. (2013). Iron-binding Haemerythrin RING ubiquitin ligases regulate plant iron responses and accumulation. *Nat Commun* 4**,** 2792.

Kobayashi, T., and Nishizawa, N.K. (2012). Iron uptake, translocation, and regulation in higher plants. *Annu Rev Plant Biol* 63**,** 131-152.

Kobayashi, T., and Nishizawa, N.K. (2014). Iron sensors and signals in response to iron deficiency. *Plant Science* 224**,** 36-43.

Koenig, R. and M.R. Kuhns. (1996). Control of iron chlorosis in ornamental and crop plants. Utah State Univ. AG-SO-01.

Koncz, C., and Schell, J. (1986). The promoter of TL-DNA gene 5 controls the tissue-specific expression of chimaeric genes carried by a novel type of Agrobacterium binary vector. *Molecular and General Genetics MGG* 204**,** 383-396.

Korshunova, Y.O., Eide, D., Clark, W.G., Guerinot, M.L., and Pakrasi, H.B. (1999). The IRT1 protein from Arabidopsis thaliana is a metal transporter with a broad substrate range. *Plant Mol Biol* 40**,** 37-44.

Kranzler, C., Lis, H., Finkel, O.M., Schmetterer, G., Shaked, Y., and Keren, N. (2014). Coordinated transporter activity shapes high-affinity iron acquisition in cyanobacteria. *ISME J* 8**,** 409-417.

Kropat, J., Tottey, S., Birkenbihl, R.P., Depege, N., Huijser, P., and Merchant, S. (2005). A regulator of nutritional copper signaling in Chlamydomonas is an SBP domain protein that recognizes the GTAC core of copper response element. *Proc Natl Acad Sci U S A* 102**,** 18730-18735.

Kunji, E.R., and Robinson, A.J. (2006). The conserved substrate binding site of mitochondrial carriers. *Biochim Biophys Acta* 1757**,** 1237-1248.

Lahner, B., Gong, J., Mahmoudian, M., Smith, E.L., Abid, K.B., Rogers, E.E., Guerinot, M.L., Harper, J.F., Ward, J.M., Mcintyre, L., Schroeder, J.I., and Salt, D.E. (2003). Genomic scale profiling of nutrient and trace elements in Arabidopsis thaliana. *Nat Biotechnol* 21**,** 1215-1221.

Landsberg, E. (1984)Regulation of iron-stress response by whole plant activity. *J, Plant Nutr.* 7, 609-621.

Lanquar, V., Lelievre, F., Bolte, S., Hames, C., Alcon, C., Neumann, D., Vansuyt, G., Curie, C., Schroder, A., Kramer, U., Barbier-Brygoo, H., and Thomine, S. (2005b). Mobilization of vacuolar iron by AtNRAMP3 and AtNRAMP4 is essential for seed germination on low iron. *EMBO J* 24**,** 4041-4051.

Leclere, S., and Bartel, B. (2001). A library of Arabidopsis 35S-cDNA lines for identifying novel mutants. *Plant Mol Biol* 46**,** 695-703.

Lee, S., Chiecko, J.C., Kim, S.A., Walker, E.L., Lee, Y., Guerinot, M.L., and An, G. (2009). Disruption of OsYSL15 leads to iron inefficiency in rice plants. *Plant Physiol* 150**,** 786-800.

Lescure, A.M., Proudhon, D., Pesey, H., Ragland, M., Theil, E.C., and Briat, J.F. (1991). Ferritin gene transcription is regulated by iron in soybean cell cultures. *Proc Natl Acad Sci U S A* 88**,** 8222-8226.

Lesuisse, E., Crichton, R.R., and Labbe, P. (1990). Iron-reductases in the yeast Saccharomyces cerevisiae. *Biochim Biophys Acta* 1038**,** 253-259.

Levi, S., Corsi, B., Bosisio, M., Invernizzi, R., Volz, A., Sanford, D., Arosio, P., and Drysdale, J. (2001). A human mitochondrial ferritin encoded by an intronless gene. *J Biol Chem* 276**,** 24437-24440.

Li, H., Wang, L., and Yang, Z.M. (2014). Co-expression analysis reveals a group of genes potentially involved in regulation of plant response to iron-deficiency. *Gene*.

Lin, Y.F., Liang, H.M., Yang, S.Y., Boch, A., Clemens, S., Chen, C.C., Wu, J.F., Huang, J.L., and Yeh, K.C. (2009). Arabidopsis IRT3 is a zinc-regulated and plasma membrane localized zinc/iron transporter. *New Phytol* 182**,** 392-404.

Ling, H.-Q., Bauer, P., Bereczky, Z., Keller, B., and Ganal, M. (2002). The tomato fer gene encoding a bHLH protein controls iron-uptake responses in roots. *Proceedings of the National Academy of Sciences* 99**,** 13938-13943.

Lingam, S., Mohrbacher, J., Brumbarova, T., Potuschak, T., Fink-Straube, C., Blondet, E., Genschik, P., and Bauer, P. (2011). Interaction between the bHLH transcription factor FIT and ETHYLENE INSENSITIVE3/ETHYLENE

INSENSITIVE3-LIKE1 reveals molecular linkage between the regulation of iron acquisition and ethylene signaling in Arabidopsis. *Plant Cell* 23**,** 1815-1829.

Long, T.A., Tsukagoshi, H., Busch, W., Lahner, B., Salt, D.E., and Benfey, P.N. (2010). The bHLH transcription factor POPEYE regulates response to iron deficiency in Arabidopsis roots. *Plant Cell* 22**,** 2219-2236.

Lopez-Millan, A.F., Morales, F., Abadia, A., and Abadia, J. (2000). Effects of iron deficiency on the composition of the leaf apoplastic fluid and xylem sap in sugar beet. Implications for iron and carbon transport. *Plant Physiol* 124**,** 873-884.

Luo, D., Bernard, D.G., Balk, J., Hai, H., and Cui, X. (2012). The DUF59 family gene AE7 acts in the cytosolic iron-sulfur cluster assembly pathway to maintain nuclear genome integrity in Arabidopsis. *Plant Cell* 24**,** 4135-4148.

Ma, J.F., Taketa, S., Chang, Y.-C., Iwashita, T., Matsumoto, H., Takeda, K., and Nomoto, K. (1999). Genes controlling hydroxylations of phytosiderophores are located on different chromosomes in barley (Hordeum vulgare L.). *Planta* 207**,** 590-596.

Maliandi, M.V., Busi, M.V., Turowski, V.R., Leaden, L., Araya, A., and Gomez-Casati, D.F. (2011). The mitochondrial protein frataxin is essential for heme biosynthesis in plants. *Febs J* 278**,** 470-481.

Marschner, H., and Marschner, P. (2012). *Marschner's mineral nutrition of higher plants.* Academic press.

Masuda, T., Suzuki, T., Shimada, H., Ohta, H., and Takamiya, K. (2003). Subcellular localization of two types of ferrochelatase in cucumber. *Planta* 217**,** 602-609.

Maurer, F., Muller, S., and Bauer, P. (2011). Suppression of Fe deficiency gene expression by jasmonate. *Plant Physiol Biochem* 49**,** 530-536.

Meiser, J., Lingam, S., and Bauer, P. (2011). Posttranslational regulation of the iron deficiency basic helix-loop-helix transcription factor FIT is affected by iron and nitric oxide. *Plant Physiol* 157**,** 2154-2166.

Mendoza-Cozatl, D.G., Xie, Q., Akmakjian, G.Z., Jobe, T.O., Patel, A., Stacey, M.G., Song, L., Demoin, D.W., Jurisson, S.S., Stacey, G., and Schroeder, J.I. (2014). OPT3 Is a Component of the Iron-Signaling Network between Leaves and Roots and Misregulation of OPT3 Leads to an Over-Accumulation of Cadmium in Seeds. *Mol Plant* 7**,** 1455-1469.

Mendoza-Cózatl, D.G., Xie, Q., Akmakjian, G.Z., Jobe, T.O., Patel, A., Stacey, M.G., Song, L., Demoin, D.W., Jurisson, S.S., Stacey, G., and Schroeder, J.I. (2014). OPT3 Is a Component of the Iron-Signaling Network between Leaves and Roots and Misregulation of OPT3 Leads to an Over-Accumulation of Cadmium in Seeds. *Molecular Plant* 7**,** 1455-1469.

Metzendorf, C., Wu, W., and Lind, M.I. (2009). Overexpression of Drosophila mitoferrin in l(2)mbn cells results in dysregulation of Fer1HCH expression. *Biochem J* 421**,** 463-471.

Morgan, L.A., Horton, R., Scrimgeour, K.G. and Perry, M.D. (2012) *Principles of Biochemistry*, 5th edition

Morrissey, J., Baxter, I.R., Lee, J., Li, L., Lahner, B., Grotz, N., Kaplan, J., Salt, D.E., and Guerinot, M.L. (2009). The ferroportin metal efflux proteins function in iron and cobalt homeostasis in Arabidopsis. *Plant Cell* 21**,** 3326-3338.

Muhlenhoff, U., Stadler, J.A., Richhardt, N., Seubert, A., Eickhorst, T., Schweyen, R.J., Lill, R., and Wiesenberger, G. (2003). A specific role of the yeast mitochondrial carriers MRS3/4p in mitochondrial iron acquisition under iron-limiting conditions. *J Biol Chem* 278**,** 40612-40620.

Mukherjee, I. (2006). Iron uptake and homeostasis in Arabidopsis. University of South Carolina, ProQuest, UMI Dissertations Publishing

Mukherjee, I., Campbell, N.H., Ash, J.S., and Connolly, E.L. (2006). Expression profiling of the Arabidopsis ferric chelate reductase (FRO) gene family reveals differential regulation by iron and copper. *Planta* 223**,** 1178-1190.

Nechushtai, R., Conlan, A.R., Harir, Y., Song, L., Yogev, O., Eisenberg-Domovich, Y., Livnah, O., Michaeli, D., Rosen, R., Ma, V., Luo, Y., Zuris, J.A., Paddock, M.L., Cabantchik, Z.I., Jennings, P.A., and Mittler, R. (2012). Characterization of Arabidopsis NEET reveals an ancient role for NEET proteins in iron metabolism. *Plant Cell* 24**,** 2139-2154.

Noorjahan, M., Durga Kumari, V., Subrahmanyam, M., and Panda, L. (2005). Immobilized Fe(III)-HY: an efficient and stable photo-Fenton catalyst. *Applied Catalysis B: Environmental* 57**,** 291-298.

Nouet, C., Motte, P., and Hanikenne, M. (2011). Chloroplastic and mitochondrial metal homeostasis. *Trends Plant Sci* 16**,** 395-404.

Nozoye, T., Nagasaka, S., Kobayashi, T., Takahashi, M., Sato, Y., Uozumi, N., Nakanishi, H., and Nishizawa, N.K. (2011). Phytosiderophore efflux transporters are crucial for iron acquisition in graminaceous plants. *J Biol Chem* 286**,** 5446-5454.

Ohnishi, T. (1998). Iron-sulfur clusters/semiquinones in complex I. *Biochim Biophys Acta* 1364**,** 186-206.

Palmer, C.M., Hindt, M.N., Schmidt, H., Clemens, S., and Guerinot, M.L. (2013). MYB10 and MYB72 are required for growth under iron-limiting conditions. *PLoS Genet* 9**,** e1003953.

Pan, X., Yuan, D.S., Xiang, D., Wang, X., Sookhai-Mahadeo, S., Bader, J.S., Hieter, P., Spencer, F., and Boeke, J.D. (2004). A Robust Toolkit for Functional Profiling of the Yeast Genome. *Molecular Cell* 16**,** 487-496.

Pao, S.S., Paulsen, I.T., and Saier, M.H. (1998). Major Facilitator Superfamily. *Microbiology and Molecular Biology Reviews* 62**,** 1-34.

Paradkar, P.N., Zumbrennen, K.B., Paw, B.H., Ward, D.M., and Kaplan, J. (2009). Regulation of mitochondrial iron import through differential turnover of mitoferrin 1 and mitoferrin 2. *Mol Cell Biol* 29**,** 1007-1016.

Perea-Garcia, A., Garcia-Molina, A., Andres-Colas, N., Vera-Sirera, F., Perez-Amador, M.A., Puig, S., and Penarrubia, L. (2013). Arabidopsis copper transport protein COPT2 participates in the cross talk between iron deficiency responses and low-phosphate signaling. *Plant Physiol* 162**,** 180-194.

Philpott, C.C., and Ryu, M.-S. (2014). Special Delivery: Distributing Iron in the Cytosol of Mammalian cells. *Frontiers in Pharmacology* 5.

Picault, N., Hodges, M., Palmieri, L., and Palmieri, F. (2004). The growing family of mitochondrial carriers in Arabidopsis. *Trends Plant Sci* 9**,** 138-146.

Punta, M., Forrest, L.R., Bigelow, H., Kernytsky, A., Liu, J., and Rost, B. (2007). Membrane protein prediction methods. *Methods* 41**,** 460-474.

Quinn, J.M., and Merchant, S. (1995). Two copper-responsive elements associated with the Chlamydomonas Cyc6 gene function as targets for transcriptional activators. *Plant Cell* 7**,** 623-628.

Raguzzi, F., Lesuisse, E., and Crichton, R.R. (1988). Iron storage in Saccharomyces cerevisiae. *FEBS Letters* 231**,** 253-258.

Ravet, K., Touraine, B., Boucherez, J., Briat, J.F., Gaymard, F., and Cellier, F. (2009). Ferritins control interaction between iron homeostasis and oxidative stress in Arabidopsis. *Plant J* 57**,** 400-412.

Rees, E.M., and Thiele, D.J. (2007). Identification of a vacuole-associated metalloreductase and its role in Ctr2-mediated intracellular copper mobilization. *J Biol Chem* 282**,** 21629-21638.

Robinson, N., Sadjuga, and Groom, Q. (1997). "The froh gene family from Arabidopsis thaliana: Putative iron-chelate reductases," in *Plant Nutrition for Sustainable Food Production and Environment*, eds. T. Ando, K. Fujita, T. Mae, H. Matsumoto, S. Mori & J. Sekiya. Springer Netherlands), 191-194.

Robinson, N.J., Procter, C.M., Connolly, E.L., and Guerinot, M.L. (1999). A ferric-chelate reductase for iron uptake from soils. *Nature* 397**,** 694-697.

Rodriguez-Celma, J., Lin, W.D., Fu, G.M., Abadia, J., Lopez-Millan, A.F., and Schmidt, W. (2013a). Mutually exclusive alterations in secondary metabolism are critical for the uptake of insoluble iron compounds by Arabidopsis and Medicago truncatula. *Plant Physiol* 162**,** 1473-1485.

Rodriguez-Celma, J., Pan, I.-C., Li, W., Lan, P., Buckhout, T.J., and Schmidt, W. (2013b). The transcriptional response of Arabidopsis leaves to Fe deficiency. *Frontiers in Plant Science* 4.

Rogers, E.E., Eide, D.J., and Guerinot, M.L. (2000). Altered selectivity in an Arabidopsis metal transporter. *Proc Natl Acad Sci U S A* 97**,** 12356-12360.

Rogers, E.E., and Guerinot, M.L. (2002). FRD3, a member of the multidrug and toxin efflux family, controls iron deficiency responses in Arabidopsis. *Plant Cell* 14**,** 1787-1799.

Romheld, V., and Marschner, H. (1983). Mechanism of iron uptake by peanut plants : I. Fe reduction, chelate splitting, and release of phenolics. *Plant Physiol* 71**,** 949-954.

Römheld, V., and Marschner, H. (1981). Iron deficiency stress induced morphological and physiological changes in root tips of sunflower. *Physiologia Plantarum* 53**,** 354-360.

Roschzttardtz, H., Conejero, G., Curie, C., and Mari, S. (2009). Identification of the endodermal vacuole as the iron storage compartment in the Arabidopsis embryo. *Plant Physiol* 151**,** 1329-1338.

Roschzttardtz, H., Conéjéro, G., Divol, F., Alcon, C., Verdeil, J.-L., Curie, C., and Mari, S. (2013). New Insights into Fe Localization in Plant Tissues. *Frontiers in Plant Science* 4.

Sabar, M., Balk, J., and Leaver, C.J. (2005). Histochemical staining and quantification of plant mitochondrial respiratory chain complexes using blue-native polyacrylamide gel electrophoresis. *Plant J* 44**,** 893-901.

Samira, R., Stallmann, A., Massenburg, L.N., and Long, T.A. (2013). Ironing out the issues: Integrated approaches to understanding iron homeostasis in plants. *Plant Science* 210**,** 250-259.

Santi, S., and Schmidt, W. (2009a). Dissecting iron deficiency-induced proton extrusion in Arabidopsis roots. *New Phytologist* 183**,** 1072-1084.

Santi, S., and Schmidt, W. (2009b). Dissecting iron deficiency-induced proton extrusion in Arabidopsis roots. *New Phytol* 183**,** 1072-1084.

Schaaf, G., Ludewig, U., Erenoglu, B.E., Mori, S., Kitahara, T., and Von Wiren, N. (2004). ZmYS1 functions as a proton-coupled symporter for phytosiderophore- and nicotianamine-chelated metals. *J Biol Chem* 279**,** 9091-9096.

Schaedler, T.A., Thornton, J.D., Kruse, I., Schwarzlander, M., Meyer, A.J., Van Veen, H.W., and Balk, J. (2014). A Conserved Mitochondrial ATP-Binding Cassette Transporter Exports Glutathione Polysulfide for Cytosolic Metal Cofactor Assembly. *J Biol Chem*.

Schagerlof, U., Wilson, G., Hebert, H., Al-Karadaghi, S., and Hagerhall, C. (2006). Transmembrane topology of FRO2, a ferric chelate reductase from Arabidopsis thaliana. *Plant Mol Biol* 62**,** 215-221.

Schagger, H., and Von Jagow, G. (1991). Blue native electrophoresis for isolation of membrane protein complexes in enzymatically active form. *Anal Biochem* 199**,** 223-231.

Schmid, N.B., Giehl, R.F., Doll, S., Mock, H.P., Strehmel, N., Scheel, D., Kong, X., Hider, R.C., and Von Wiren, N. (2014). Feruloyl-CoA 6'-Hydroxylase1-

dependent coumarins mediate iron acquisition from alkaline substrates in arabidopsis. *Plant Physiol* 164**,** 160-172.

Schmidt, H., Gunther, C., Weber, M., Sporlein, C., Loscher, S., Bottcher, C., Schobert, R., and Clemens, S. (2014). Metabolome analysis of Arabidopsis thaliana roots identifies a key metabolic pathway for iron acquisition. *PLoS One* 9**,** e102444.

Schmidt, W., Michalke, W., and Schikora, A. (2003). Proton pumping by tomato roots. Effect of Fe deficiency and hormones on the activity and distribution of plasma membrane H+-ATPase in rhizodermal cells. *Plant Cell Environ* 26**,** 361-370.

Schneider, C.A., Rasband, W.S., and Eliceiri, K.W. (2012). NIH Image to ImageJ: 25 years of image analysis. *Nat Meth* 9**,** 671-675.

Schwab, R., Ossowski, S., Riester, M., Warthmann, N., and Weigel, D. (2006). Highly Specific Gene Silencing by Artificial MicroRNAs in Arabidopsis. *The Plant Cell Online* 18**,** 1121-1133.

Seguela, M., Briat, J.F., Vert, G., and Curie, C. (2008). Cytokinins negatively regulate the root iron uptake machinery in Arabidopsis through a growth-dependent pathway. *Plant J* 55**,** 289-300.

Shaw, G.C., Cope, J.J., Li, L., Corson, K., Hersey, C., Ackermann, G.E., Gwynn, B., Lambert, A.J., Wingert, R.A., Traver, D., Trede, N.S., Barut, B.A., Zhou, Y., Minet, E., Donovan, A., Brownlie, A., Balzan, R., Weiss, M.J., Peters, L.L., Kaplan, J., Zon, L.I., and Paw, B.H. (2006). Mitoferrin is essential for erythroid iron assimilation. *Nature* 440**,** 96-100.

Shikanai, T., Muller-Moele, P., Munekage, Y., Niyogi, K.K. and Pilon, M. (2003) PAA1, a P-type ATPase of Arabidopsis, functions in copper transport in chloroplast. *Plant Cell* 15, 1333-1346

Shimoni-Shor, E., Hassidim, M., Yuval-Naeh, N., and Keren, N. (2010). Disruption of Nap14, a plastid-localized non-intrinsic ABC protein in Arabidopsis thaliana results in the over-accumulation of transition metals and in aberrant chloroplast structures. *Plant Cell Environ* 33**,** 1029-1038.

Shin, L.J., Lo, J.C., Chen, G.H., Callis, J., Fu, H., and Yeh, K.C. (2013). IRT1 degradation factor1, a ring E3 ubiquitin ligase, regulates the degradation of iron-regulated transporter1 in Arabidopsis. *Plant Cell* 25**,** 3039-3051.

Sickmann, A., Reinders, J., Wagner, Y., Joppich, C., Zahedi, R., Meyer, H.E., Schonfisch, B., Perschil, I., Chacinska, A., Guiard, B., Rehling, P., Pfanner, N., and Meisinger, C. (2003). The proteome of Saccharomyces cerevisiae mitochondria. *Proc Natl Acad Sci U S A* 100**,** 13207-13212.

Singh, A., Kaur, N., and Kosman, D.J. (2007). The metalloreductase Fre6p in Fe-efflux from the yeast vacuole. *J Biol Chem* 282**,** 28619-28626.

Sivitz, A., Grinvalds, C., Barberon, M., Curie, C., and Vert, G. (2011). Proteasome-mediated turnover of the transcriptional activator FIT is required for plant iron-deficiency responses. *Plant J* 66**,** 1044-1052.

Sivitz, A.B., Hermand, V., Curie, C., and Vert, G. (2012). Arabidopsis bHLH100 and bHLH101 control iron homeostasis via a FIT-independent pathway. *PLoS One* 7**,** e44843.

Solti, Á., Kovács, K., Basa, B., Vértes, A., Sárvári, É., and Fodor, F. (2012). Uptake and incorporation of iron in sugar beet chloroplasts. *Plant Physiology and Biochemistry* 52**,** 91-97.

Solti, A., Muller, B., Czech, V., Sarvari, E., and Fodor, F. (2014). Functional characterization of the chloroplast ferric chelate oxidoreductase enzyme. *New Phytol* 202**,** 920-928.

Sun, W., Cao, Z., Li, Y., Zhao, Y., and Zhang, H. (2007). A simple and effective method for protein subcellular localization using Agrobacterium-mediated transformation of onion epidermal cells. *Biologia* 62**,** 529-532.

Takahashi, M., Terada, Y., Nakai, I., Nakanishi, H., Yoshimura, E., Mori, S., and Nishizawa, N.K. (2003). Role of nicotianamine in the intracellular delivery of metals and plant reproductive development. *Plant Cell* 15**,** 1263-1280.

Takahashi, M., Yamaguchi, H., Nakanishi, H., Shioiri, T., Nishizawa, N.K., and Mori, S. (1999). Cloning two genes for nicotianamine aminotransferase, a critical enzyme in iron acquisition (Strategy II) in graminaceous plants. *Plant Physiol* 121**,** 947-956.

Tarantino, D., Casagrande, F., Soave, C., and Murgia, I. (2010a). Knocking out of the mitochondrial AtFer4 ferritin does not alter response of Arabidopsis plants to abiotic stresses. *J Plant Physiol* 167**,** 453-460.

Tarantino, D., Morandini, P., Ramirez, L., Soave, C., and Murgia, I. (2011). Identification of an Arabidopsis mitoferrinlike carrier protein involved in Fe metabolism. *Plant Physiol Biochem* 49**,** 520-529.

Tarantino, D., Petit, J.M., Lobreaux, S., Briat, J.F., Soave, C., and Murgia, I. (2003). Differential involvement of the IDRS cis-element in the developmental and environmental regulation of the AtFer1 ferritin gene from Arabidopsis. *Planta* 217**,** 709-716.

Tarantino, D., Santo, N., Morandini, P., Casagrande, F., Braun, H.P., Heinemeyer, J., Vigani, G., Soave, C., and Murgia, I. (2010b). AtFer4 ferritin is a determinant of iron homeostasis in Arabidopsis thaliana heterotrophic cells. *J Plant Physiol* 167**,** 1598-1605.

Terry. N. and Abadia, J. (1986) Function of iron in chloroplast. *J. Plant Nutr*. 9, 609-646

Tiffin, L.O. (1966). Iron Translocation II. Citrate/Iron Ratios in Plant Stem Exudates. *Plant Physiol* 41**,** 515-518.

Tiffin, L.O. (1970). Translocation of iron citrate and phosphorus in xylem exudate of soybean. *Plant Physiol* 45**,** 280-283.

Varotto, C., Maiwald, D., Pesaresi, P., Jahns, P., Salamini, F., and Leister, D. (2002). The metal ion transporter IRT1 is necessary for iron homeostasis and efficient photosynthesis in Arabidopsis thaliana. *Plant J* 31**,** 589-599.

Vazzola, V., Losa, A., Soave, C., and Murgia, I. (2007). Knockout of frataxin gene causes embryo lethality in Arabidopsis. *FEBS Lett* 581**,** 667-672.

Vert, G., Grotz, N., Dedaldechamp, F., Gaymard, F., Guerinot, M.L., Briat, J.F., and Curie, C. (2002). IRT1, an Arabidopsis transporter essential for iron uptake from the soil and for plant growth. *Plant Cell* 14**,** 1223-1233.

Vigani, G. (2012). Discovering the role of mitochondria in the iron deficiency-induced metabolic responses of plants. *J Plant Physiol* 169**,** 1-11.

Vigani, G., Maffi, D., and Zocchi, G. (2009). Iron availability affects the function of mitochondria in cucumber roots. *New Phytologist* 182**,** 127-136.

Vigani, G., and Zocchi, G. (2009). The fate and the role of mitochondria in Fe-deficient roots of strategy I plants. *Plant Signal Behav* 4**,** 375-379.

Vigani, G., Zocchi, G., Bashir, K., Philippar, K., and Briat, J.F. (2013). Signals from chloroplasts and mitochondria for iron homeostasis regulation. *Trends Plant Sci*.

Vignais, P.V. (2002). The superoxide-generating NADPH oxidase: structural aspects and activation mechanism. *Cell Mol Life Sci* 59**,** 1428-1459.

Voss, P., Horakova, L., Jakstadt, M., Kiekebusch, D., and Grune, T. (2006). Ferritin oxidation and proteasomal degradation: protection by antioxidants. *Free Radic Res* 40**,** 673-683.

Walker, E.L., and Connolly, E.L. (2008). Time to pump iron: iron-deficiency-signaling mechanisms of higher plants. *Current Opinion in Plant Biology* 11**,** 530-535.

Walker, J.E. (1992). The mitochondrial transporter family. *Current Opinion in Structural Biology* 2**,** 519-526.

Waters, B., Blevins, D., and Eide, D. (2002). Characterization of FRO1, a pea ferric-chelate reductase involved in root iron acquisition. *Plant Physiol* 129**,** 85 - 94.

Waters, B.M., Chu, H.H., Didonato, R.J., Roberts, L.A., Eisley, R.B., Lahner, B., Salt, D.E., and Walker, E.L. (2006). Mutations in Arabidopsis yellow stripe-like1 and yellow stripe-like3 reveal their roles in metal ion homeostasis and loading of metal ions in seeds. *Plant Physiol* 141**,** 1446-1458.

Weaver, J., and Pollack, S. (1990). Two types of receptors for iron on mitochondria. *Biochem J* 271**,** 463-466.

Weaver, J., Zhan, H., and Pollack, S. (1990). Mitochondria have Fe(III) receptors. *Biochem J* 265**,** 415-419.

Welch, R., Norvell, W., Schaefer, S., Shaff, J., and Kochian, L. (1993). Induction of iron(III) and copper(II) reduction in pea (Pisum sativum L.) roots by Fe and Cu status: Does the root-cell plasmalemma Fe(III)-chelate reductase perform a general role in regulating cation uptake? *Planta* 190**,** 555-561.

Wickson, M., and Thimann, K.V. (1958). The Antagonism of Auxin and Kinetin in Apical Dominance. *Physiologia Plantarum* 11**,** 62-74.

Wiesemann, K., Gross, L.E., Sommer, M., Schleiff, E., and Sommer, M.S. (2013). self-assembling GFP: a versatile tool for plant (membrane) protein analyses. *Methods Mol Biol* 1033**,** 131-144.

Wu, A.C., Lesperance, L., and Bernstein, H. (2002). Screening for iron deficiency. *Pediatr Rev* 23**,** 171-178.

Wu, H., Li, L., Du, J., Yuan, Y., Cheng, X., and Ling, H.Q. (2005). Molecular and biochemical characterization of the Fe(III) chelate reductase gene family in Arabidopsis thaliana. *Plant Cell Physiol* 46**,** 1505-1514.

Wu, T., Zhang, H.-T., Wang, Y., Jia, W.-S., Xu, X.-F., Zhang, X.-Z., and Han, Z.H. (2012). Induction of root Fe(lll) reductase activity and proton extrusion by iron deficiency is mediated by auxin-based systemic signalling in Malus xiaojinensis. *Journal of Experimental Botany* 63**,** 859-870.

Yadavalli, V., Jolley, C.C., Malleda, C., Thangaraj, B., Fromme, P., and Subramanyam, R. (2012). Alteration of Proteins and Pigments Influence the Function of

Photosystem I under Iron Deficiency from <italic>Chlamydomonas reinhardtii</italic>. *PLoS One* 7**,** e35084.

Yamasaki, H., Hayashi, M., Fukazawa, M., Kobayashi, Y., and Shikanai, T. (2009). SQUAMOSA Promoter Binding Protein-Like7 Is a Central Regulator for Copper Homeostasis in Arabidopsis. *Plant Cell* 21**,** 347-361.

Yi, Y., and Guerinot, M.L. (1996). Genetic evidence that induction of root Fe(III) chelate reductase activity is necessary for iron uptake under iron deficiency. *Plant J* 10**,** 835-844.

Yoon, T., and Cowan, J.A. (2004). Frataxin-mediated iron delivery to ferrochelatase in the final step of heme biosynthesis. *J Biol Chem* 279**,** 25943-25946.

Yuan, Y., Wu, H., Wang, N., Li, J., Zhao, W., Du, J., Wang, D., and Ling, H.Q. (2008). FIT interacts with AtbHLH38 and AtbHLH39 in regulating iron uptake gene expression for iron homeostasis in Arabidopsis. *Cell Res* 18**,** 385-397.

Zancani, M., Peresson, C., Biroccio, A., Federici, G., Urbani, A., Murgia, I., Soave, C., Micali, F., Vianello, A., and Macri, F. (2004). Evidence for the presence of ferritin in plant mitochondria. *Eur J Biochem* 271**,** 3657-3664.

Zhai, Z., Gayomba, S.R., Jung, H.I., Vimalakumari, N.K., Pineros, M., Craft, E., Rutzke, M.A., Danku, J., Lahner, B., Punshon, T., Guerinot, M.L., Salt, D.E., Kochian, L.V., and Vatamaniuk, O.K. (2014). OPT3 Is a Phloem-Specific Iron Transporter That Is Essential for Systemic Iron Signaling and Redistribution of Iron and Cadmium in Arabidopsis. *Plant Cell* 26**,** 2249-2264.

Zhang, X., Krause, K.-H., Xenarios, I., Soldati, T., and Boeckmann, B. (2013). Evolution of the Ferric Reductase Domain (FRD) Superfamily: Modularity, Functional Diversification, and Signature Motifs. *PLoS One* 8**,** e58126.

Zhang, Y., Mikhael, M., Xu, D., Li, Y., Soe-Lin, S., Ning, B., Li, W., Nie, G., Zhao, Y., and Ponka, P. (2010). Lysosomal proteolysis is the primary degradation pathway for cytosolic ferritin and cytosolic ferritin degradation is necessary for iron exit. *Antioxid Redox Signal* 13**,** 999-1009.

Zhao, G., Ceci, P., Ilari, A., Giangiacomo, L., Laue, T.M., Chiancone, E., and Chasteen, N.D. (2002). Iron and hydrogen peroxide detoxification properties of DNA-binding protein from starved cells. A ferritin-like DNA-binding protein of Escherichia coli. *J Biol Chem* 277**,** 27689-27696.

Appendix A

Permission to use copy right material

Dear Mr Jain,

Thank you for your email.

Just to reassure you, according to the CCBY license under which we operate, you have full permission to refer to text and figures from your published articles (and any Frontiers articles) so long as they are properly cited. For further information, please see our "Copyright Policy" in our FAQ section.

All the best,

Gearóid Ó Faoleán, PhD

Frontiers | Plant Science Editorial Office

Journal Manager: Dr Amanda Baker

EPFL - Innovation Park, building I

1015 Lausanne, Switzerland | T +41(0)21 510 17 11

www.frontiersin.org | twitter.com/FrontiersIn

For technical issues, please contact our IT Helpdesk <support@frontiersin.org>.

On 18 September 2014 05:13, JAIN, ANSHIKA <anshika@biol.sc.edu> wrote:

Dear Sir or madam

I am Anshika Jain, a graduate student at the University of South Carolina. I am the first author of two published mini reviews in Frontiers in Plant Science: one being 'Mitochondrial Iron transport and homeostasis in plants' and the other being 'The diverse role of FRO family metalloreducatses in iron and copper homeostasis'. I understand that the copyright for both these manuscripts are reserved by Frontiers. However, being the 1st author in both the manuscripts, I was wondering if I could adapt some portions (both text and figures) from these manuscripts and combine them into an introduction for my dissertation. The portions adapted will be properly cited and referenced.

I would really appreciate your consideration.

Thank you

Anshika Jain

Doctoral candidate
Dept. of Biological Sciences
University of South Carolina
715, Sumter street
Columbia, SC- 29208

Appendix B

Permission to use copy right material

Dear Anshika,

Sorry that it took me so long to get back to you!

I have no issues if you adapt my data in your dissertation as long as Erin is ok with that.

Good luck!

Regards,

Indrani

On Tue, Oct 28, 2014 at 12:15 PM, Anshika Jain <11.anshika@gmail.com> wrote:

Dear Dr. Mukherjee

I am Anshika Jain, a current graduate student with Dr. Erin Connolly at University of South Carolina.

I have worked on the FRO3 project that you had initiated years ago in Connolly lab. In order for a proper dissemination of this work, I need to include/adapt some data (such as transcript analysis, ICP analysis of the mutant) from your dissertation into mine as the foundation of the project.

I understand that your dissertation is your copyright material and I do not mean to infringe upon it in anyway. Therefore, I was hoping to get your permission to adapt some figures from your thesis into mine.

All the work will be properly cited and credited. Please let me know if it would be fine by you..

I would really appreciate your consideration

Thank You

Anshika

Anshika Jain
Doctoral candidate
Univ of South Carolina
715, sumter street
Columbia, SC- 29208